Perspectives on Nanoscience

Mildred Dresselhaus

Massachusetts Institute of Technology

Cambridge, MA

21st Century COE Symposium

Tohoku University, March 6, 2004

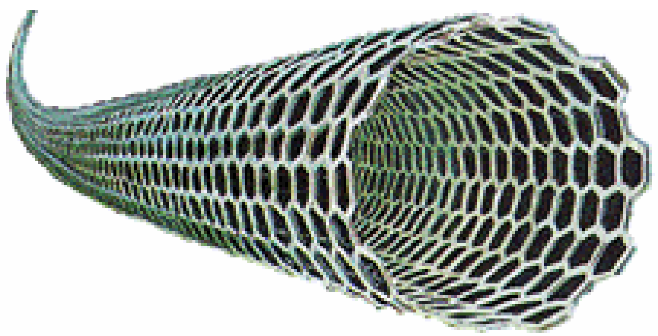

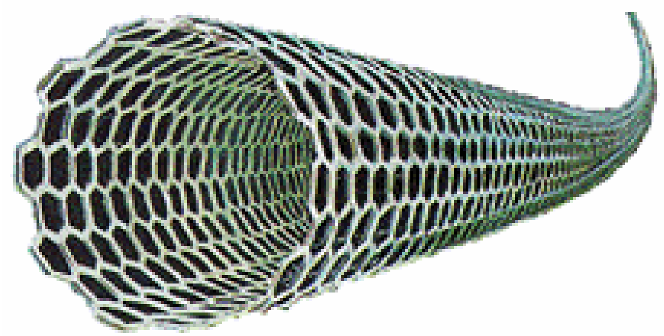

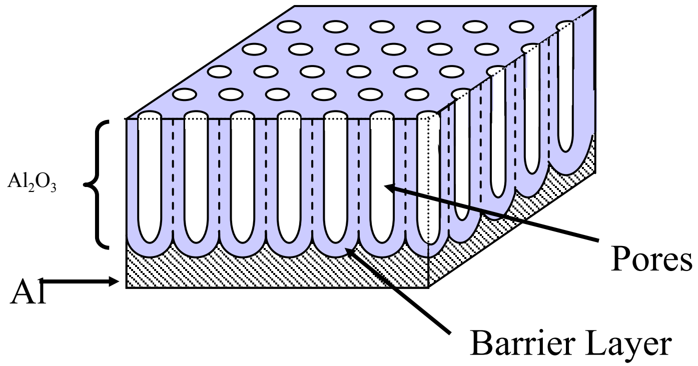

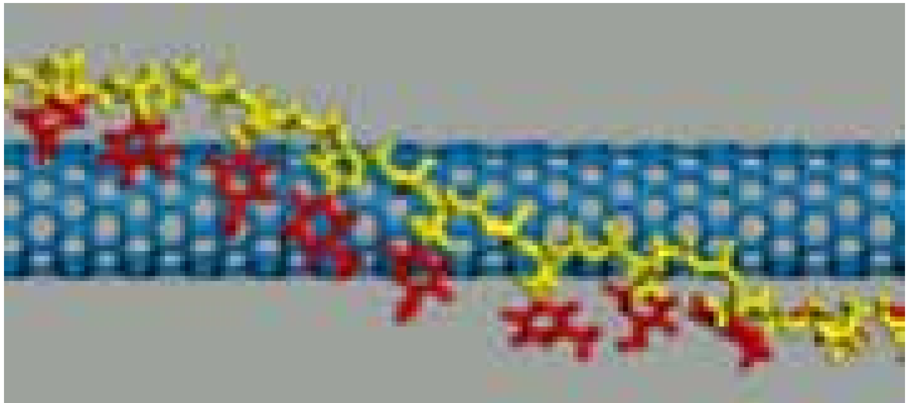

Outline

- Broad overview of nanoscience
- One dimensional nanostructures
- Nanowire structure and properties
- Carbon nanotubes as 1D model systems
- An example of the connection between Science and Science policy in the U.S.: Nanoscience and the Hydrogen Economy

The Incredible Tininess of Nano

Billions of nanometers
A two meter tall male is two billion nanometers.

A million nanometers
The pinhead sized patch of this thumb is a million nanometers across.

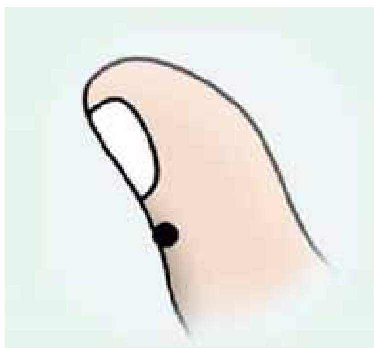

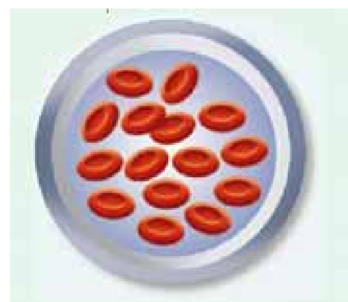

Thousands of nanometers
Biological cells have diameters in the range of thousands of nanometers.

Nanometers
Ten shoulder-to-shoulder hydrogen atoms span 1 nanometer. DNA molecules are about 2.5 nanometers wide.

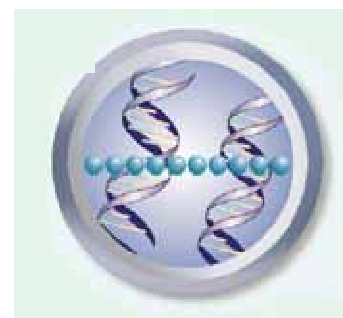

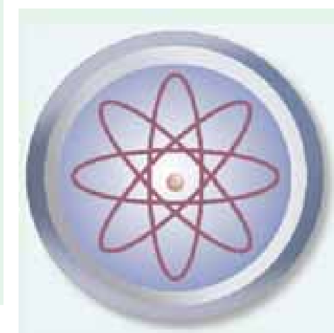

Less than a nanometer
Individual atoms are up to a few tenths of a nanometer in diameter.

1 nm is 70,000 times smaller than a human hair

Science Introduction

- Nanostructures (< 30 nm) have become an exciting research field
  - New quantum phenomena occur at this length scale
  - New structure – property relations are expected
  - Materials behave differently in 2D, 1D and 0D as compared to 3D
  - Promising applications are expected in optics, electronics, thermoelectric, magnetic storage, NEMS (nano-electro-mechanical systems)

- Low-dimensional systems are realized by creating nanostructures that are quantum confined in one or more directions

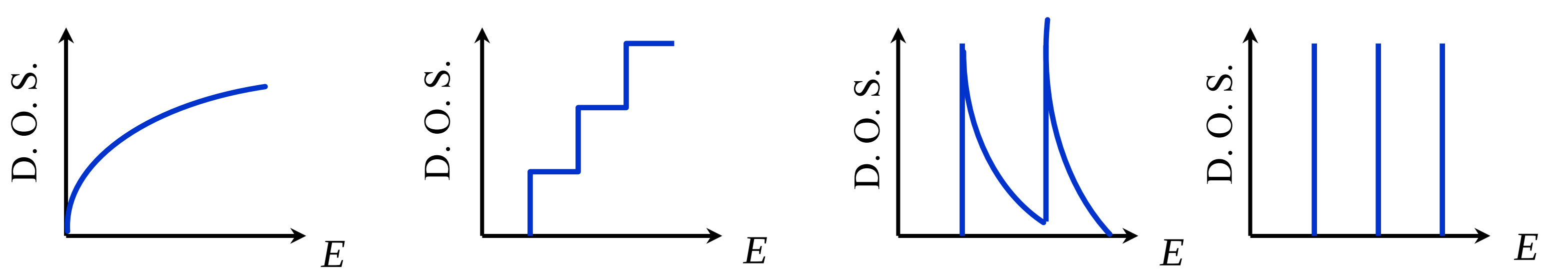

3D Bulk Semiconductor | 2D Quantum Well | 1D Quantum Wire | 0D Quantum Dot

Context – Nanotechnology in the World

Government investments 1997-2002

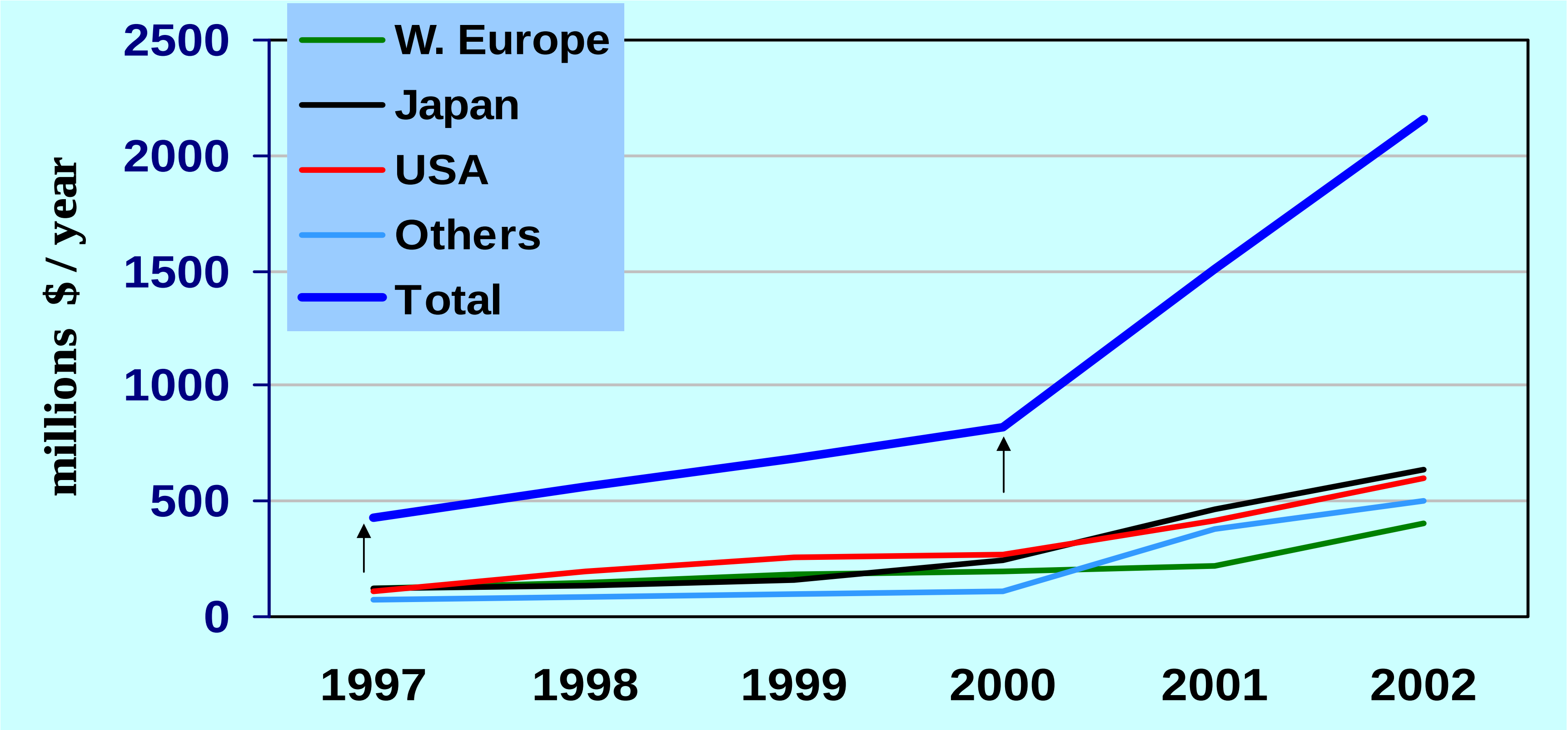

Note:

- U.S. begins FY in October, six month before EU & Japan in March/April
- Japan is the leading investor in nano

The incredible shrinking disk drive for data storage

1956 IBM Ramac 305	**vs.**	**2000 IBM Microdrive**
5 MB		**1 GB**
50 x 24” dia. disks		**1 x 1” disk**
weighs “a ton”		**< 1 oz.**
$50,000		**$500**

Decreasing Head/media spacing

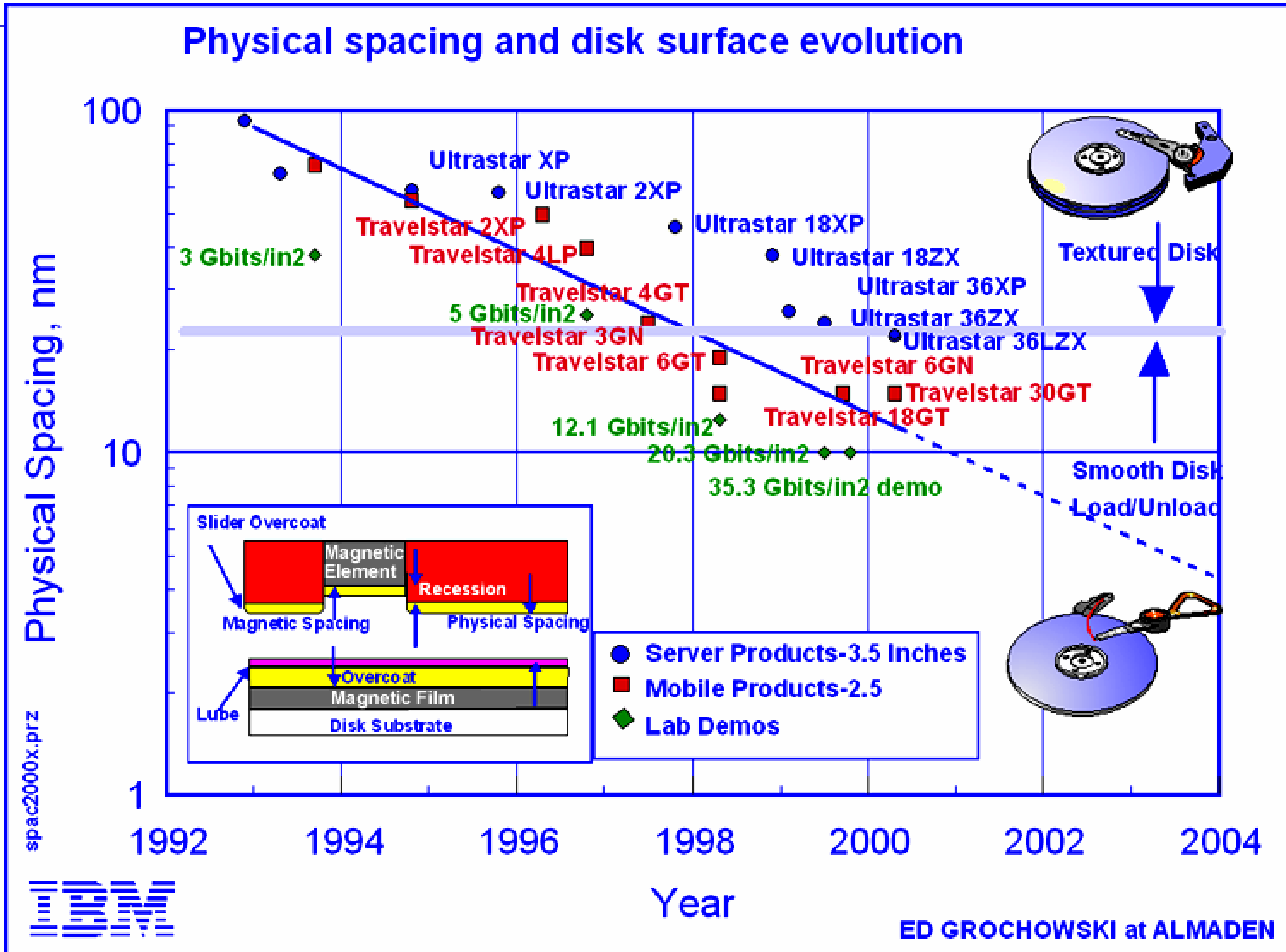

- Moore's law applies to semiconductor electronics, optoelectronics, magnetic storage, etc.

Magnetic Recording at the Nanoscale

• **Simplest Case of Giant Magnetoresistance**

scattering of majority electrons shown in film cross-section

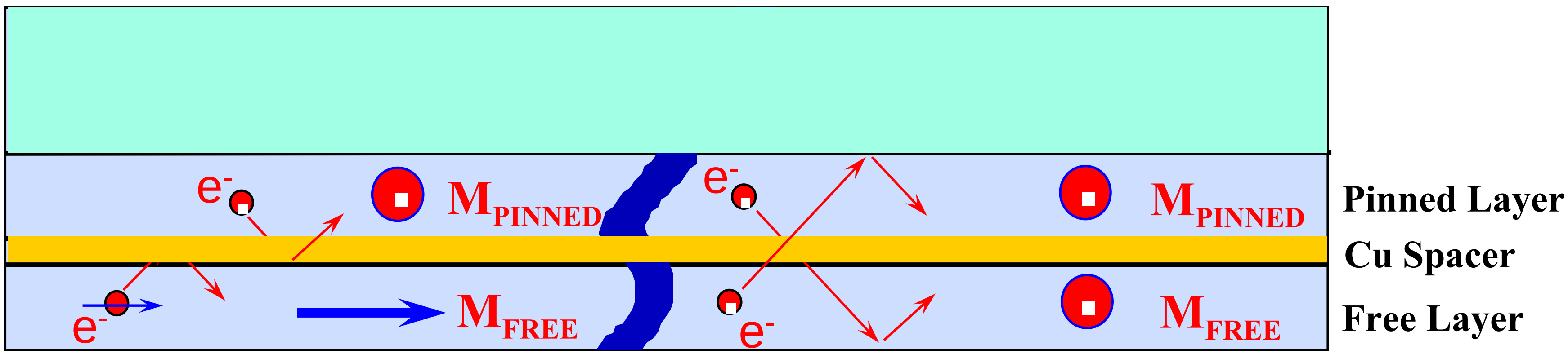

Higher Resistance
Perpendicular State

Lowest Resistance
Parallel State

Sense Current Direction

Active layer is 15-25 nm thick

Picture from Allan Shultz, Seagate Technology

A "Nano Tool-box"

To fabricate/probe nanostructures

Nanofabrication

<u>Top-down Method</u>

- create nanostructures out of macrostructures

<u>Bottom-up Method</u>

- self assembly of atoms or molecules into nanostructures

Various Bi Nanostructures

All are one-dimensional and all are Bi

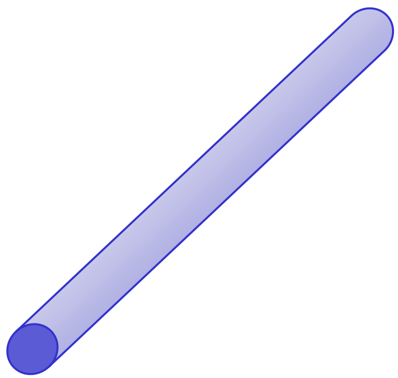

(a) Bi Nanowire

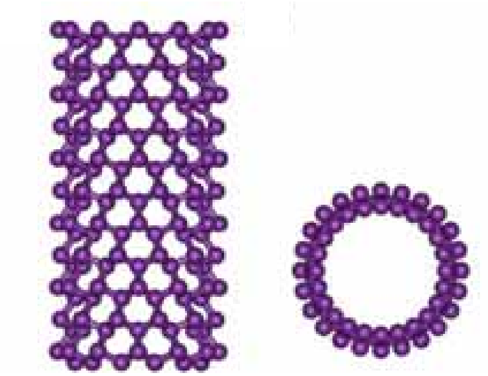

(b) Bi Nanotube

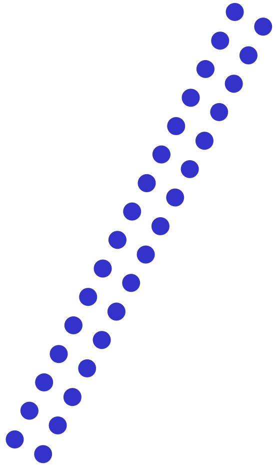

(c) Bi Atomic Line

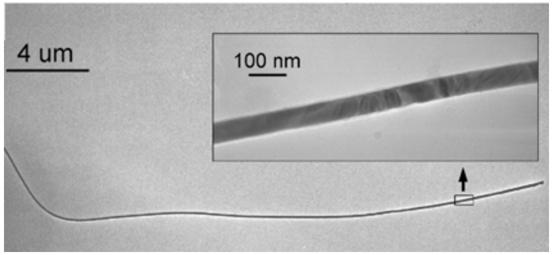

Dresselhaus Group
US

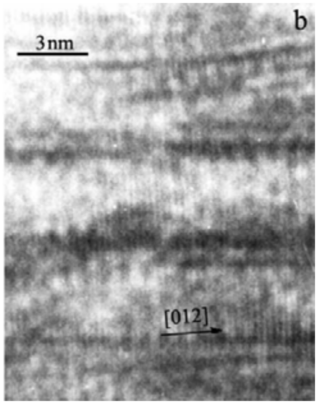

X.Y. Liu *et al.*
China

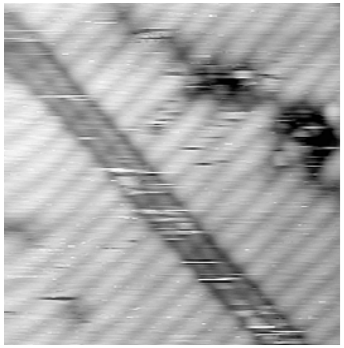

K. Miki
Japan

Wiring on Si with ultra-fine Bi lines

Structure different from 3D Bismuth

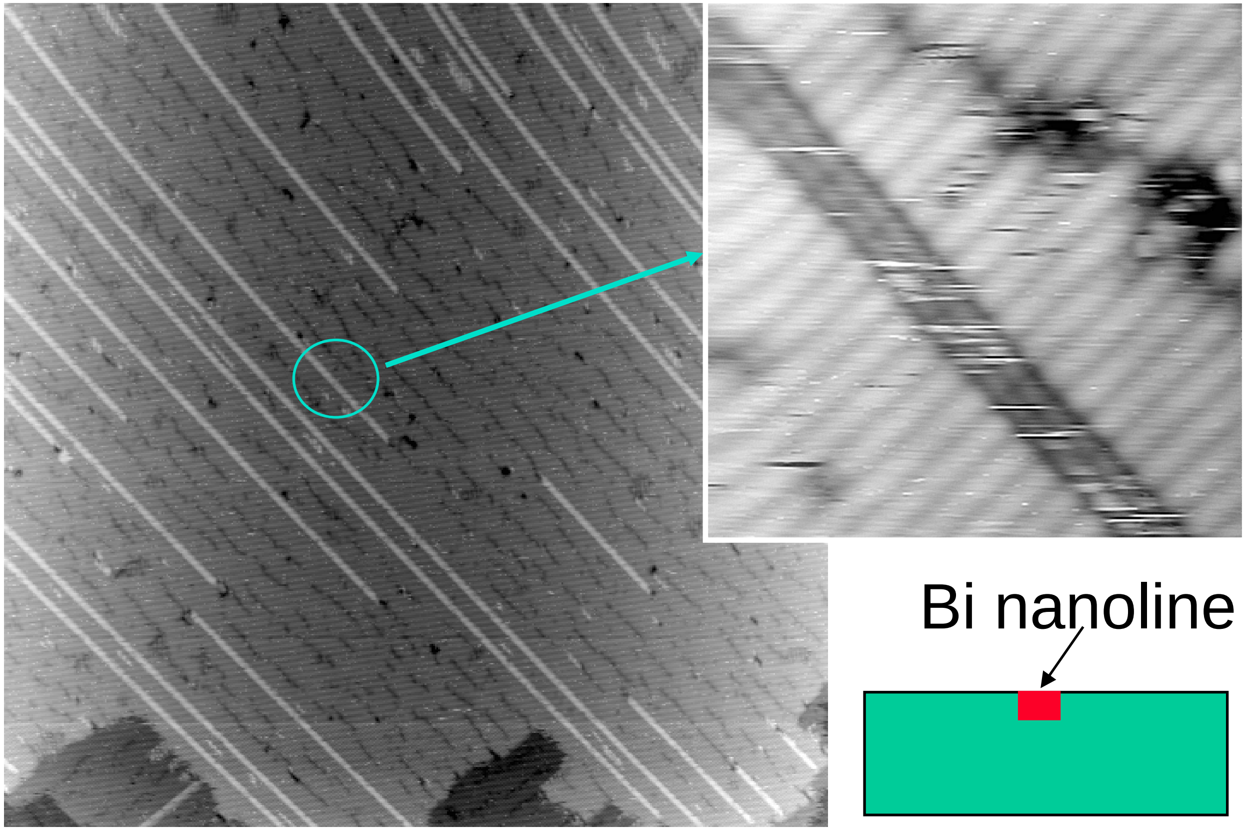

- *Features:*
- over 300 nm long
- 1 nm (3 Si dimers) wide
- without kink
- in terrace (not on top layer)

K. Miki et al. Surf. Sci. 421 (1999) 397

Bi Nanotubes – Unit Cell like 3D bismuth

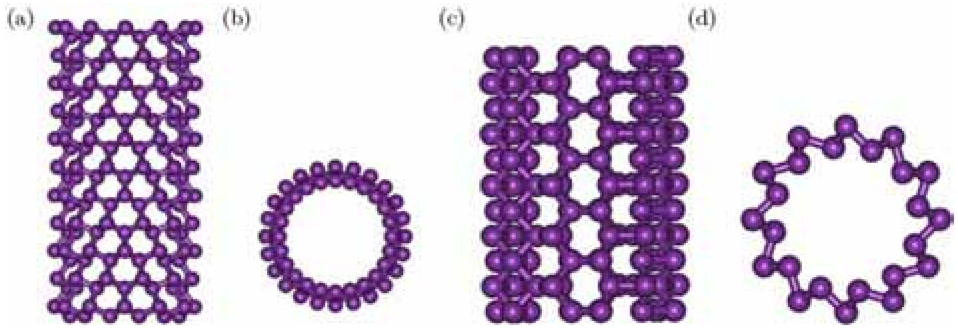

C. Su et al., *Nanotech.* 13 (2002) 746

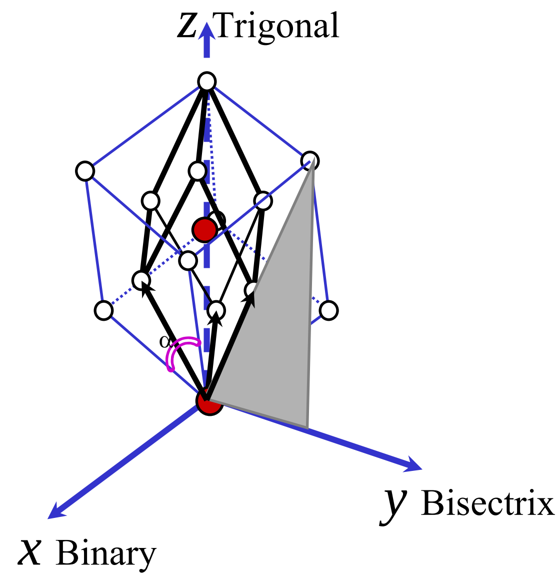

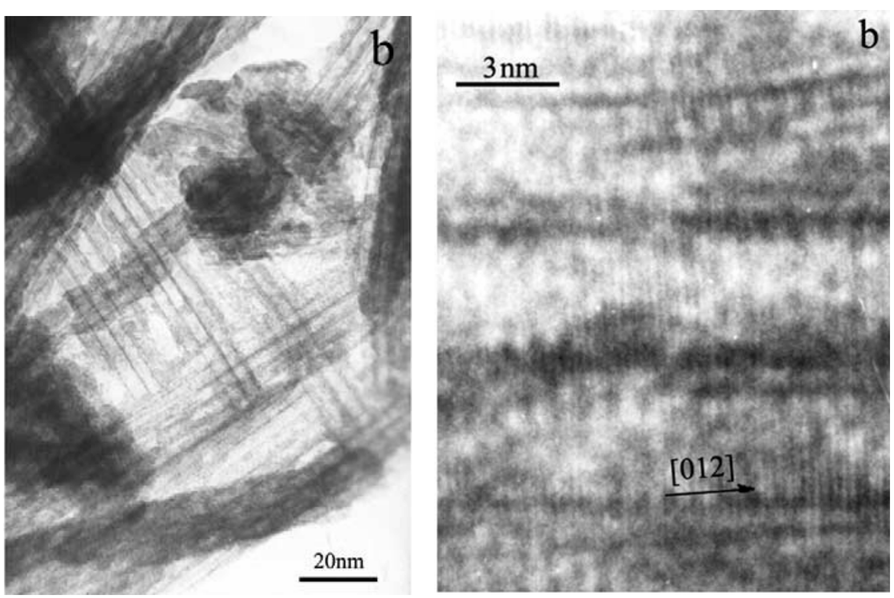

X.-Y. Liu et al., *Chem. Phys. Lett.* 374 (2003) 348

Self-Assembled Nanopores in Alumina for growing nanowires/nanotubes

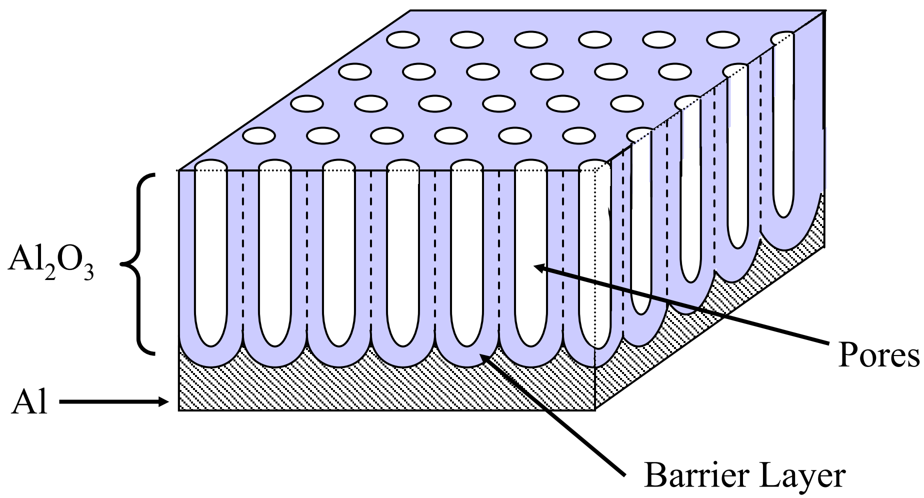

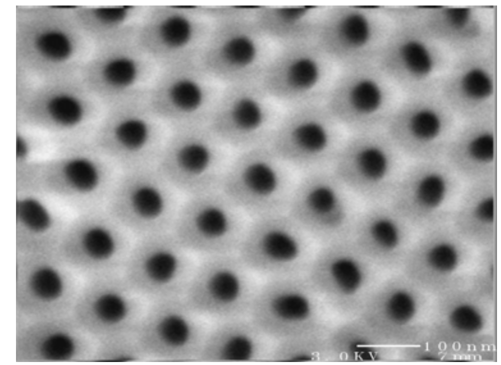

SEM image of the surface of an anodic alumina template with self-assembled nanopore structure

- Applications
  - Templates for ordered arrays of nanowires and nanotubes
  - 2D photonic crystal
  - High density magnetic storage media
  - Filters and gas sensors

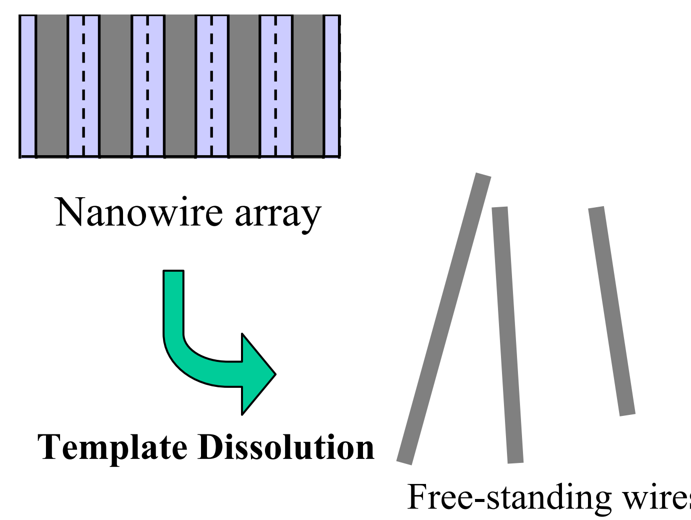

Single Crystal Nanowires

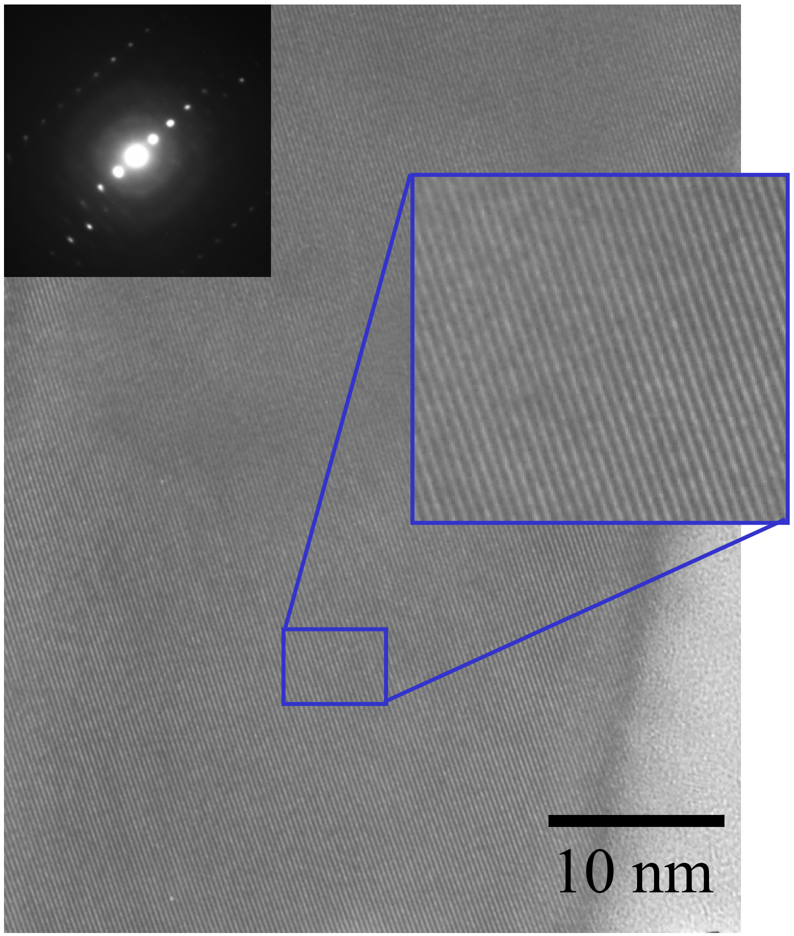

TEM and electron diffraction of a 40-nm nanowire ($Bi_{0.85}Sb_{0.15}$)

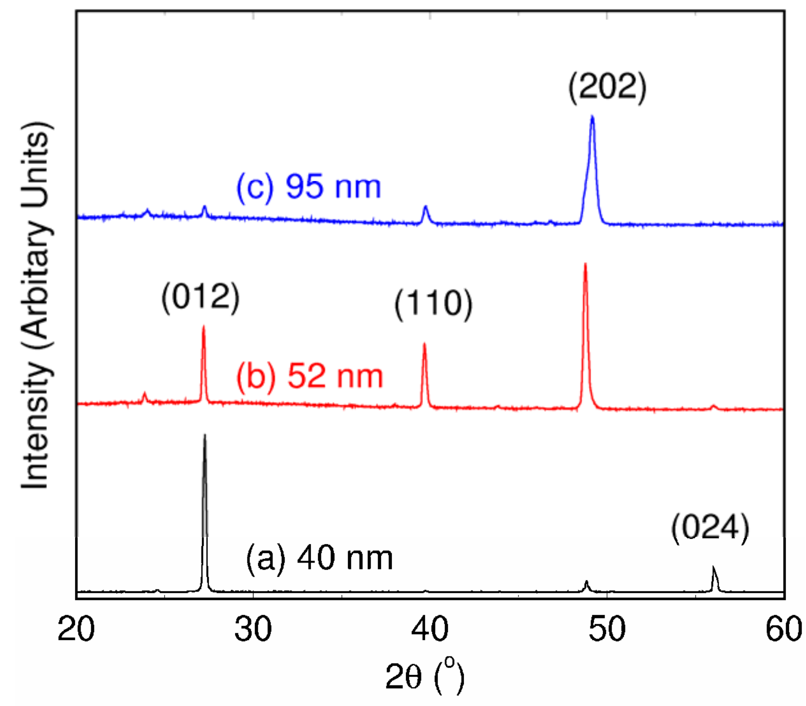

X-ray diffraction of Bi nanowire arrays with different diameters.

Quantum Confinement Produces New Materials Classes

- Bi
  - Group V element
  - Semimetal in bulk form
  - The conduction band (*L*-electron) overlaps with the valence band (*T*-hole) by 38 meV
- Bi nanowire
  - Semimetal-semiconductor transition at a wire diameter about 50 nm due to quantum confinement effects

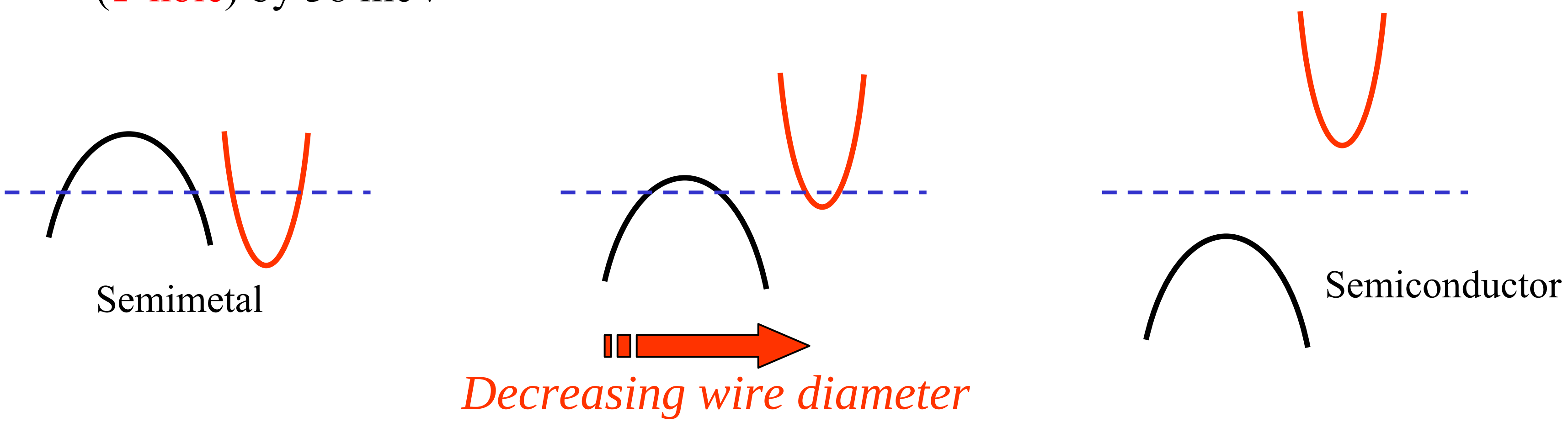

Semimetal-Semiconductor Transition

Semimetal-Semiconductor Transition in $Bi_{1-x}Sb_x$ (SM-SC)

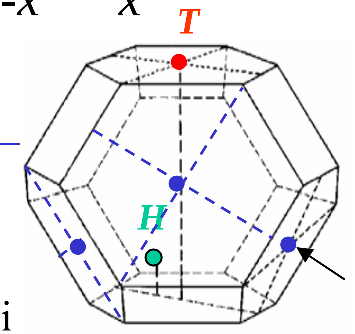

- Bi
  - Group V element
  - Semimetal in bulk form
  - The conduction band (*L*-electron) overlaps with the valence band (*T*-hole) by ~ 38 meV (77 K)

- Sb alloying
  - Group V element
  - Complete solubility with Bi
  - Moves down the *T*-point valence band edge in energy relative to the *L*-point carriers

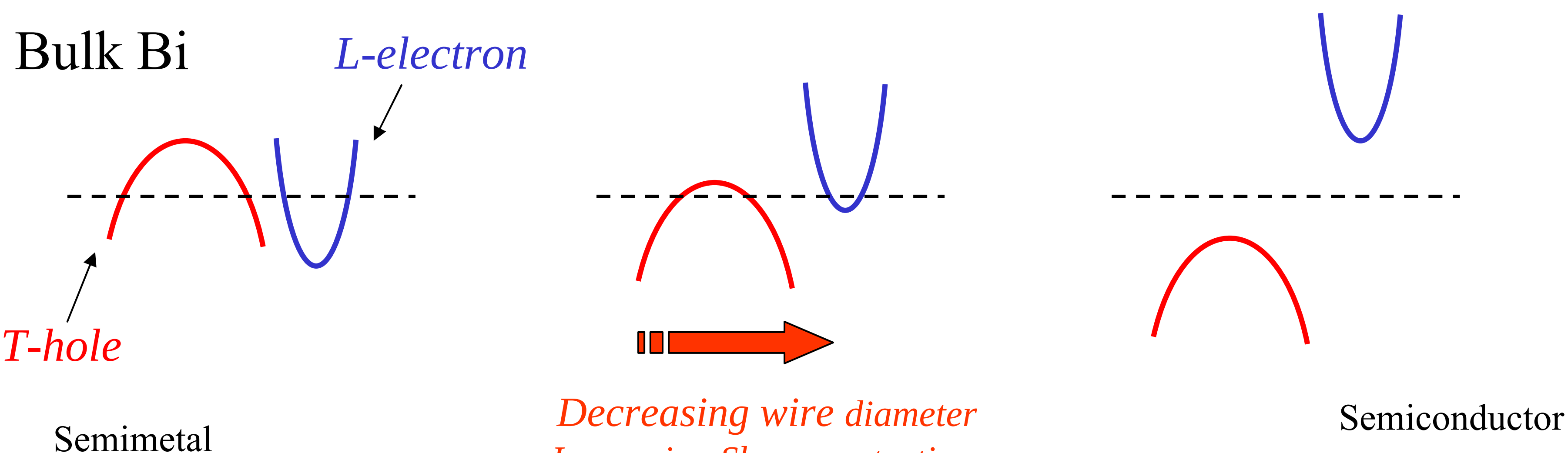

Lin *et al*., Phys. Rev. B **62**, 4610 (2001)
Rabin *et al*., Appl. Phys. Lett. 79, 81 (2001)

Electronic Phases of 3D & 1D $Bi_{1-x}Sb_x$

Electronic phases of bulk $Bi_{1-x}Sb_x$ alloy

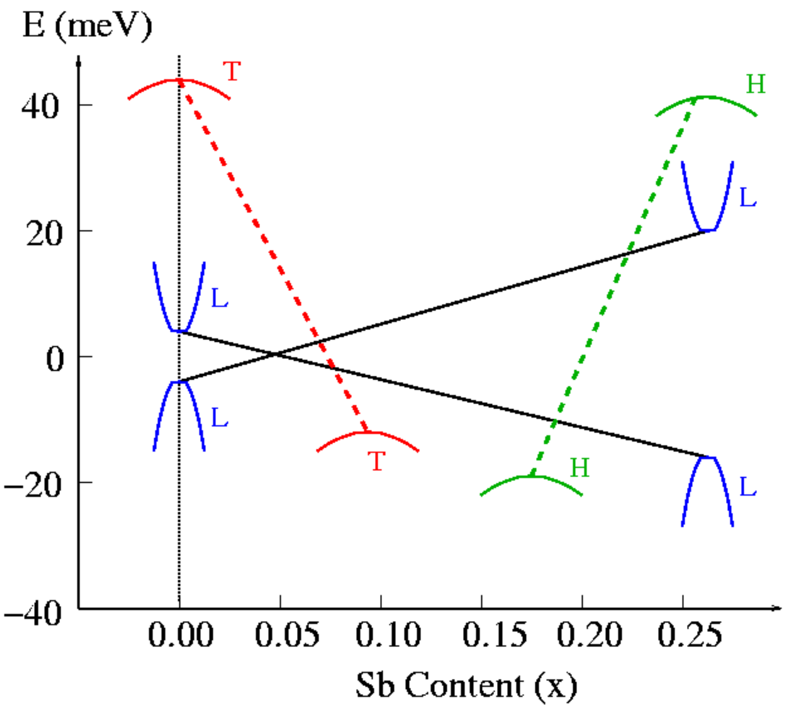

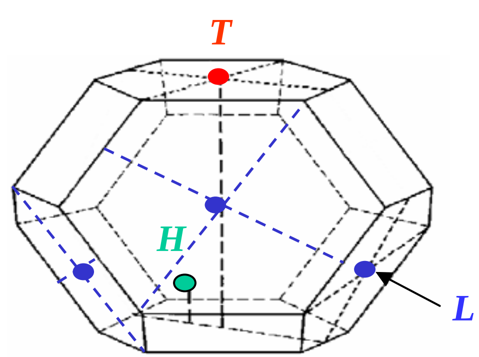

Phase diagram of $Bi_{1-x}Sb_x$ nanowires

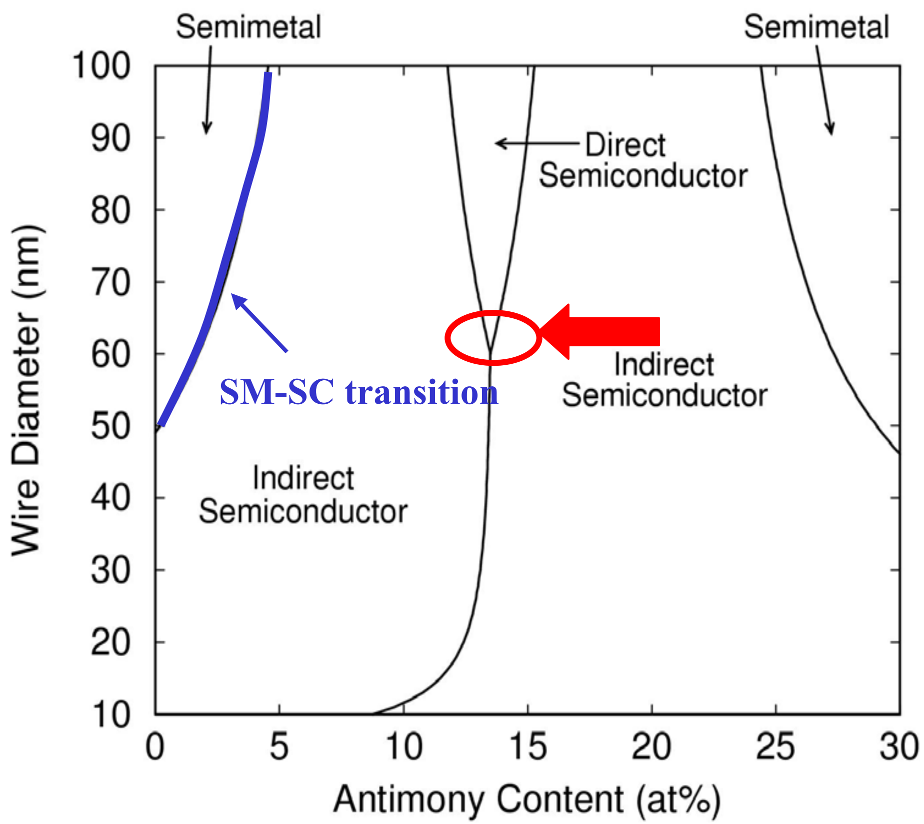

Rabin *et al.*, Appl. Phys. Lett. 79, 81 (2001)

Superlattice Nanowires for Thermoelectric Applications

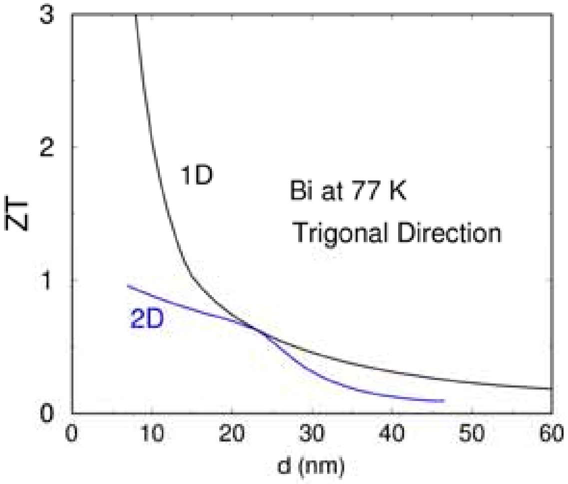

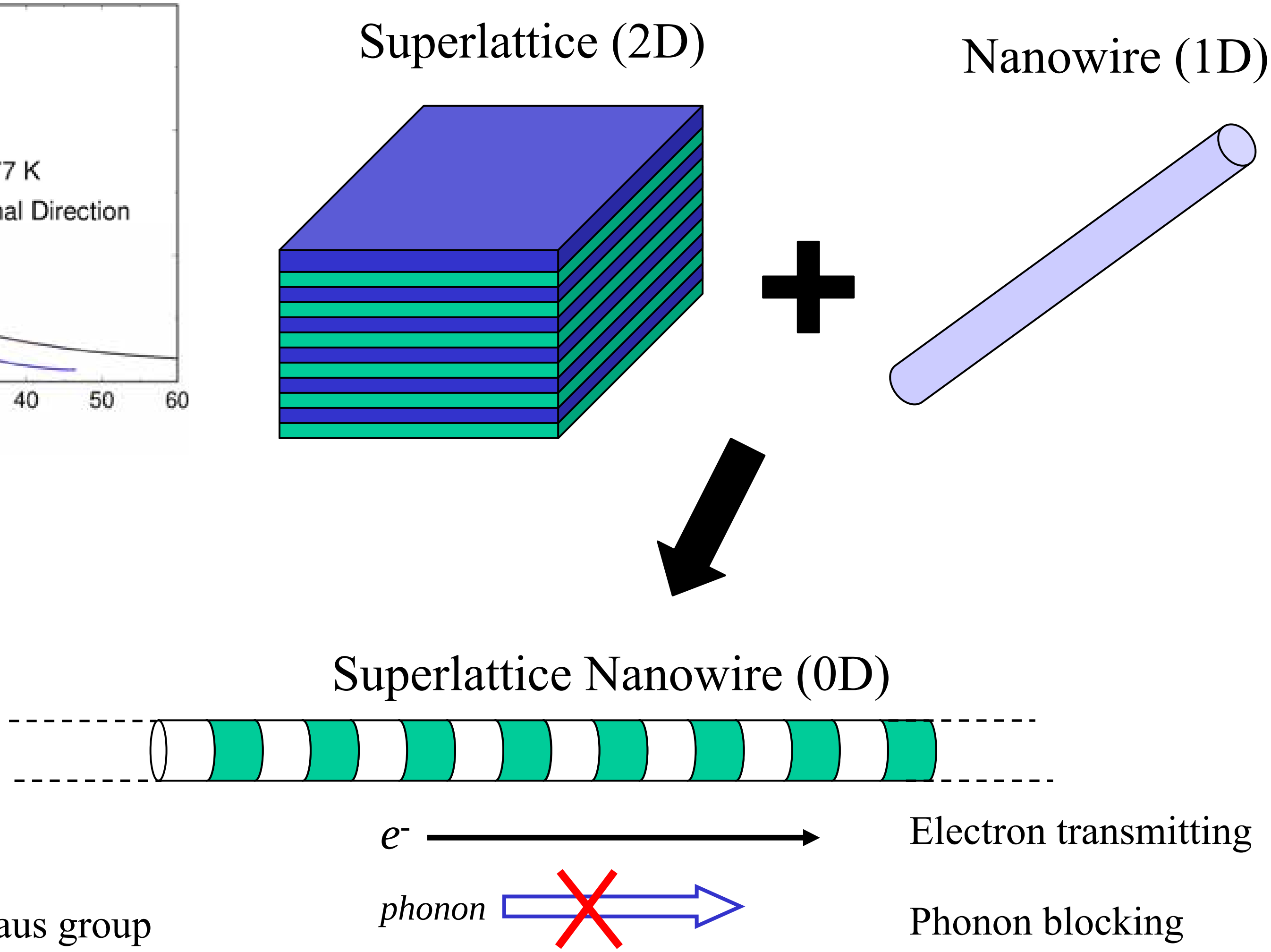

Y. M. Lin in Dresselhaus group

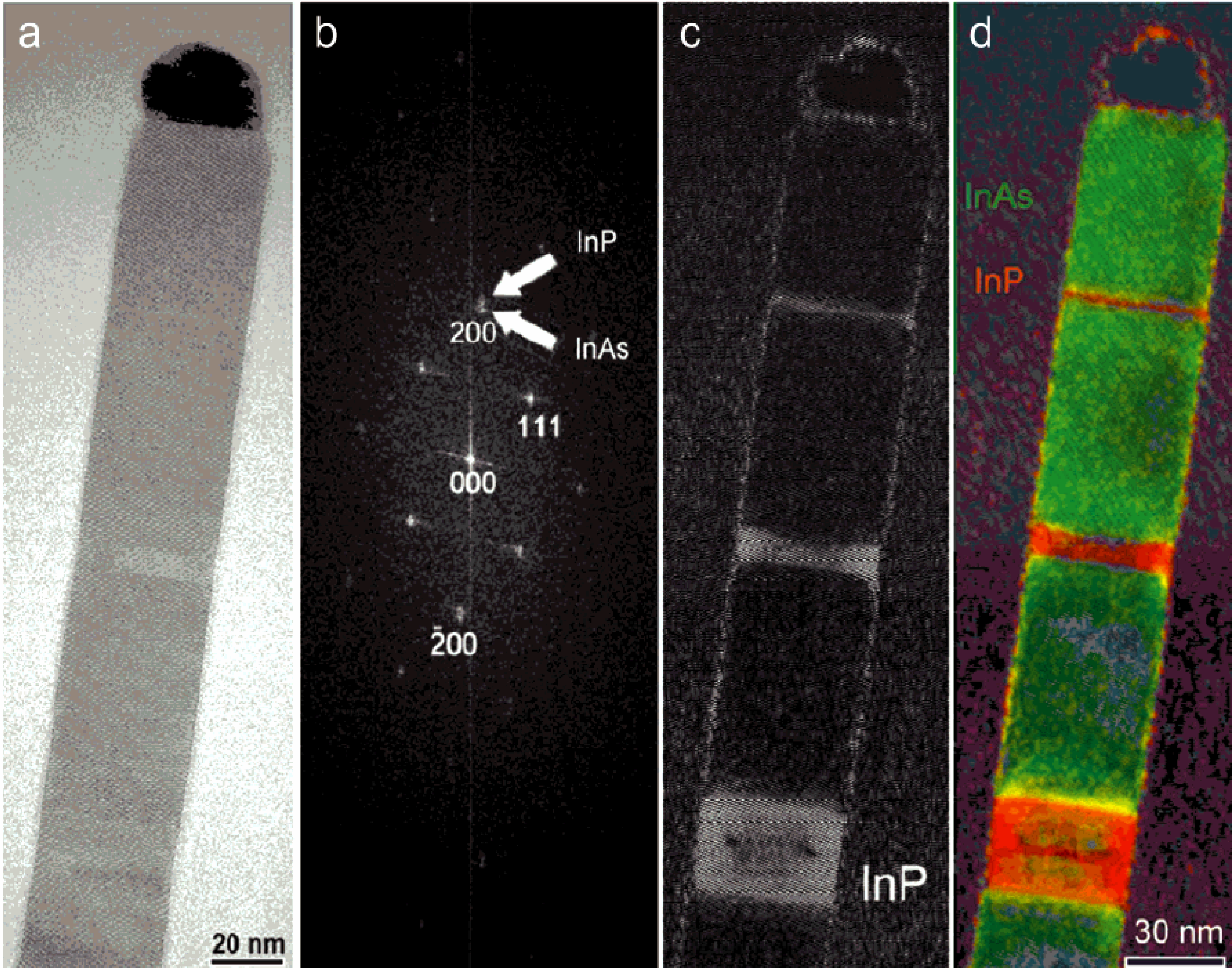

Samuelson *et al.*, *Nano Lett.* **2** (2002) 87

Growth of Semiconductor Nanowires by VLS method

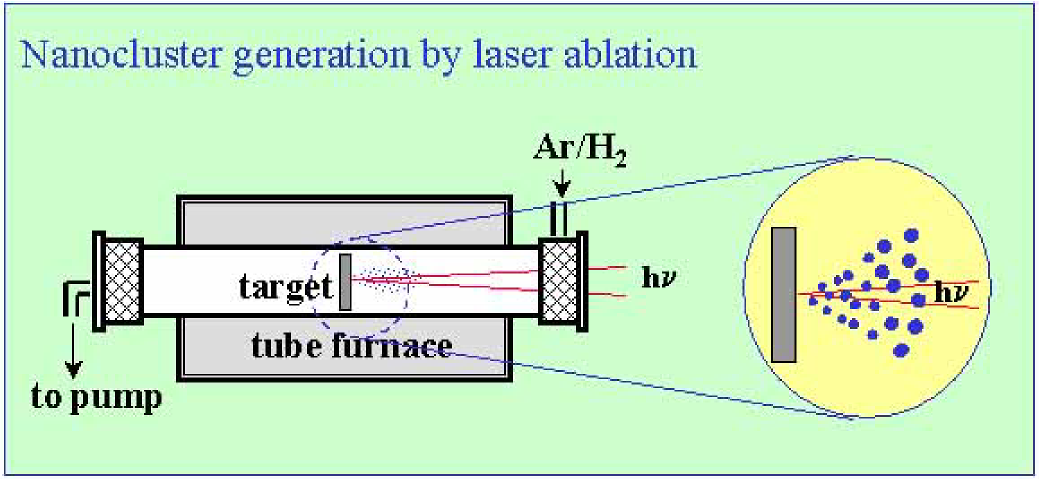

Laser ablation overcomes thermodynamic equilibrium constraints, and enables liquid nanocluster formation.

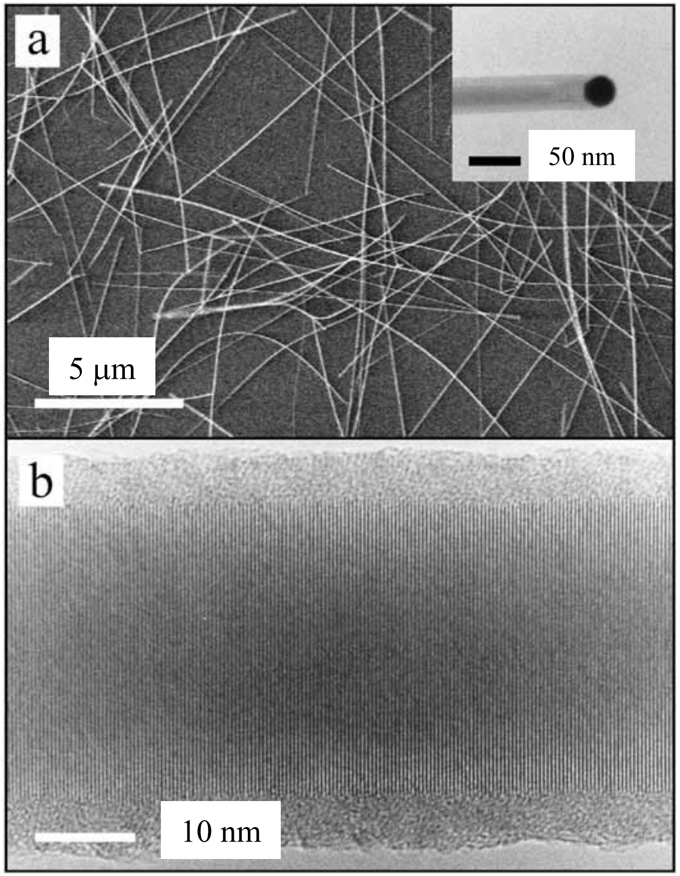

a) FESEM image of GaP nanowires. The inset is a TEM image of the end of one of these wires.
b) TEM image of a GaP wire. The [111] lattice planes are resolved, showing that wire growth occurs along this axis.

Lieber et al., JACS 122 (2000) 8801

ZnO Nanowires on Sapphire by VLS method

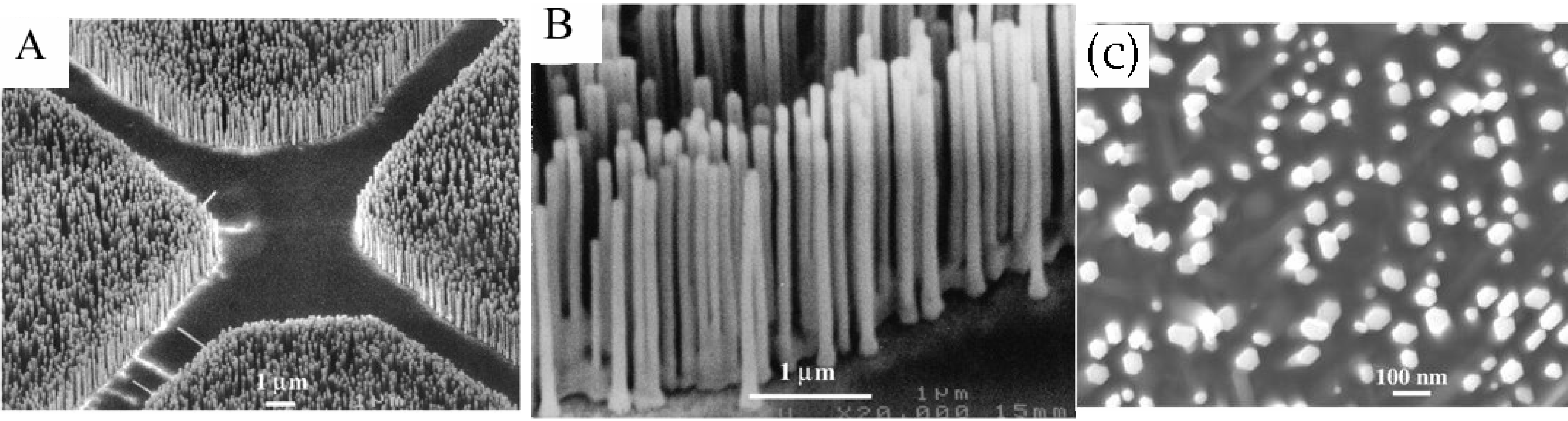

*SEM images of ZnO nanowire arrays grown on a sapphire substrate, where (a) shows patterned growth, (b) shows a higher resolution image of the parallel alignment of the nanowires, and (c) shows the faceted side-walls and the hexagonal cross-section of the nanowires. For nanowire growth, the sapphire substrates were coated with a 1.0 to 3.5nm thick patterned layer of Au as the catalyst, using a TEM grid as the shadow mask. These nanowires have been used for nanowire laser applications (Huang et al., 2001a).
*Patterned growth can be arranged.
*Proper selection of nanowires and substrate materials can lead to facets, useful for nanowire lasers.

P. Yang et al., Science 292 (2001) 1897

Nano-Lasers using ZnO Nanowires

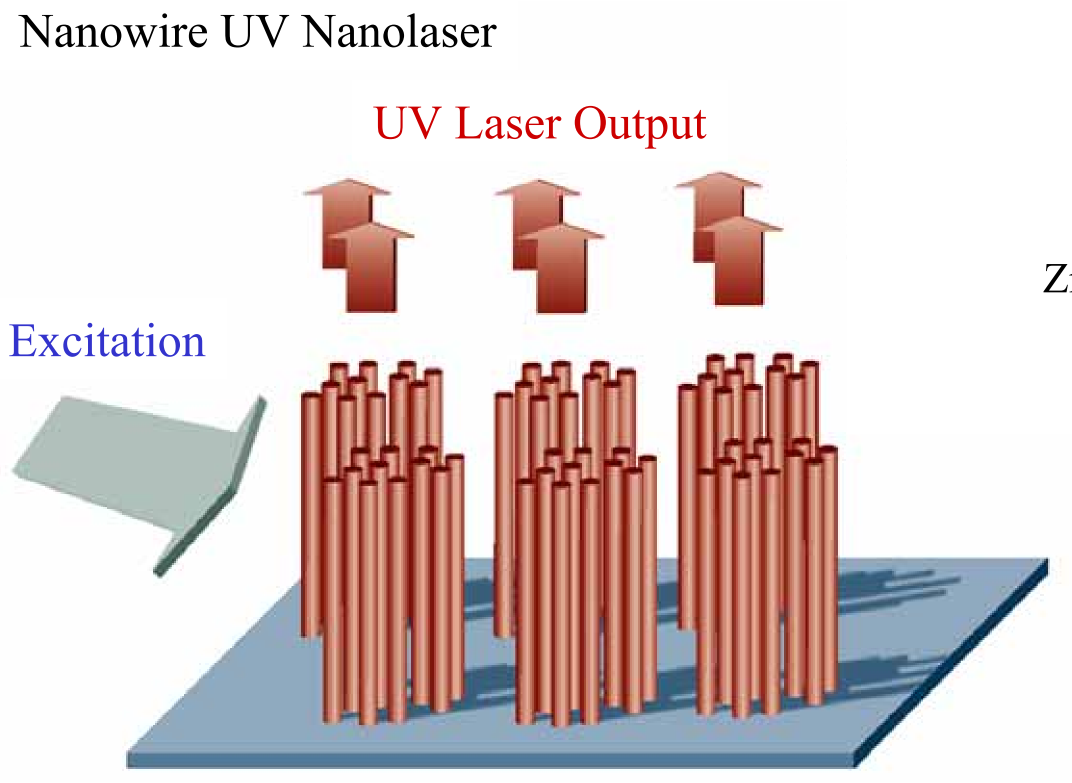

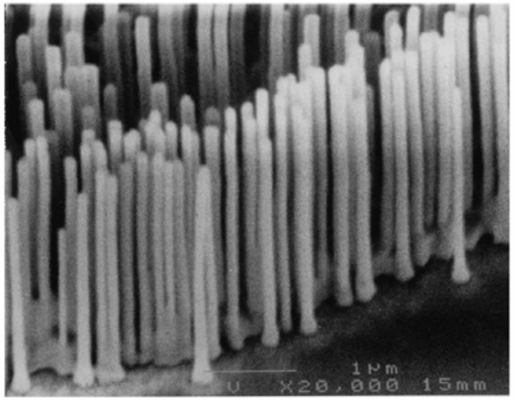

ZnO nanowires grown by VLS method.

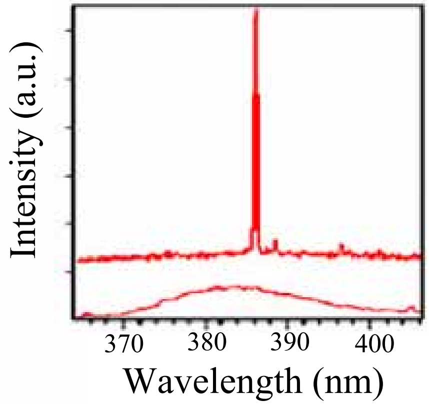

Emission spectrum from ZnO nanowires.

P. Yang et al., Science 292 (2001) 1897

Tunable Bandgap in Nanowires

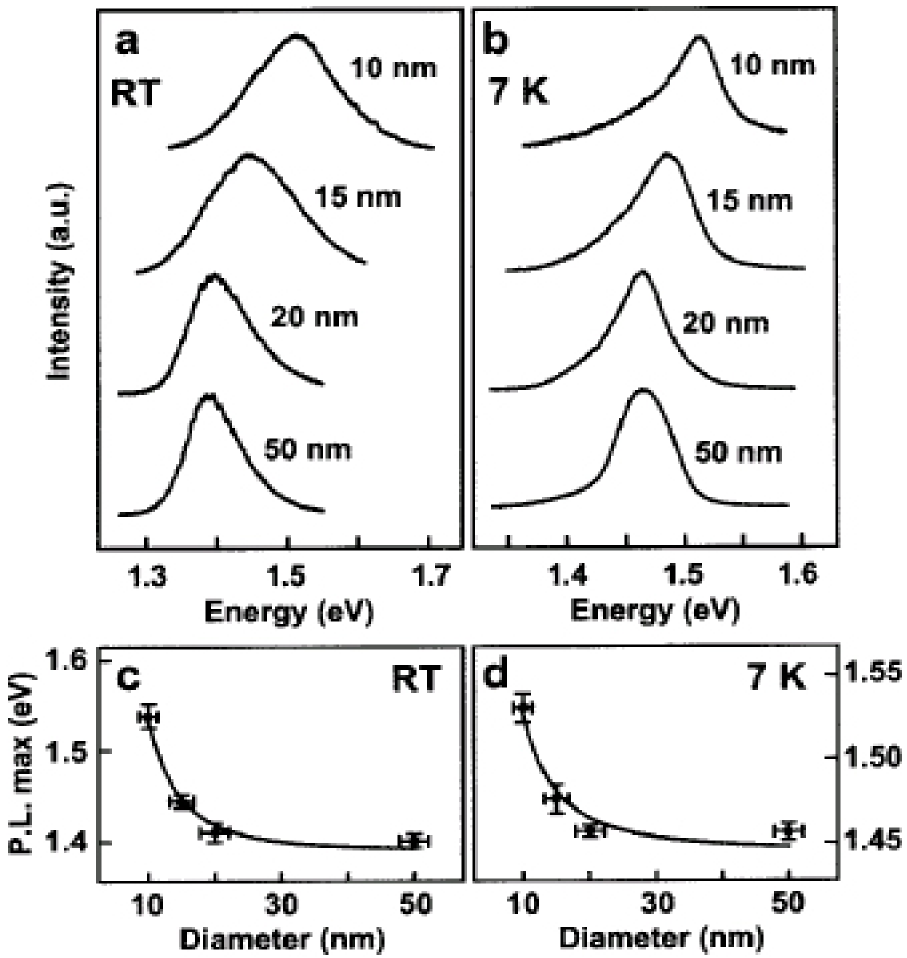

InP nanowire

diameter ↓

energy ↑

M. S. Gudiksen et al., J. Phys. Chem B 106, 4036 (2002)

Quantum Confinement in Si Nanowires

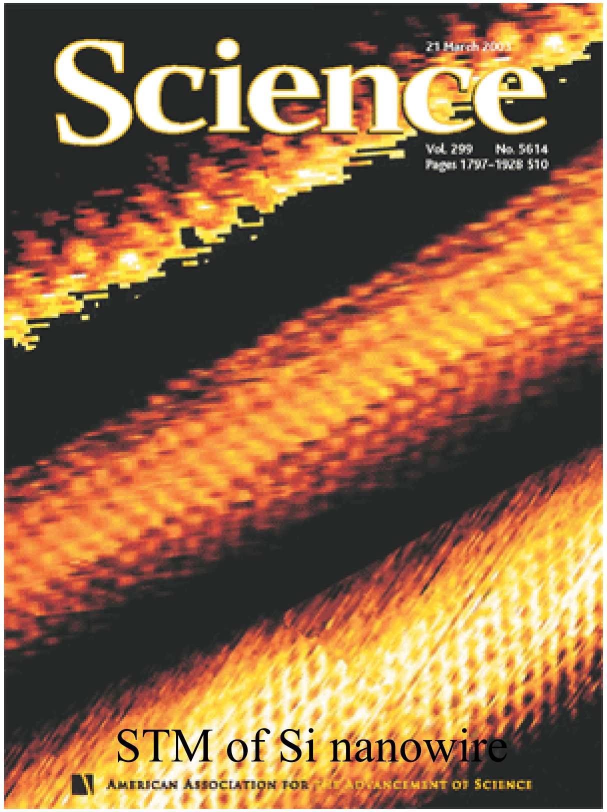

Ma et al., Science 299, 1874 (2003)

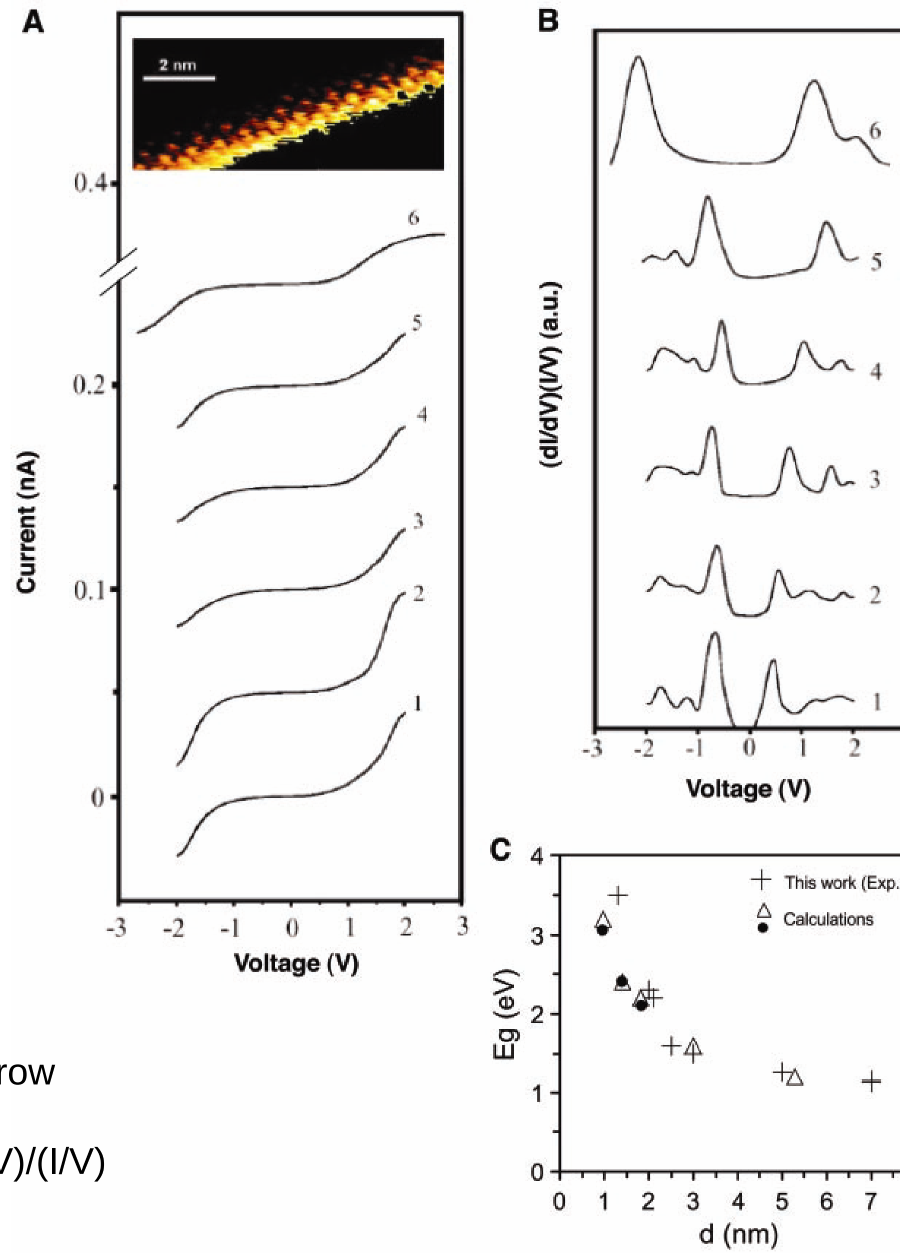

- STM studies show that Si nanowires grow along (110) and ($11\bar{2}$) directions.
- STS studies give I-V curves, and (dI/dV)/(I/V) gives DOS and E_g vs tube diameter.

Luminescence from Nanowire Junctions

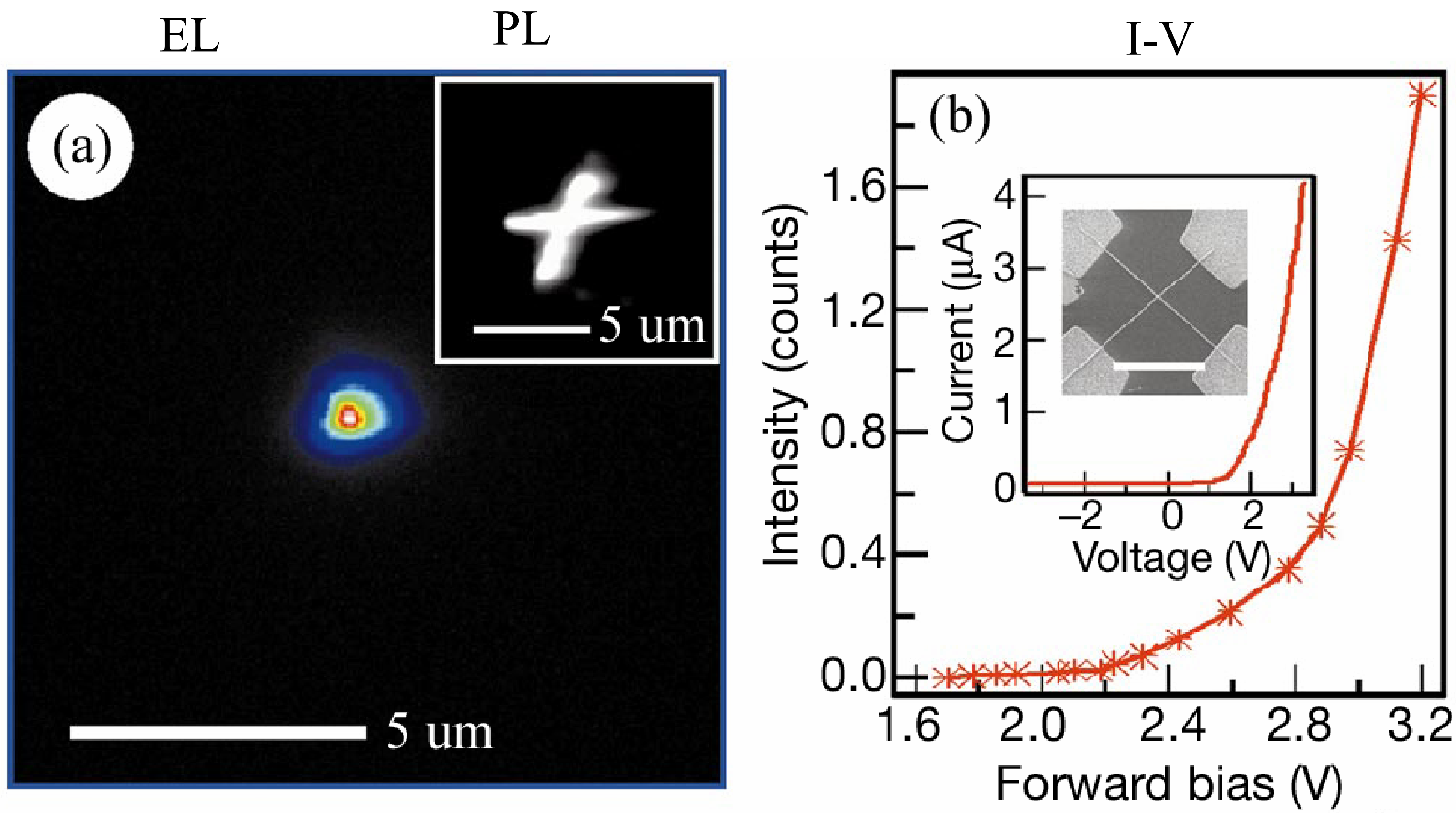

Optoelectrical characterization of a crossed nanowire junction formed between 65-nm n-type and 68-nm p-type InP nanowires. (a) Electroluminescence (EL) image of the light emitted from a forward-biased nanowire p-n junction at 2.5 V. Inset, photoluminescence (PL) image of the junction. (b) EL intensity as a function of operation voltage. Inset, the SEM image and the I-V characteristics of the junction (Duan et al., 2001). The scale bar in the inset is 5 microns.

Lieber et al., Nature 409 (2001) 66

Unique Properties of Carbon Nanotubes

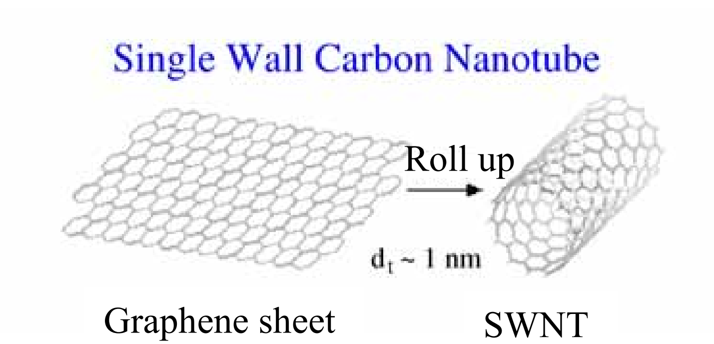

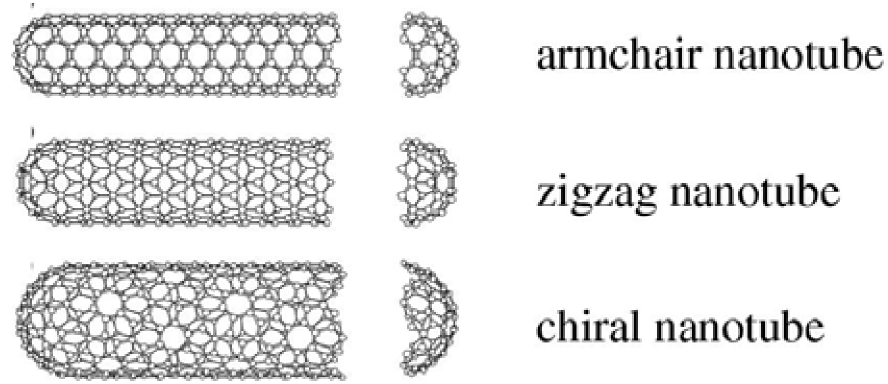

- Size: Nanostructures with dimensions of ~1 nm diameter (~20 atoms around the cylinder)
- Electronic Properties: Can be either metallic or semiconducting depending on the tube diameter or orientation of the hexagons
- Mechanical: Very high strength and modulus. Good properties on compression and extension
- Heat pipe and electromagnetic pipe
- Single nanotube spectroscopy yields structure
- Many applications are being attempted worldwide

Applications for Nanotubes

Scanning tips and Electronics

- STM/AFM tips
- Semiconductor devices
- Field Emitters
- New Materials
- Many other proposals

Field Emitter

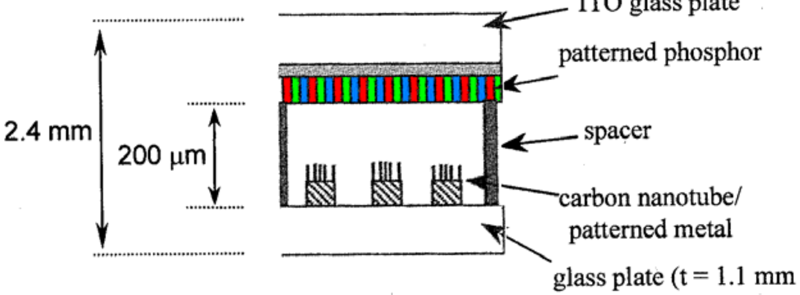

Transistor

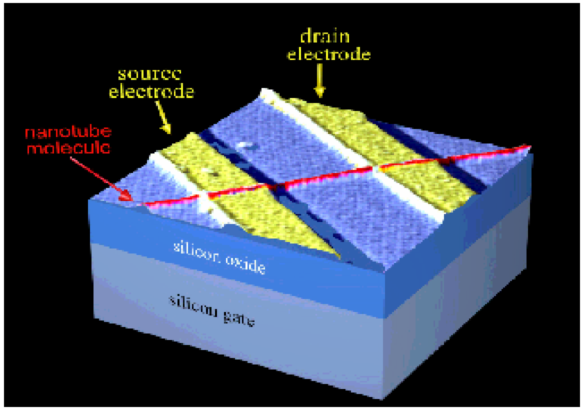

S.J. Tans *et al. Nature*, 393, 49 (1998)

New Materials

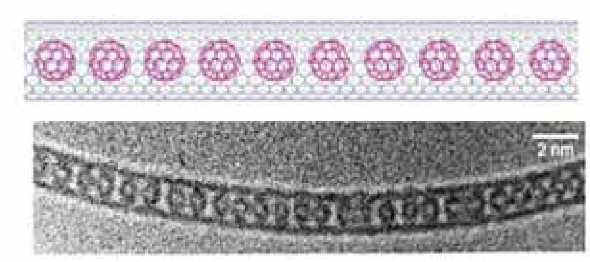

Fullerene C_{60} inside nanotubes

Imaging biological molecules

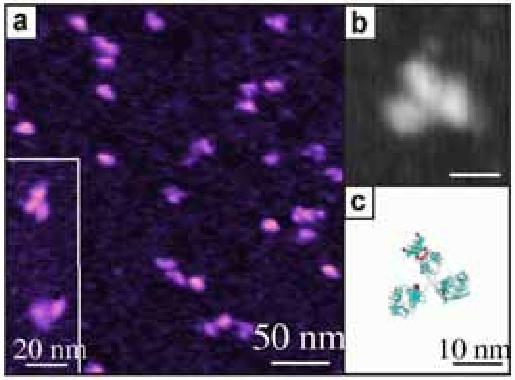

AFM image of Immunoglobulin G resolved by nanotube tips

Rolling up graphene layer $\Rightarrow$ Nanotube

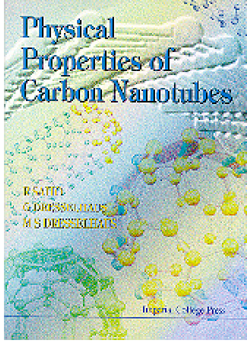

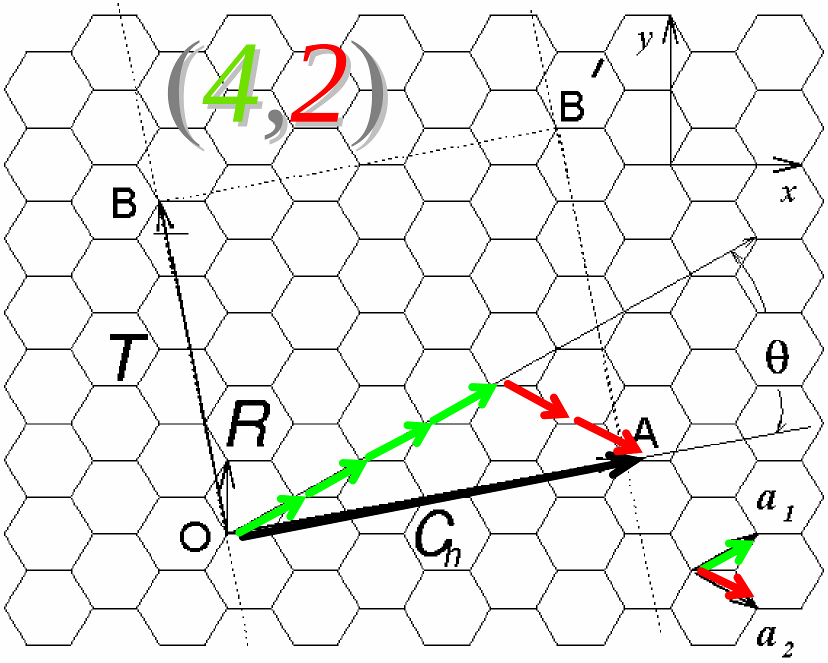

armchair $\theta = 30°$

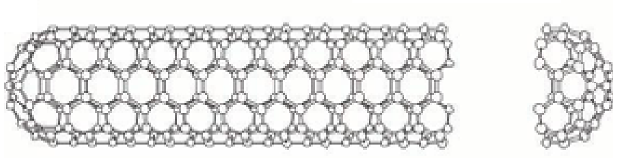

zigzag $\theta = 0°$

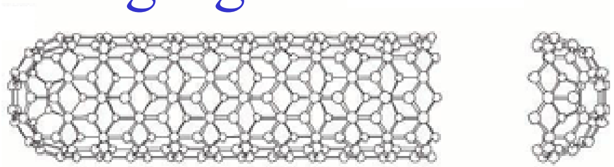

chiral $0 < \theta < 30°$

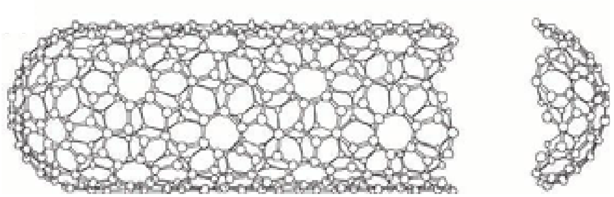

$$\mathbf{C}_h = n\mathbf{a}_1 + m\mathbf{a}_2$$

$$d_t = \frac{C_h}{\pi} = \frac{a}{\pi}\sqrt{n^2 + nm + m^2}$$

$$\tan\theta = \frac{\sqrt{3}m}{2n + m}$$

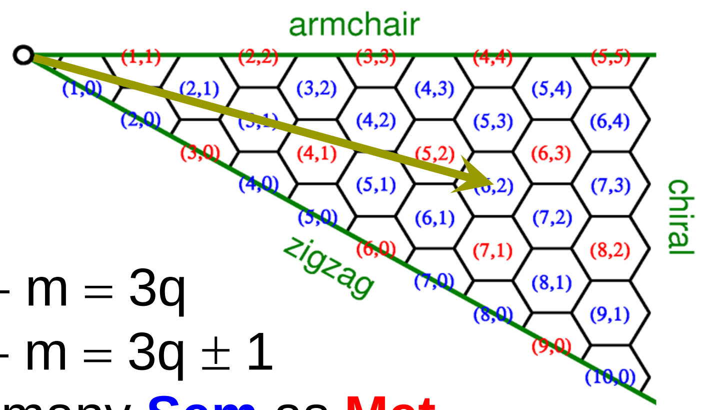

Met : n – m = 3q

Sem: n – m = 3q ± 1

twice as many **Sem** as **Met**

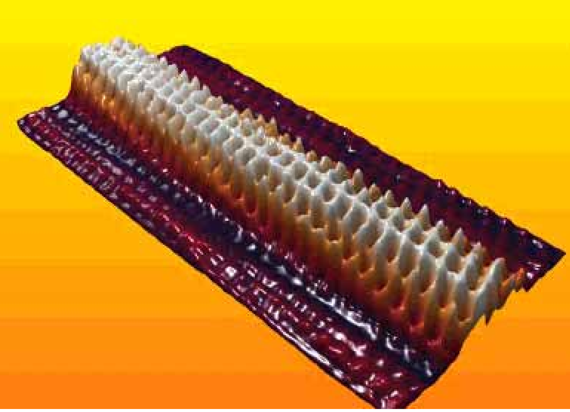

STM/STS *Experiments*

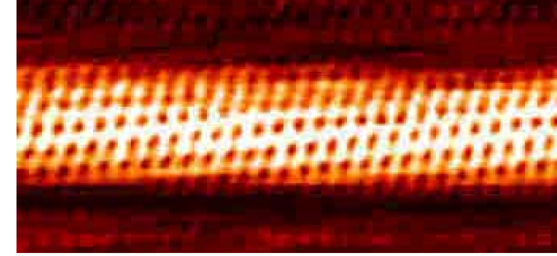

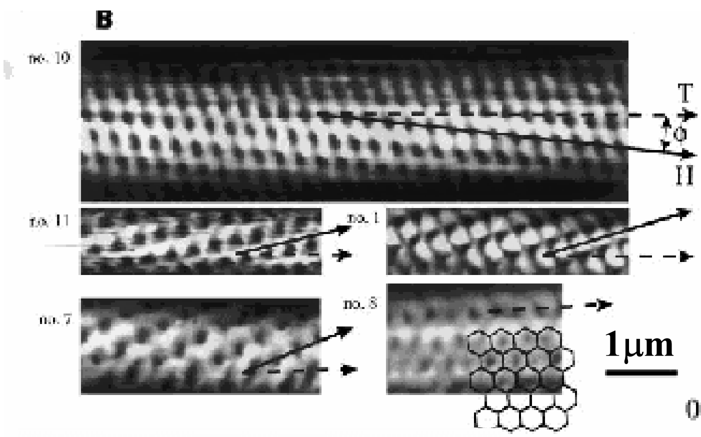

P. Kim et al., Phys. Rev. Lett. 82, 1225 (1999)

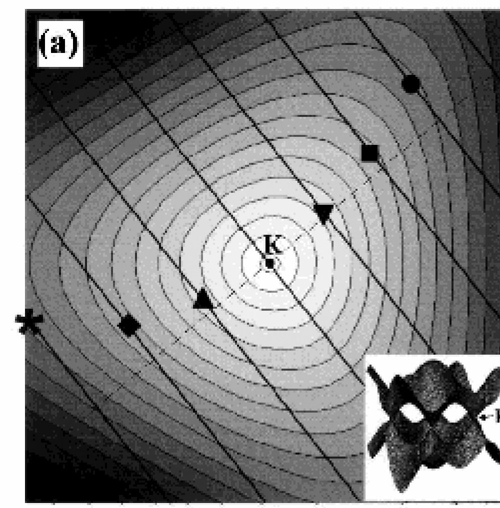

cutting lines (13,7)

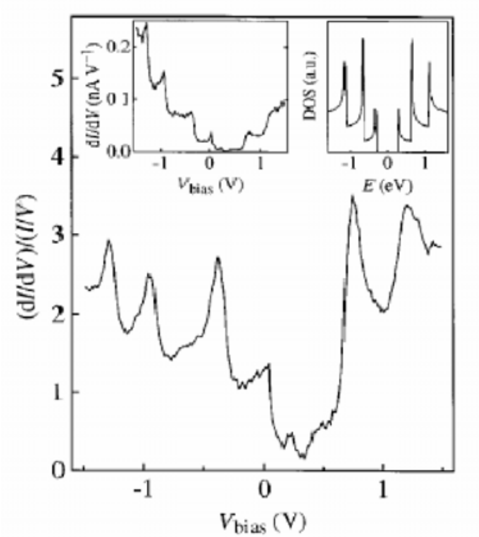

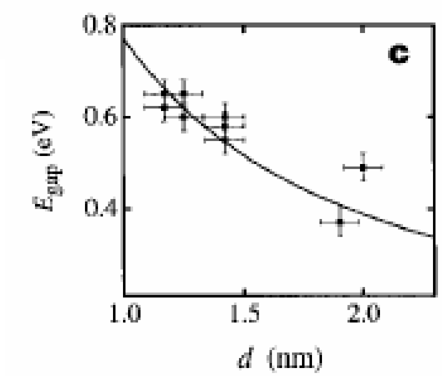

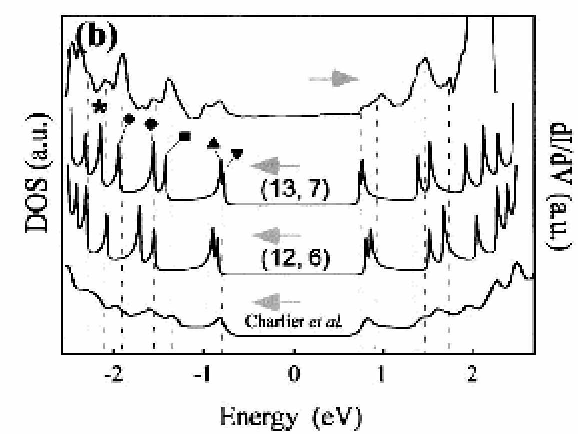

J. W. G. Wildoer et al., Nature 391, 59 (1998)

Phonons in single wall carbon nanotubes

Graphite Brillouin Zone

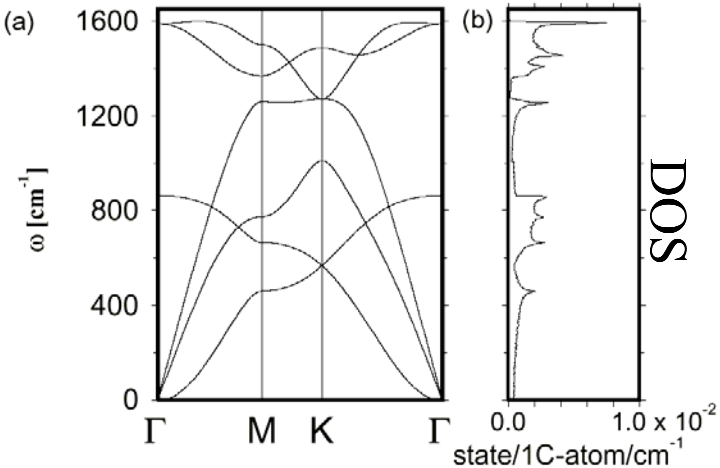

(Figs. From Prof. R. Saito)

(10,10) Brillouin Zone

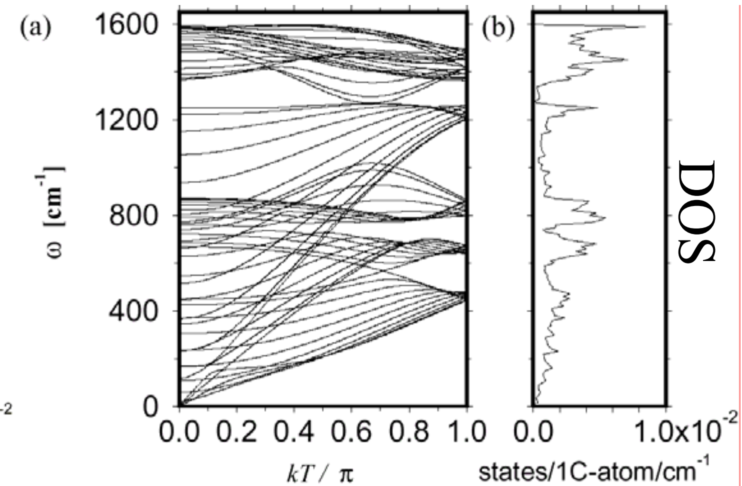

Zone folding of graphene sheet

Main Features

Radial Breathing Mode (RBM)

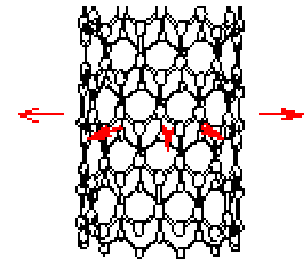

Raman Spectra of SWNTs:

Raman active modes:

- Chiral 15
- Zigzag 15
- Armchair
  - Even n 16
  - Odd n 15

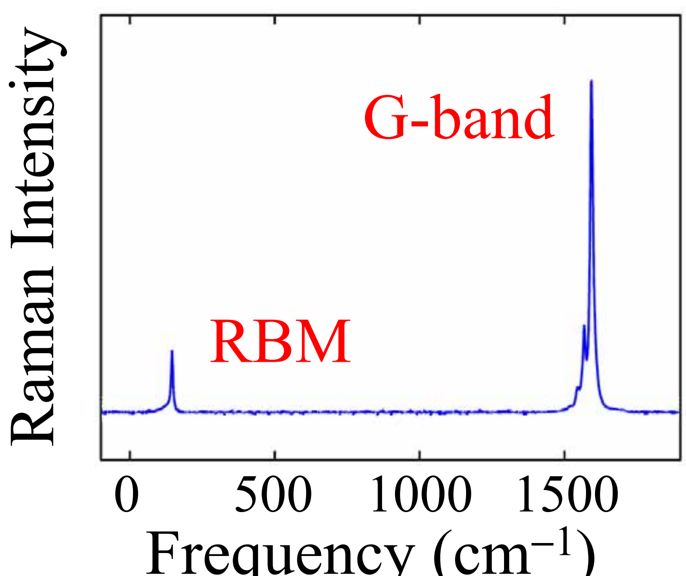

Tangential Modes (G-band)

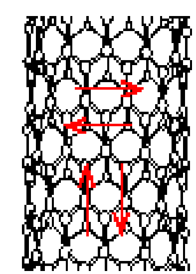

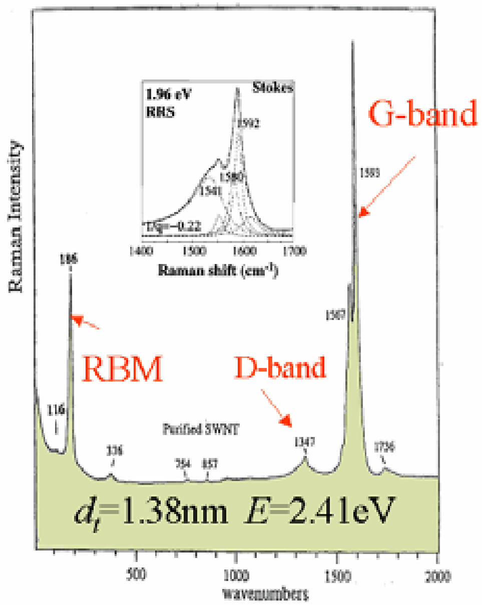

Raman Spectroscopy of Carbon Nanotubes

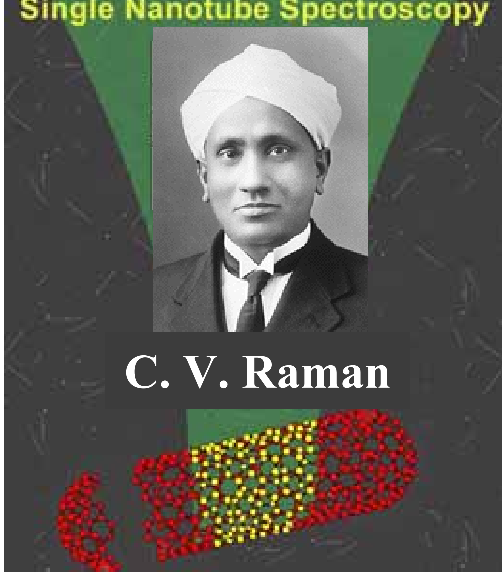

M. S. Dresselhaus and P. C. Eklund, Advances in Physics 49 705 (2000)

- Non-destructive, contactless measurement
  - Room Temperature
  - In Air at Ambient Pressure
  - Quick (1min), Accurate in Energy
- Diameter Selective (Resonant Raman Effect)
- Diameter and Chirality dependent phonons
  - Characterization of *(n,m)*
  - Related to Low Dimensional Physics

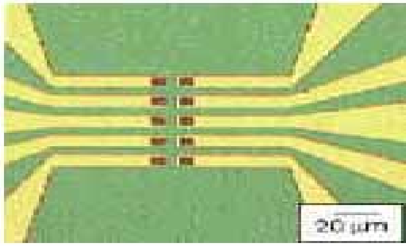

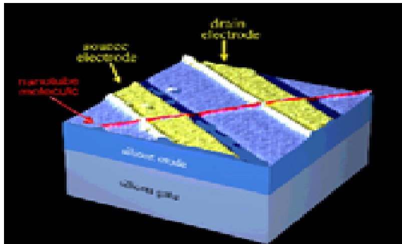

Resonant Raman Spectroscopy

A. M. Rao *et al.*, *Science* **275**, 187 (1997)

- Enhanced Signal
  - ✓ Optical Absorption
  - ✓ e-DOS peaks

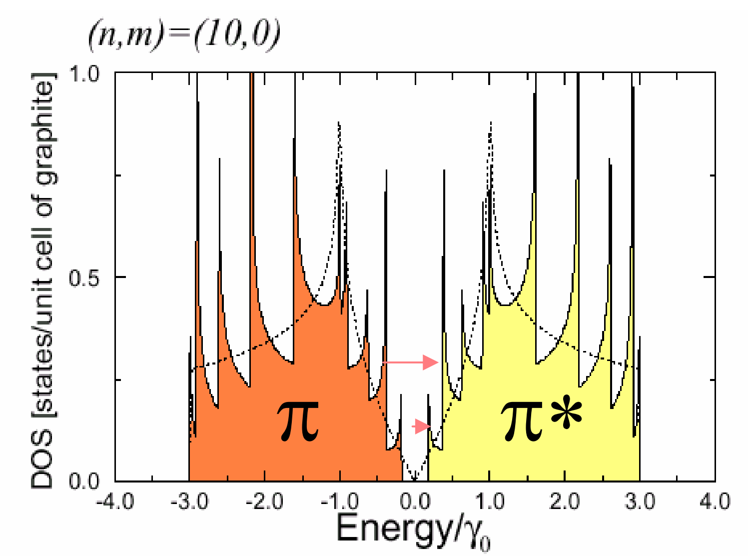

diameter-selective resonance process

$$\omega_{RBM} = \alpha / d_t$$

Raman spectra from nanotube bundles

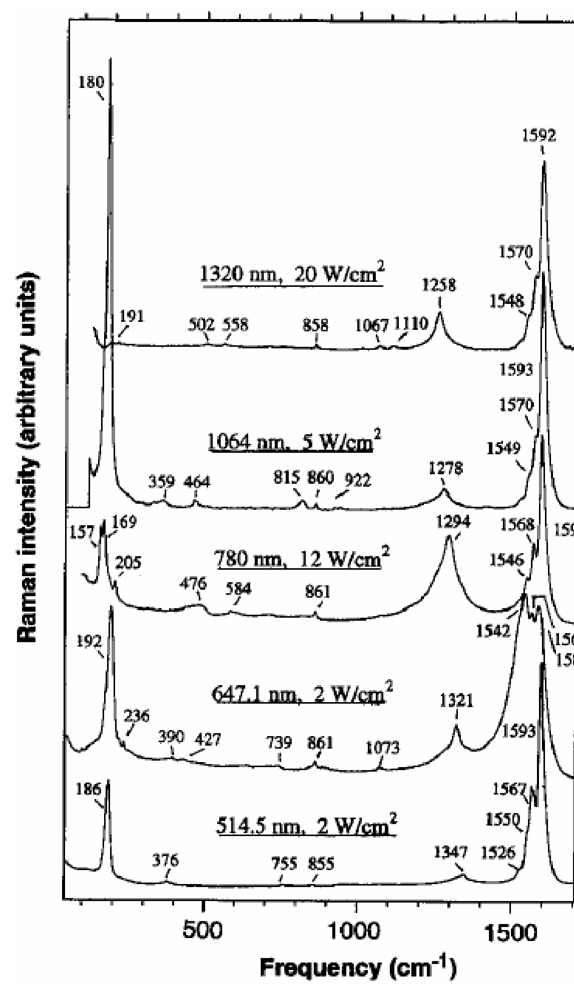

$E = 0.94\text{eV}$

$= 1.17\text{eV}$

$= 1.58\text{eV}$

$= 1.92\text{eV}$

$= 2.41\text{eV}$

Resonant Raman Spectra of Carbon Nanotube Bundles

M. A. Pimenta *et al.*, *Phys. Rev.* B **58**, R16016 (1998)

G-band resonant Raman spectra

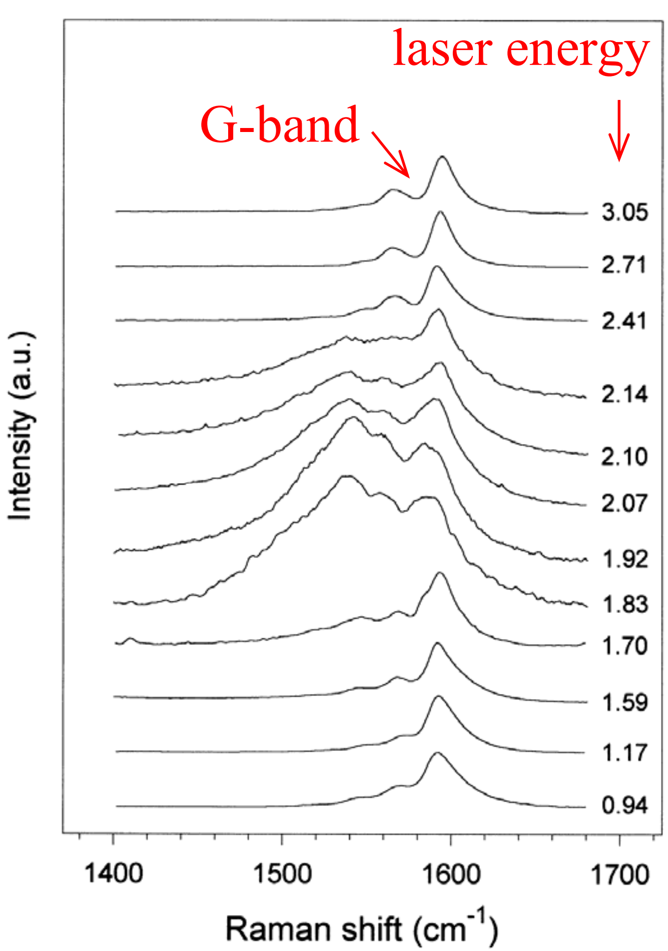

$d_t = 1.37 \pm 0.18$ nm

Diameter dependence of the Van-Hove singularities

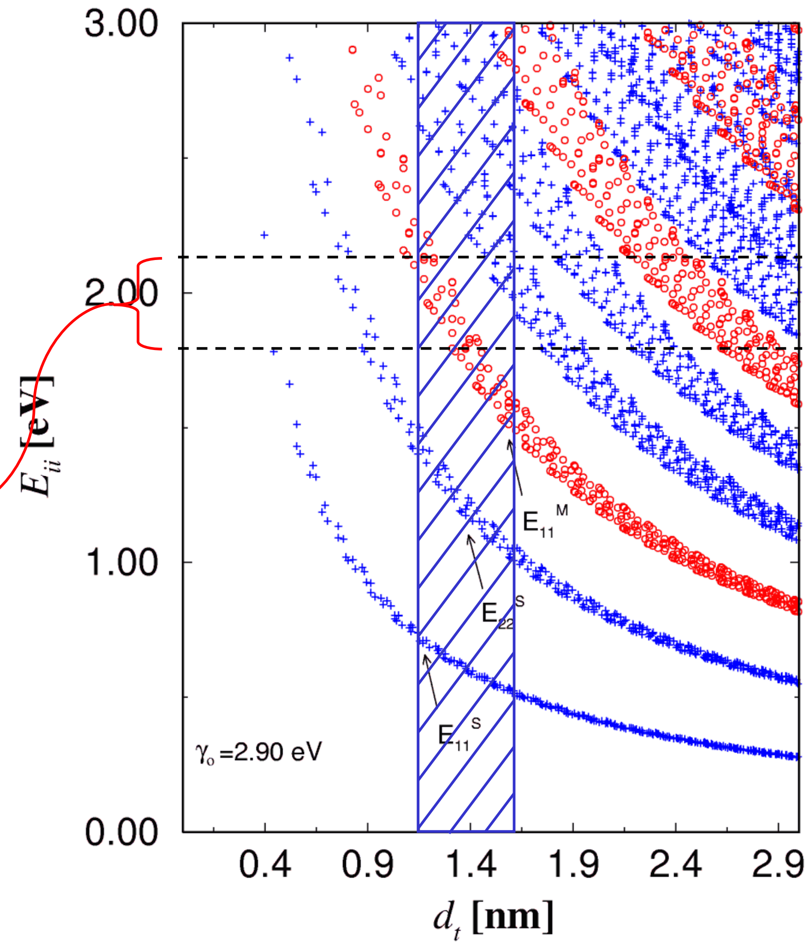

Single Nanotube Spectroscopy yields E_{ii}

Resonant Raman spectra for isolated single-wall carbon nanotubes grown on Si/SiO_2 substrate by the CVD method

A. Jorio et al., Phys. Rev. Lett. 86, 1118 (2001)

RBM

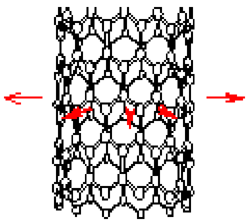

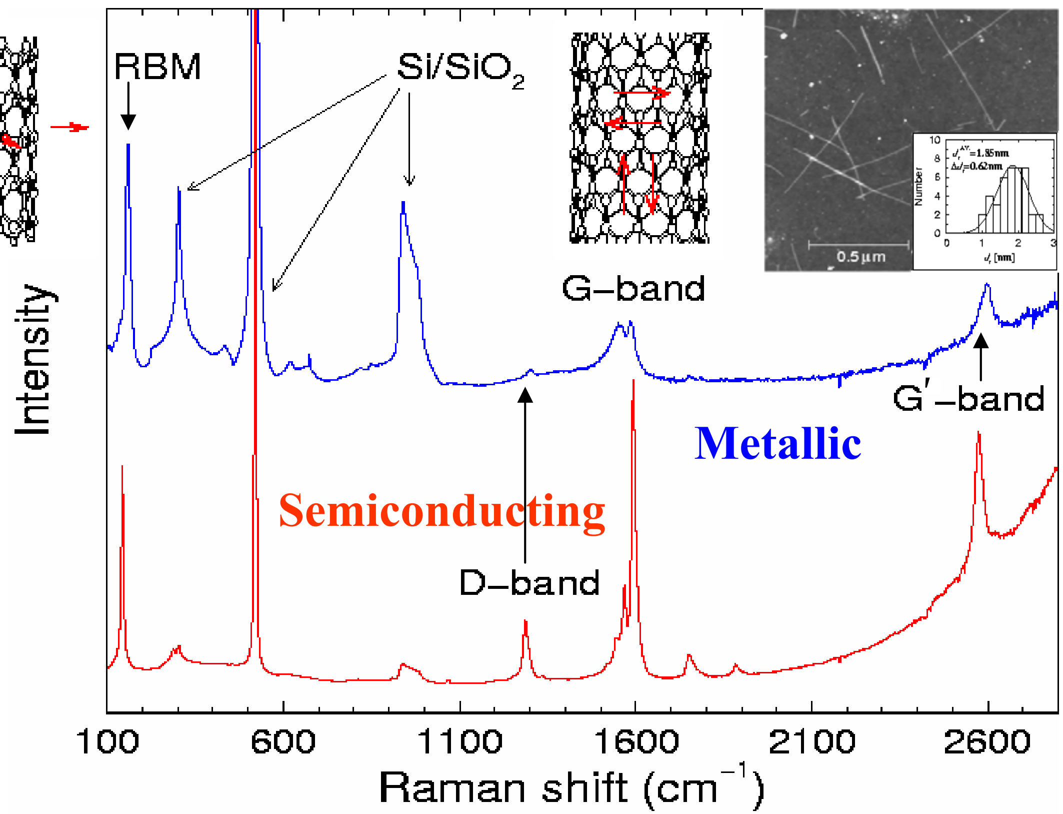

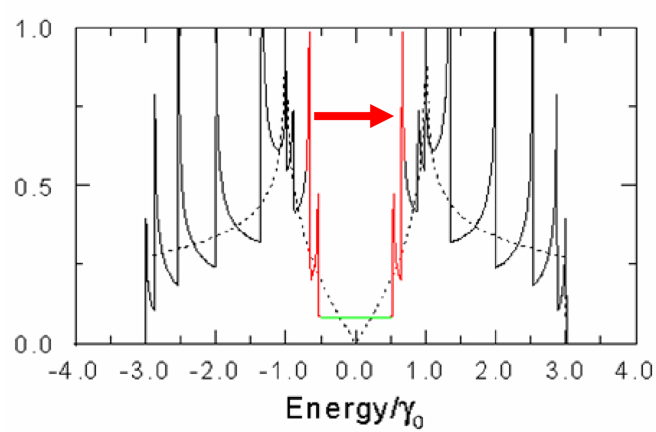

Each nanotube has a unique DOS because of trigonal warping effects *R. Saito et al., Phys. Rev. B 61, 2981 (2000)*

$(\omega_{RBM}, E_{ii}) \rightarrow (n,m)$

Raman signal from *one* SWNT indicates a strong resonance process

Single nanotube Raman spectroscopy

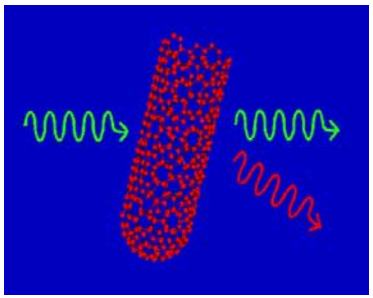

(n,m), JDOS, E_{ii}
Resonant Raman window

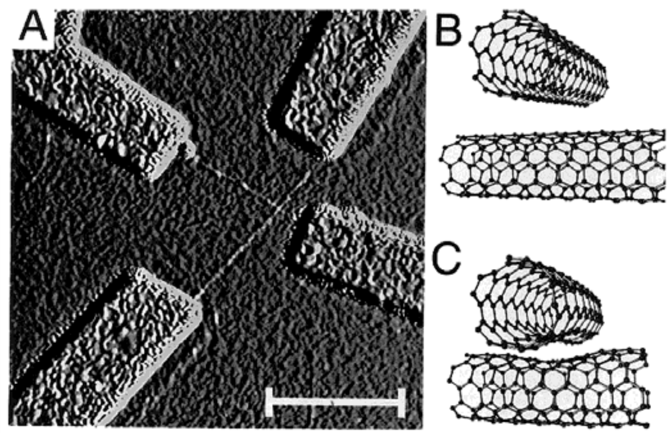

(Fig. From Prof. S. G. Louie)

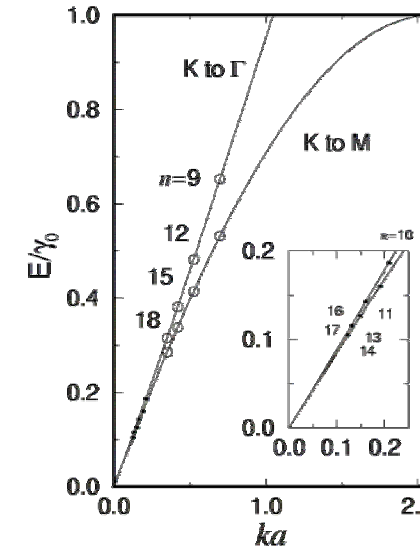

to compare directly experiments and theory on (n,m) SWNTs

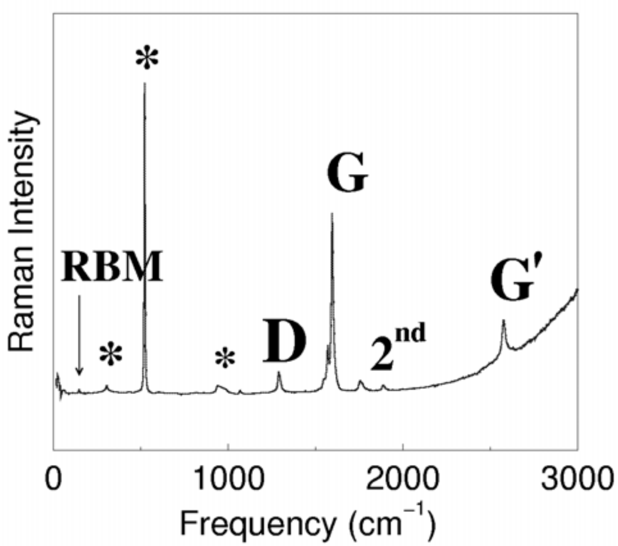

to perform different experiments and to build devices on a characterized (n,m) SWNT

to improve the knowledge about the nanotube spectroscopy
to improve the characterization capability

Raman Spectra and Transport for One SWNT

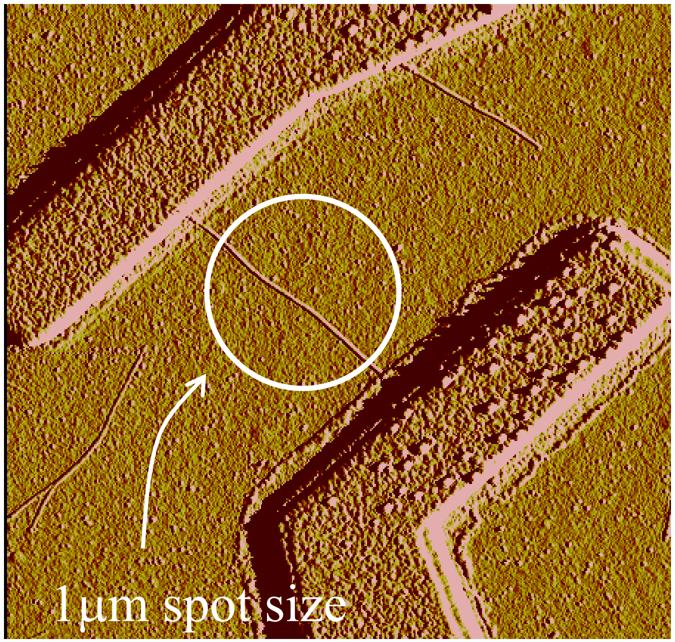

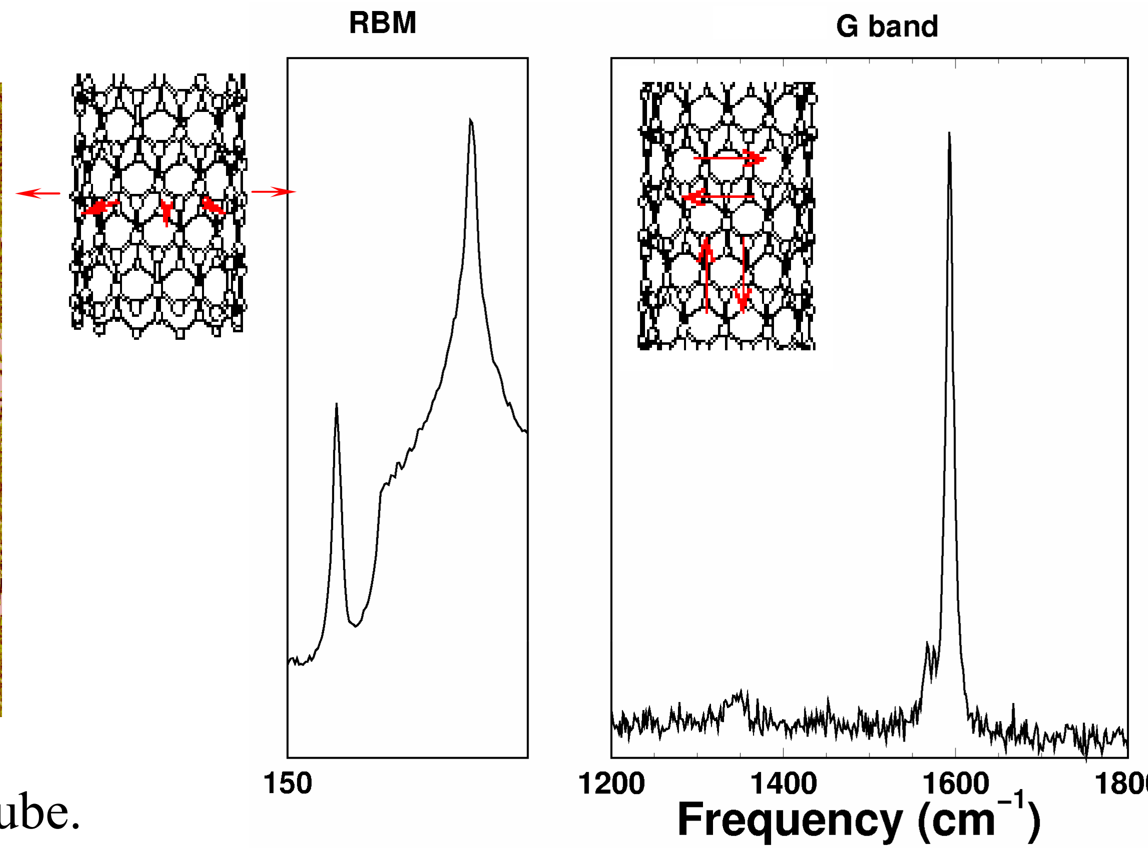

- AFM d_t =1-2nm => single tube.
- No voltage applied to sample during Raman Spectroscopy.

$$\omega_{RBM} = \frac{248}{d_t}$$

$$\omega_{RBM} = 185\,\mathrm{cm}^{-1} \Rightarrow d_t = 1.34\,\mathrm{nm}$$

S. B. Cronin *et al.*, *Appl. Phys. Lett.* (2004) in press

Electrochemical Gating of Single Nanotube

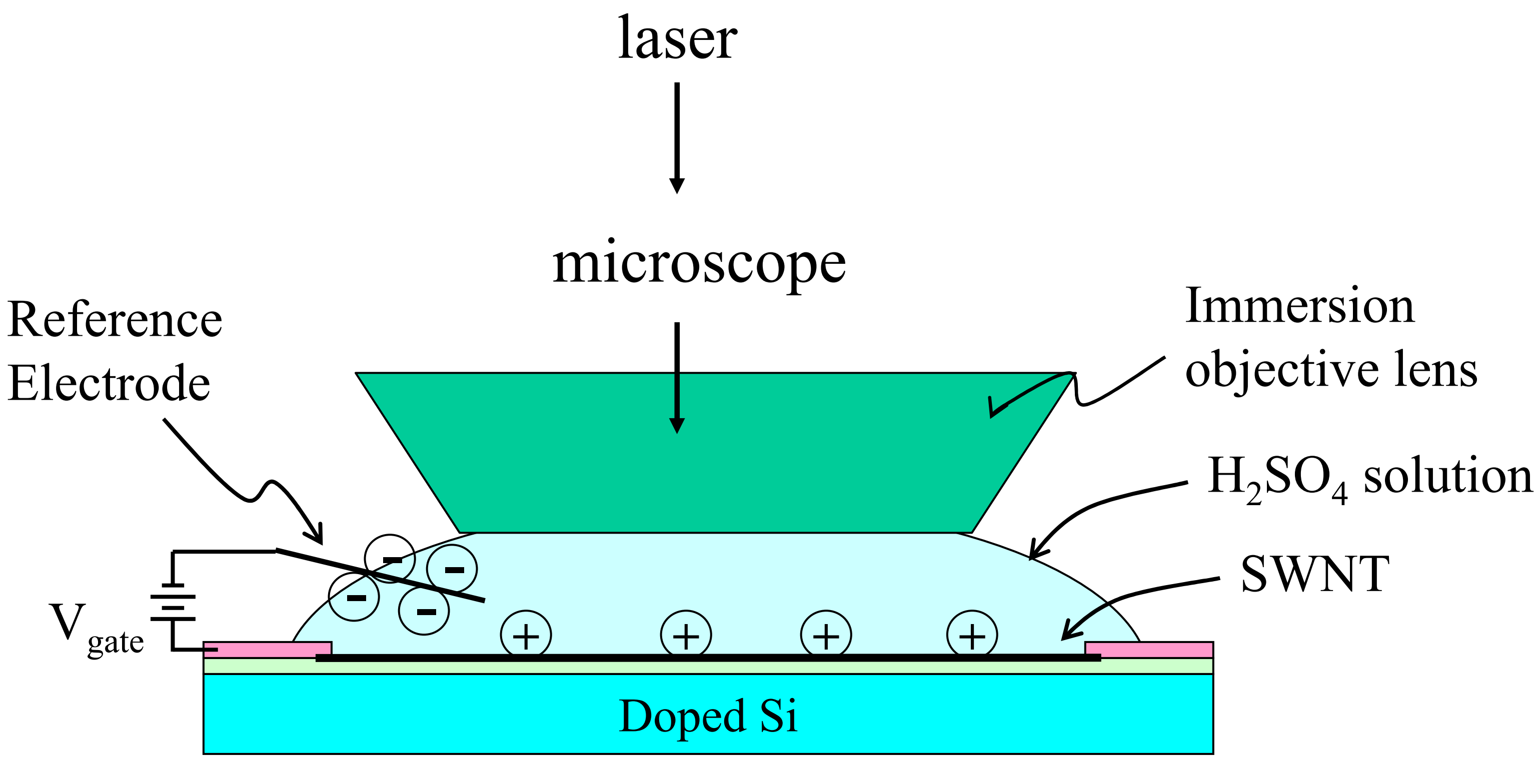

- Because of a large surface to volume ratio, nanotubes are very sensitive to guest chemical species on its surface.
- By applying a voltage in an electrolytic solution, the Fermi energy of the nanotube can be changed.

S. B. Cronin *et al*., *Appl*. *Phys*. *Lett*. (2004) in press

Stokes/anti-Stokes Processes

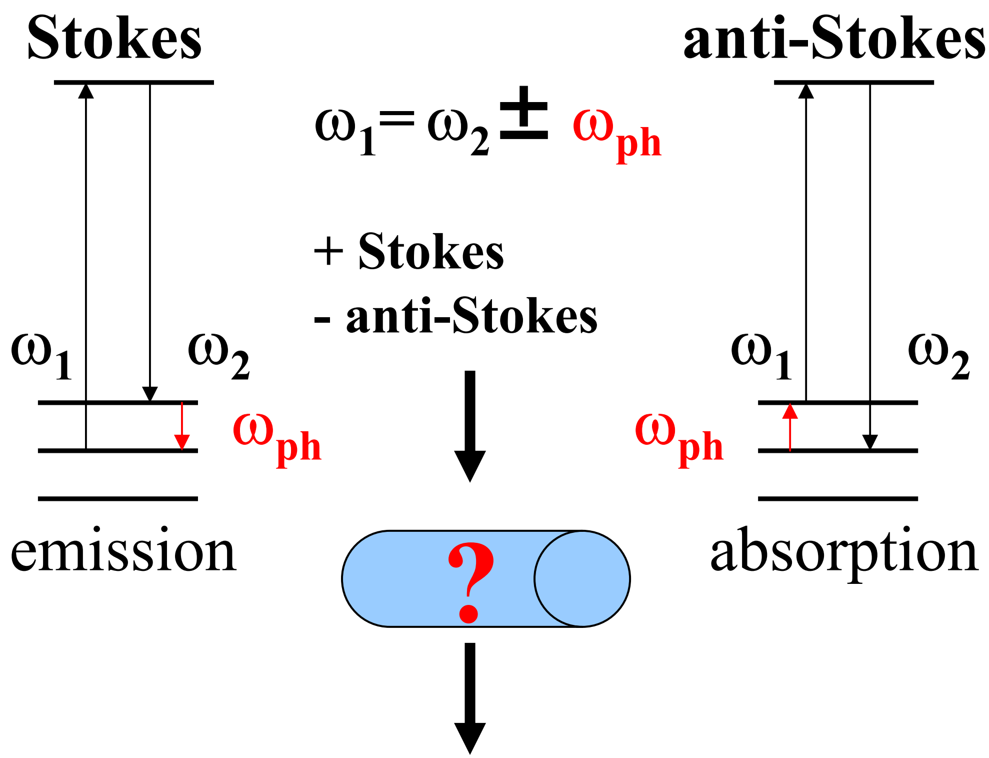

Experimental determination of energy transition between van Hove singularities E_{ii}

Yields reliable (n,m) assignment

Intensity Ratio Stokes/anti-Stokes

From I_{Stokes} / $I_{anti\text{-}Stokes}$

$E_{ii}(d_t)$ is obtained with

10 meV accuracy

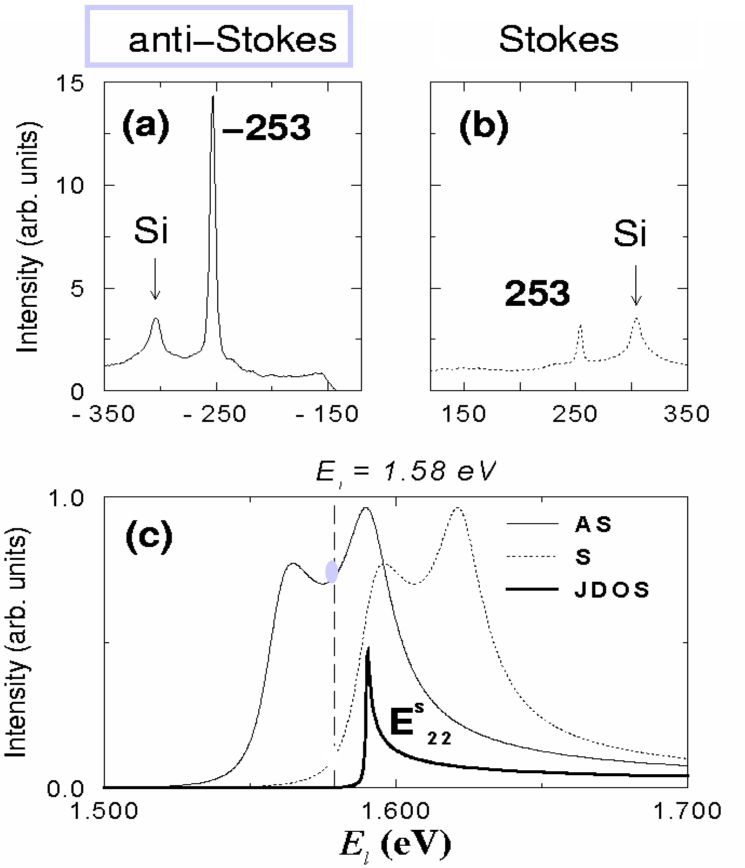

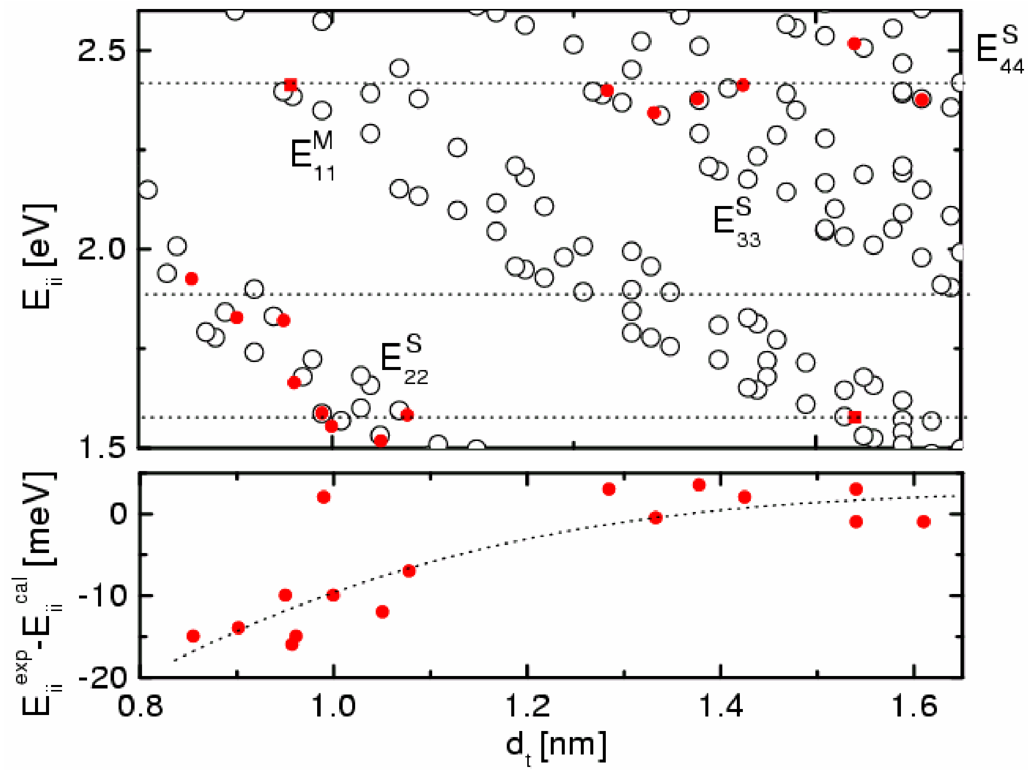

A.G. Souza Filho et al., PRB 63, 241404(R) (2001)

- Accurate (n,m) assignment with Stokes/anti-Stokes measurements for 15 SWNTs using three E_{laser}

- σ-π mixing is important for SWNTs with diameter below d_t = 1.1nm

G-band frequency dependence on tube diameter

A. Jorio *et al.*,
Phys. Rev. B
65, 155412 (2002)

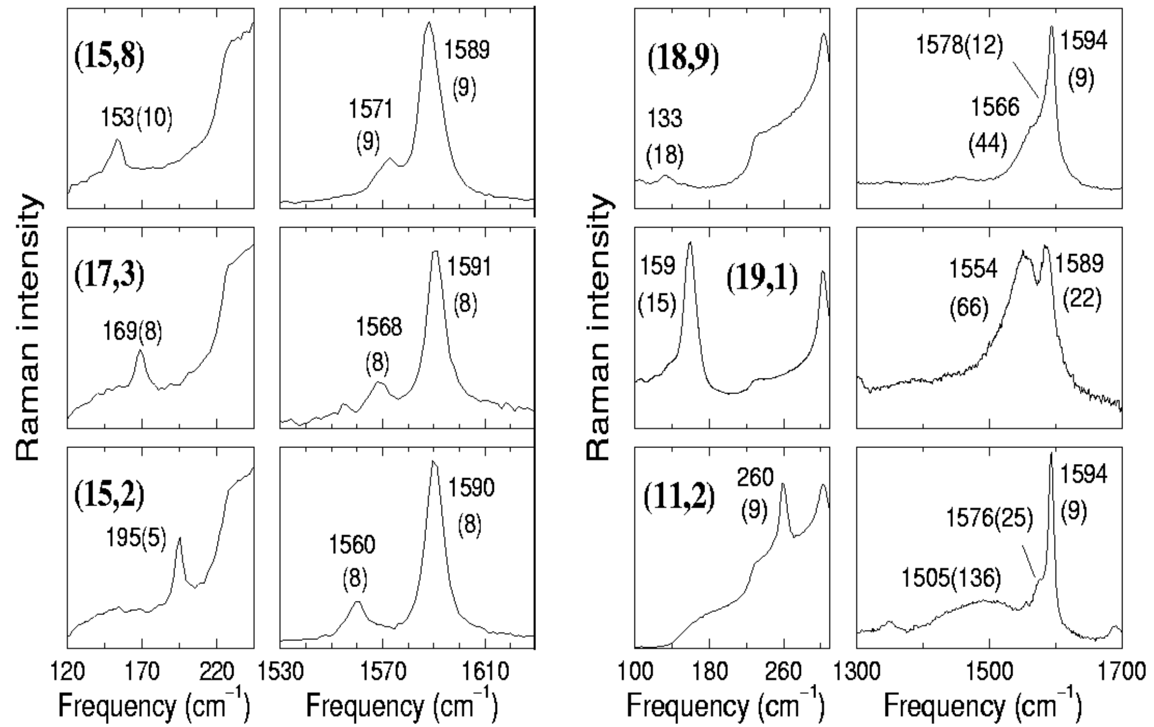

RBM | G band | RBM | G band

Semiconducting | **Metallic**

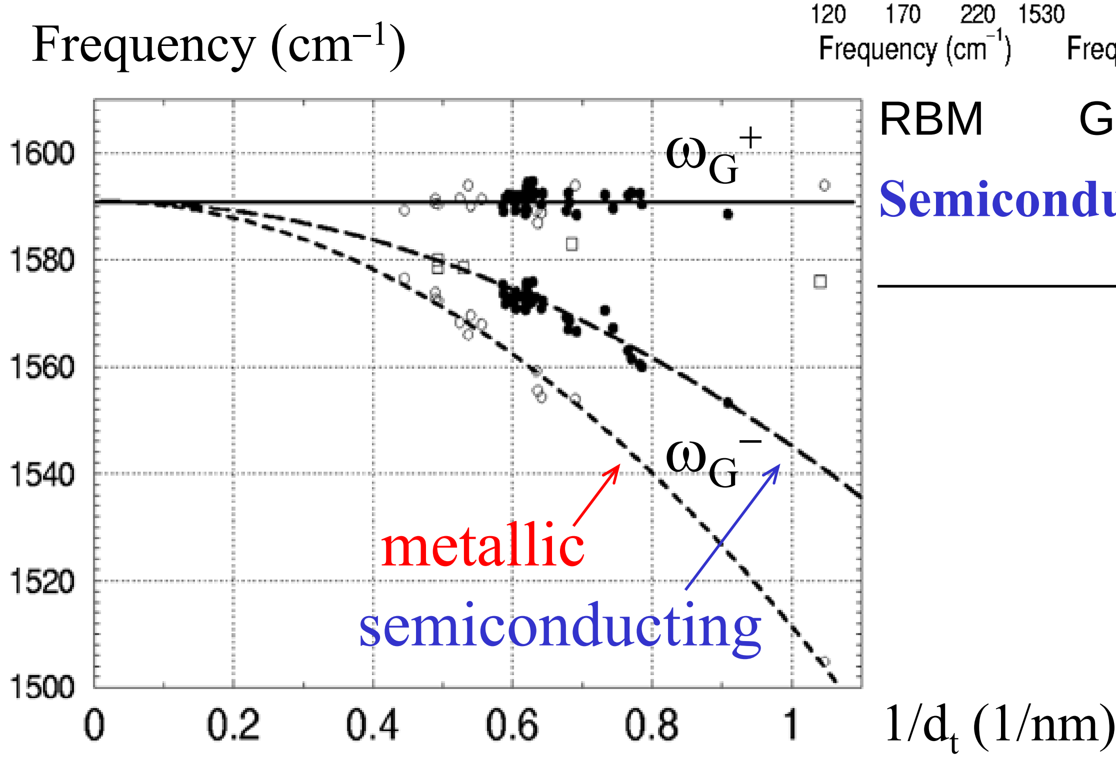

$$\omega_G^{\ +} \sim 1591\text{cm}^{-1}$$

$$\omega_G^{\ -} = \omega_G^{\ +} - C/d_t^{\,2}$$

$$C_S \;= 47.7\text{cm}^{-1}\text{nm}^2$$

$$C_M \;= 79.5\text{cm}^{-1}\text{nm}^2$$

Polarization Effects in Isolated Semiconducting SWNTs

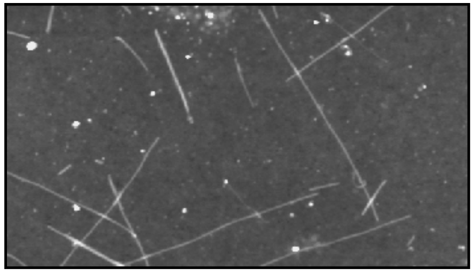

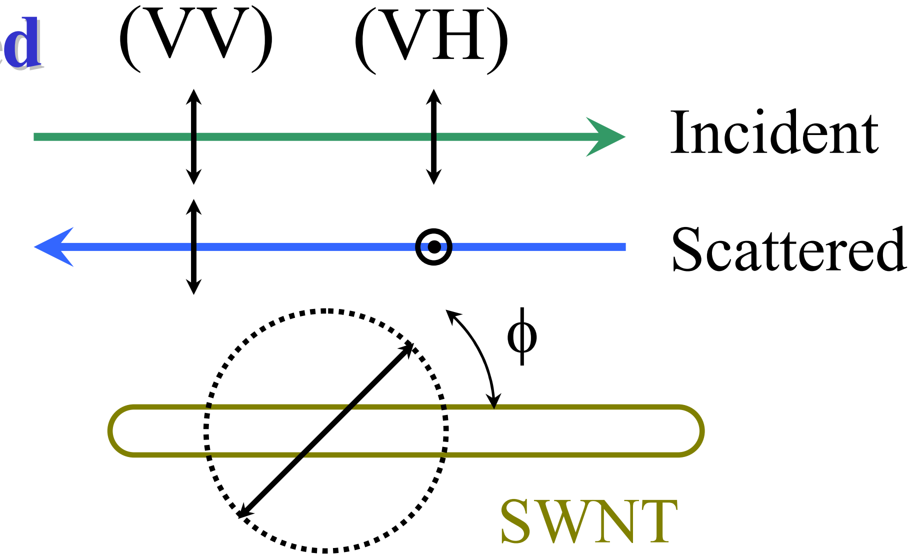

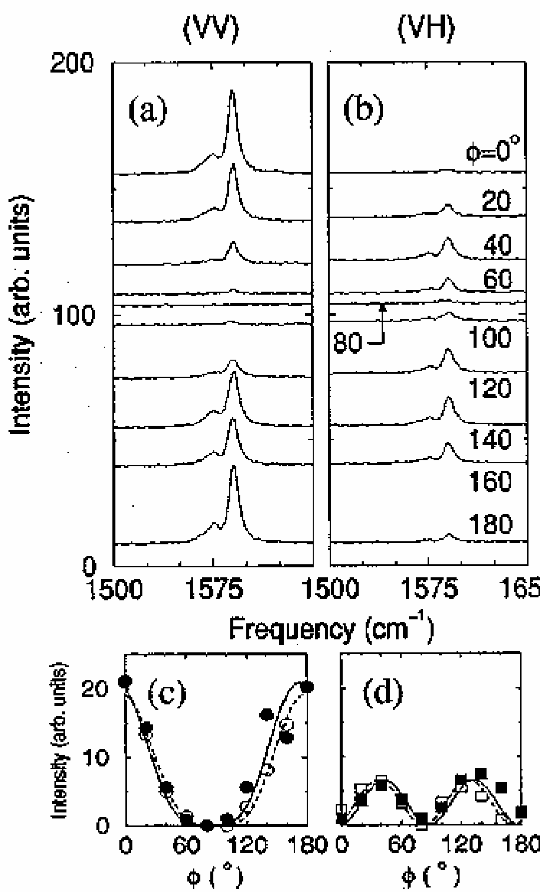

$$(VV) - I(\phi) = \alpha \cos^4(\phi+\Delta\phi)$$
$$(VH) - I(\phi) = \alpha \cos^2(\phi+\Delta\phi) \sin^2(\phi+\Delta\phi)$$

- For G-band on 2 different SWNTs and for RBM on 1 SWNT
- The antenna effect of each SWNT creates a local field along the tube axis that dominates polarization effect
- The local field is strongly affected by the presence of neighboring SWNTs, and for two crossed SWNTs, the full dipolar antenna effect above is not observed

Dispersive Raman Modes: D-band and G'-band

Electron dispersion

$$q_{phonons} \approx 2\,k_{electrons}$$

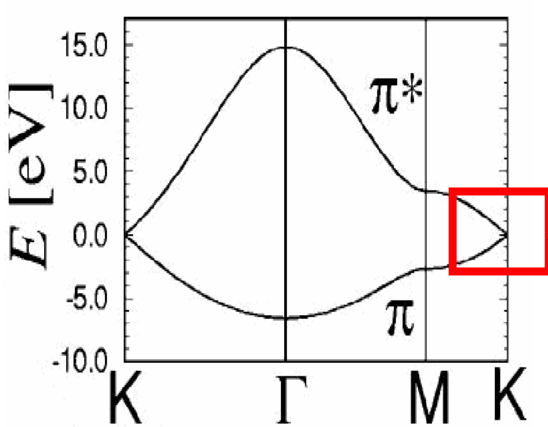

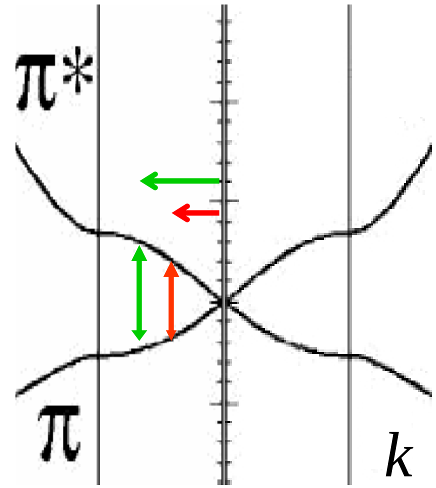

Phonon dispersion

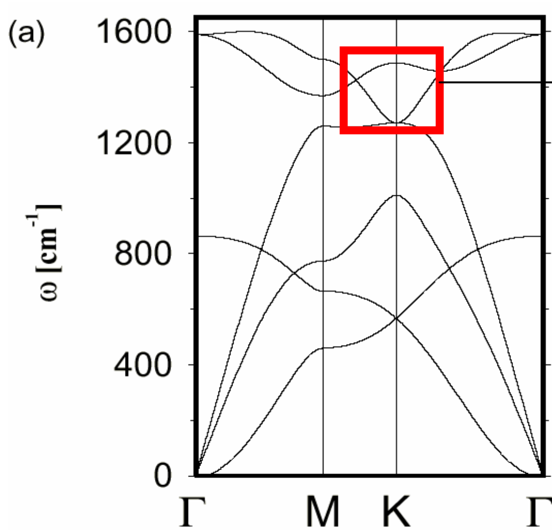

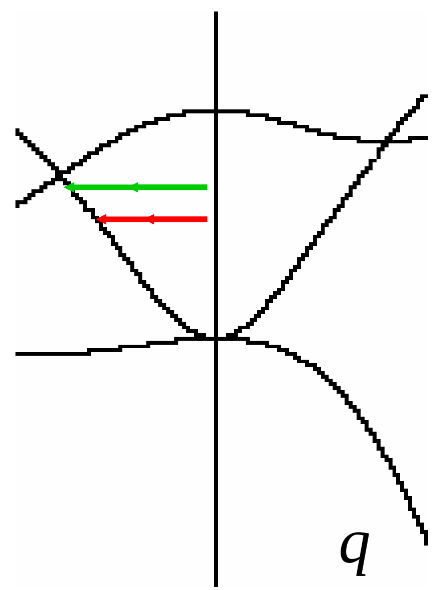

Resonances with E^S_{33} and E^S_{44} transitions

Two peaks 9 predicted **5 observed**

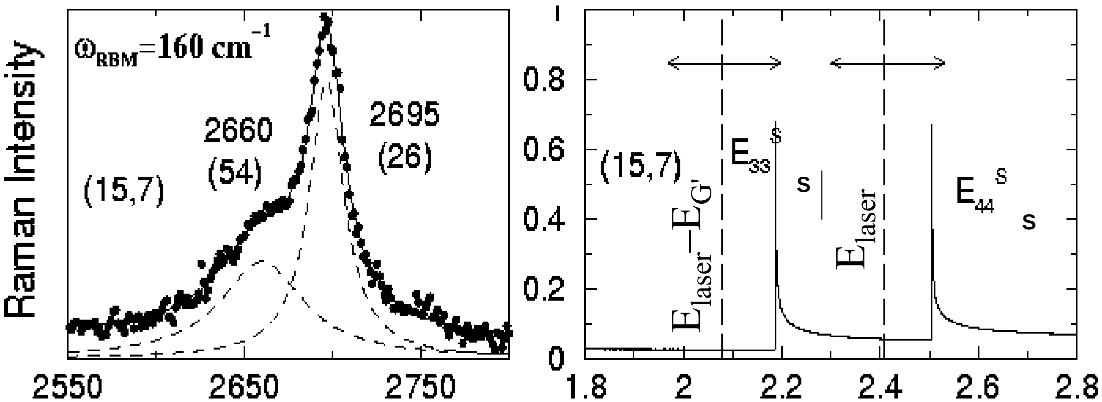

Double peak structure of the G'-band feature in Semiconducting SWNTs

$\Delta\omega_{G'}/\Delta E_{ii}$=106cm^{-1}/eV

One peak 8 predicted **4 observed**

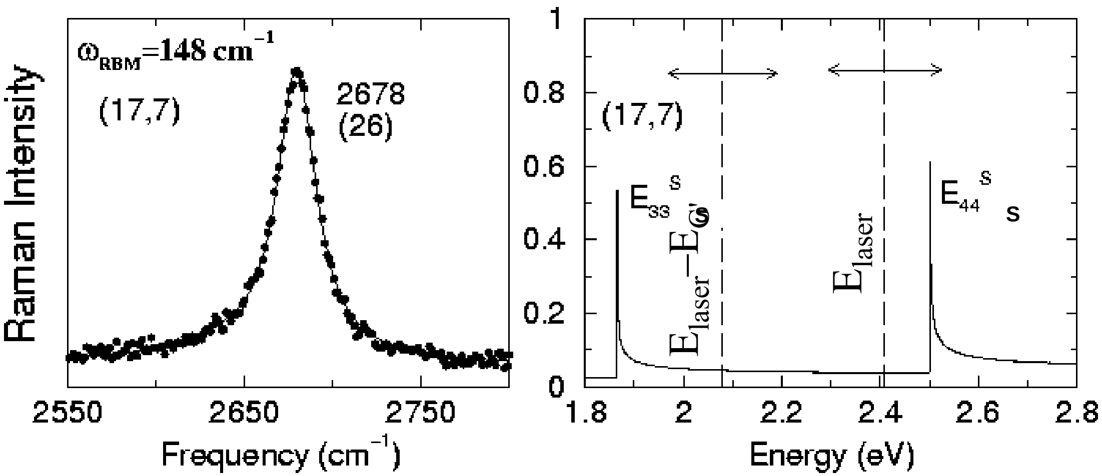

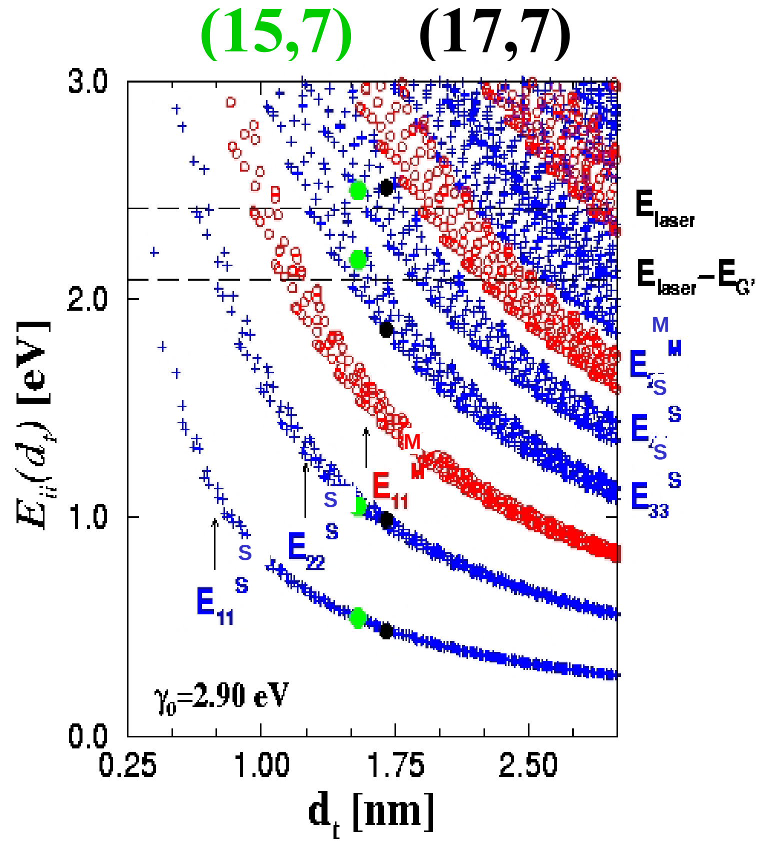

A. G. Souza Filho *et al*, PRB 65, 085417 (2002)

Resonances with E_{22} and E_{22} transitions: Metallic tubes

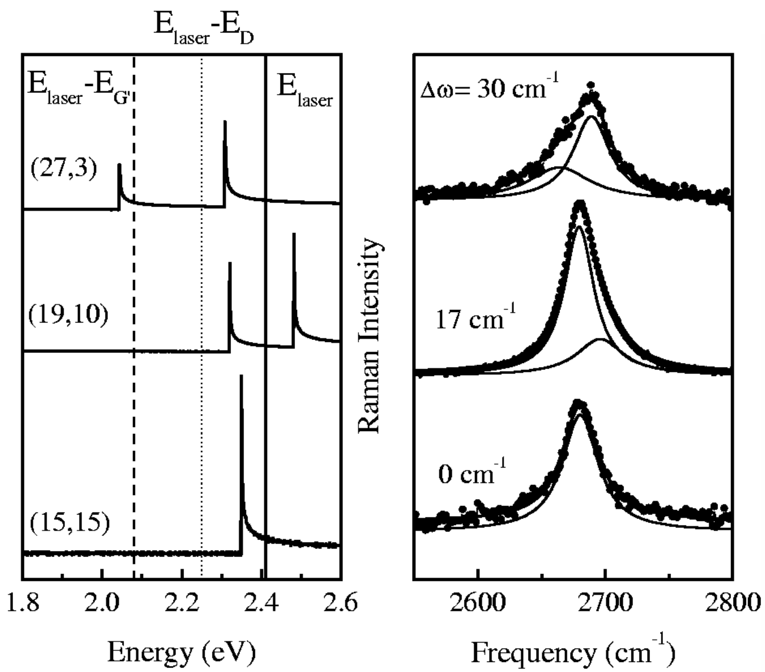

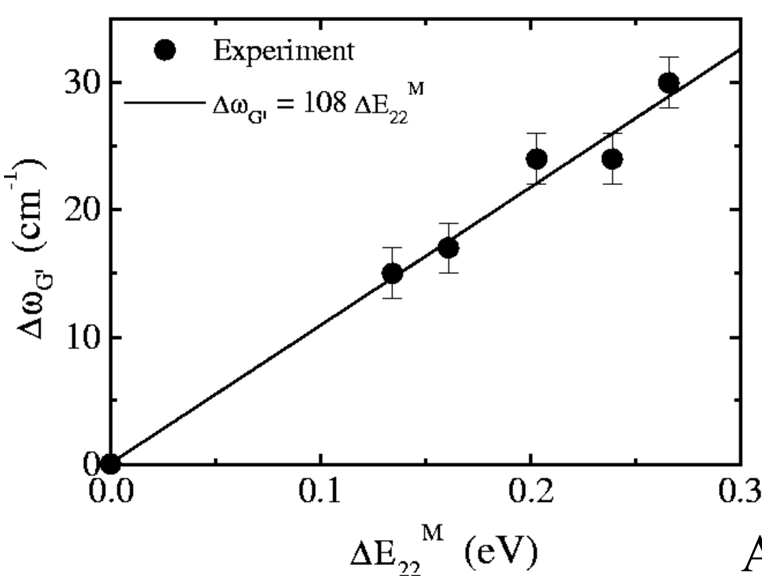

lower & upper

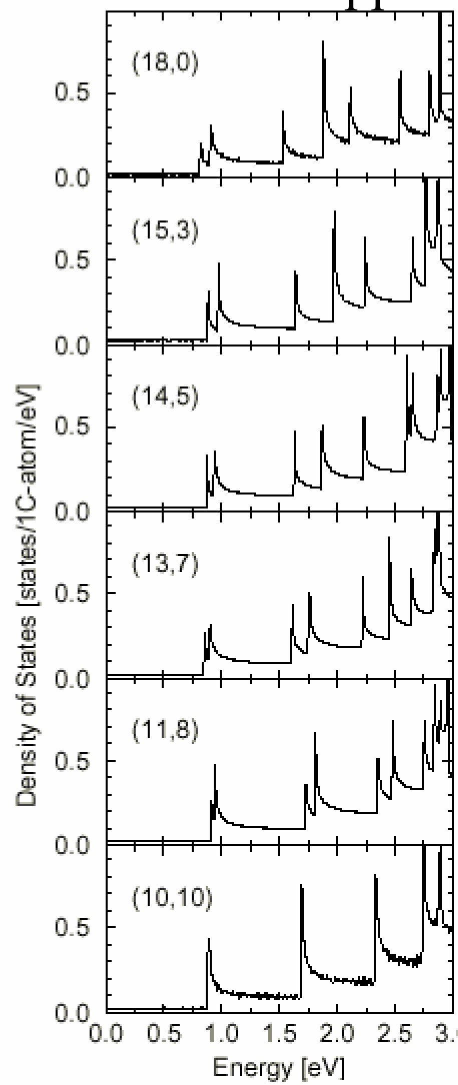

Double peak structure of the G'-band feature in Metallic SWNTs

$\Delta\omega_{G'}/\Delta E_{ii}$=108cm^{-1}/eV

Trigonal Warping

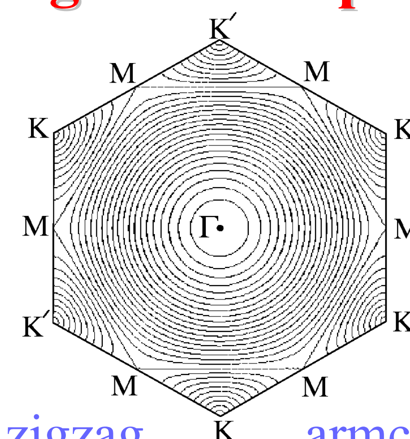

zigzag armchair

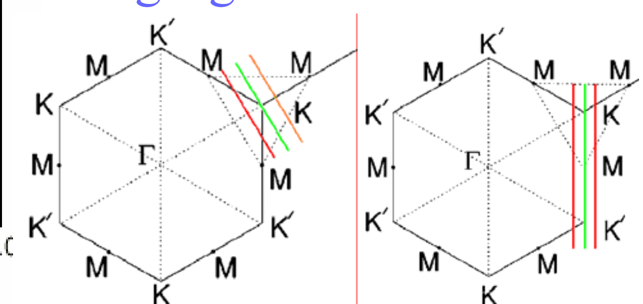

R. Saito *et al*, PRB 61, 2981 (2000)

A. G. Souza Filho *et al*, CPL 354, 62 (2002)

CUTTING LINES

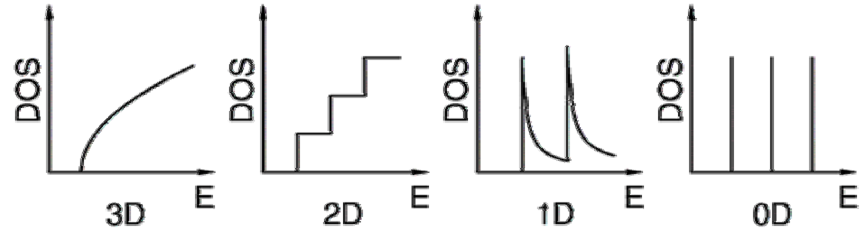

Energy-momentum contours
(linear dispersion & degenerate point)

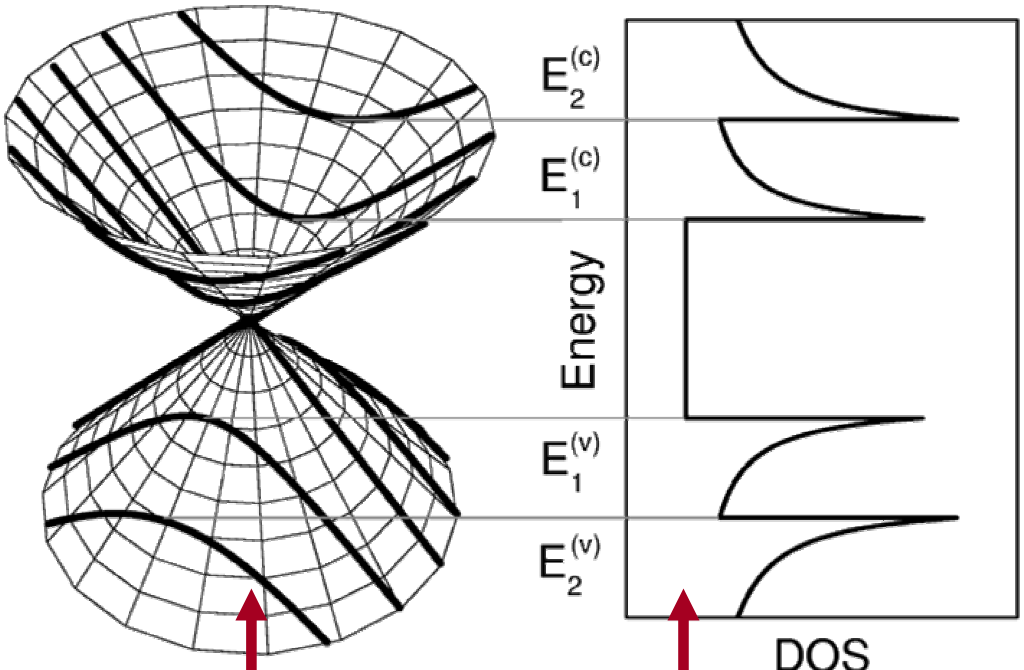

cutting lines

density of states

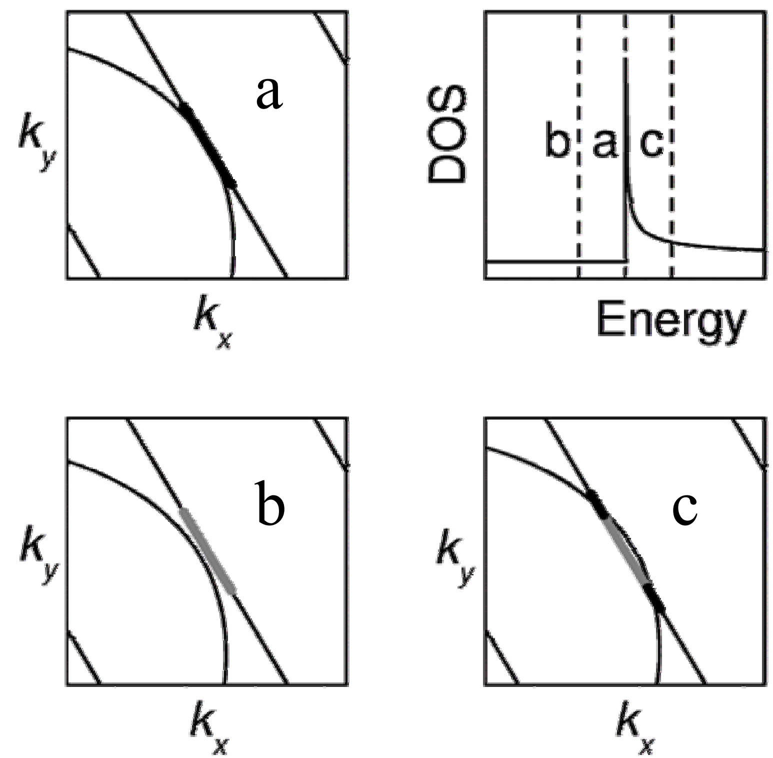

Pre-resonant conditions
(cutting lines & DOS profile)

TWO PEAK G'-BAND

SEMICONDUCTING

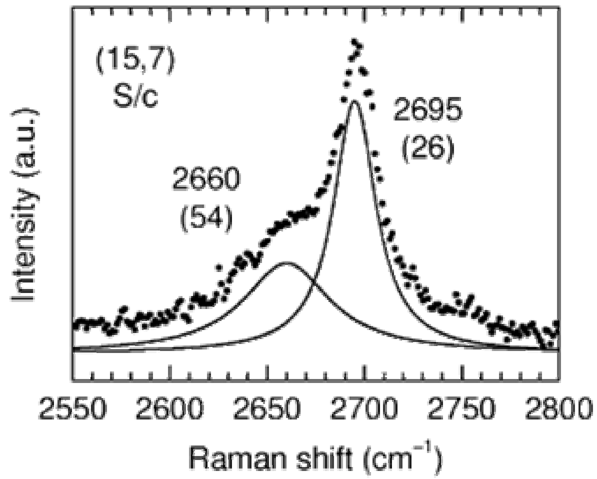

METALLIC

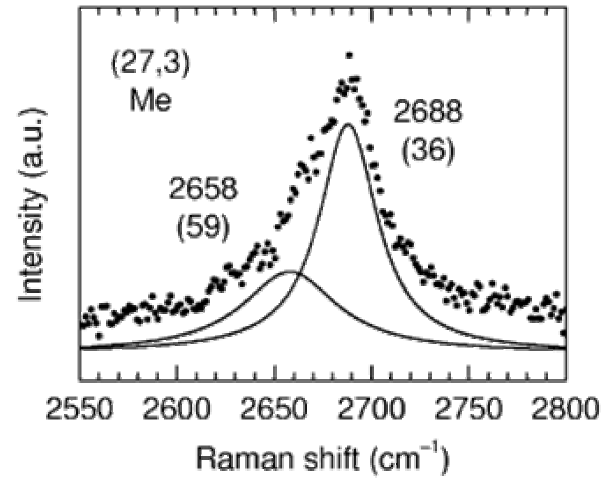

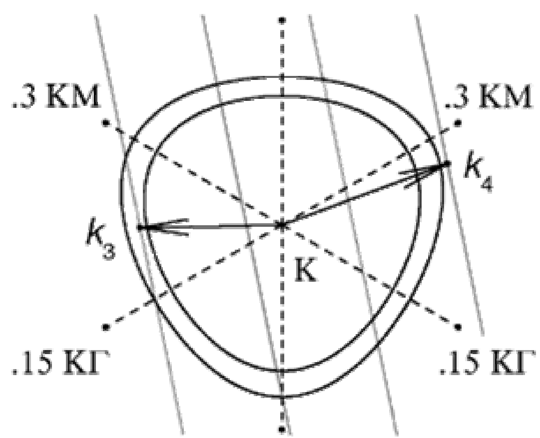

PHONON DISPERSION

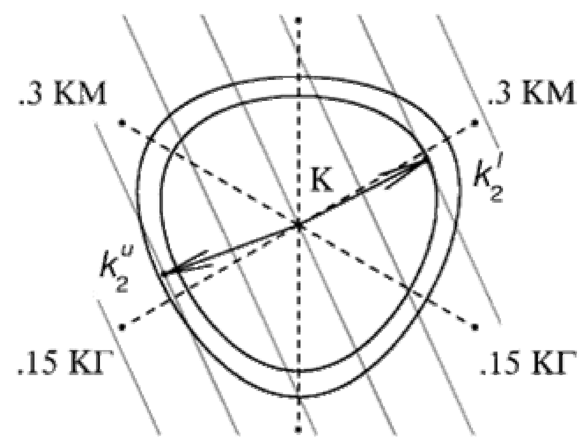

PHONON ANISOTROPY

Trigonal warping effect for phonons

Measured by Raman spectroscopy

SWNT chiral angle θ defines *q* direction on 2D Brillouin zone

Experimental results

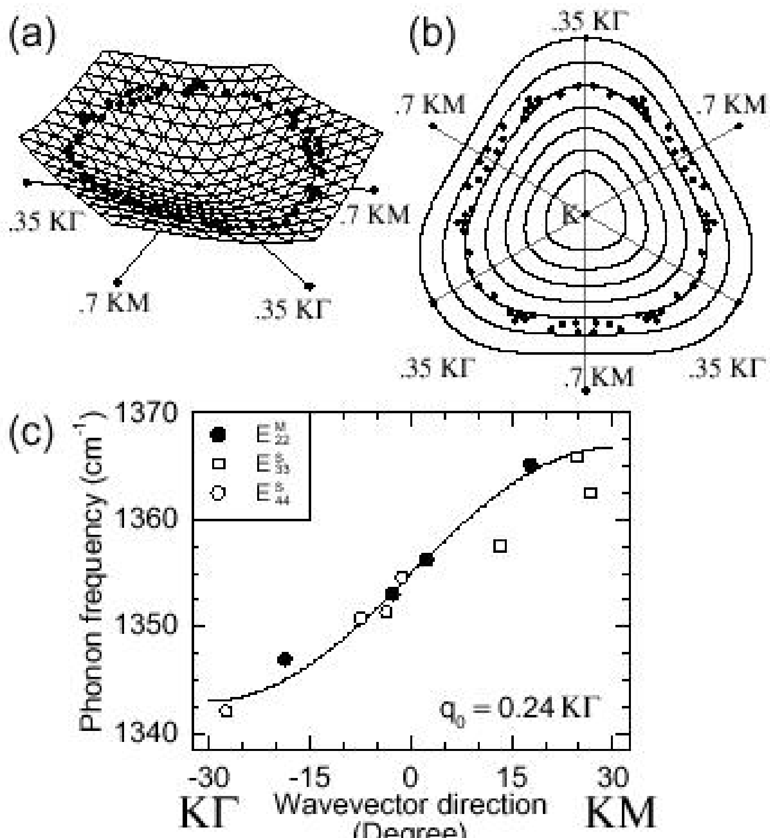

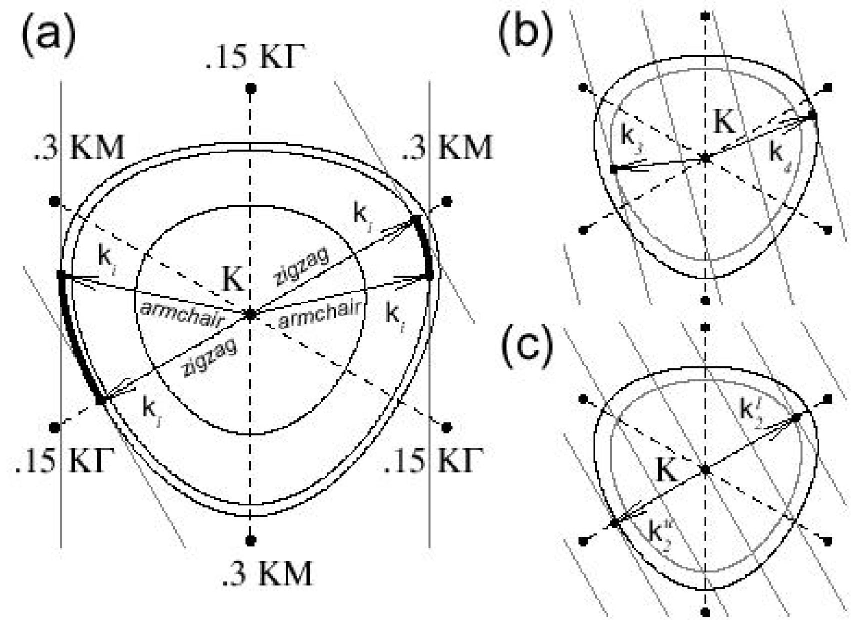

Cutting lines allow determination of not only magnitude of *q* but also direction

Samsonidze et al., *PRL.* ***90****, 027403* (2003)

Phonon trigonal warping around K point ~ 24cm^{-1}

Raman Spectra of Carbon Nanotubes

Fantini et al., (unpublished)

- Radial breathing mode
- D band
- G band
- Intermediate frequency modes (IFM)

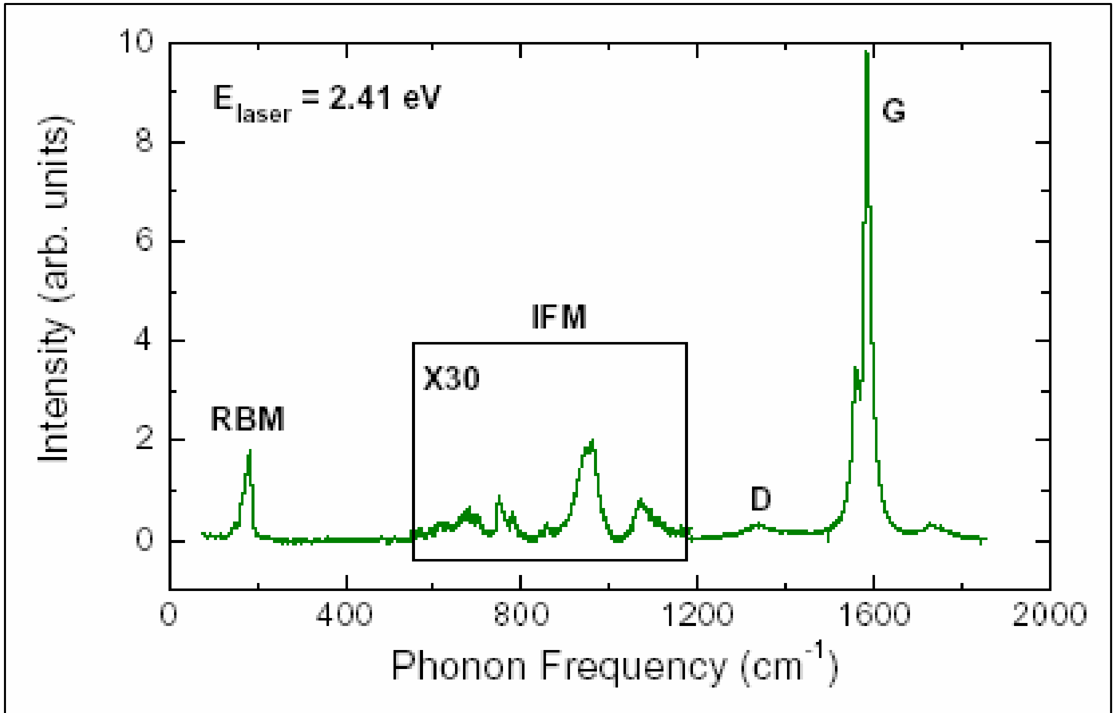

Detailed E_{laser} dispersion of the IFMs

Fantini et al., (unpublished)

Raman spectra obtained with 22 different E_{laser} between 1.92 and 2.71eV

Observation of many peaks

Raman spectra show strong E_{laser} dependence

Raman peaks with constant frequency appear and disappear in the spectra

Step-like dispersion is observed, positive for IFMs above 860cm^{-1} and negative for IFMs below 860cm^{-1}

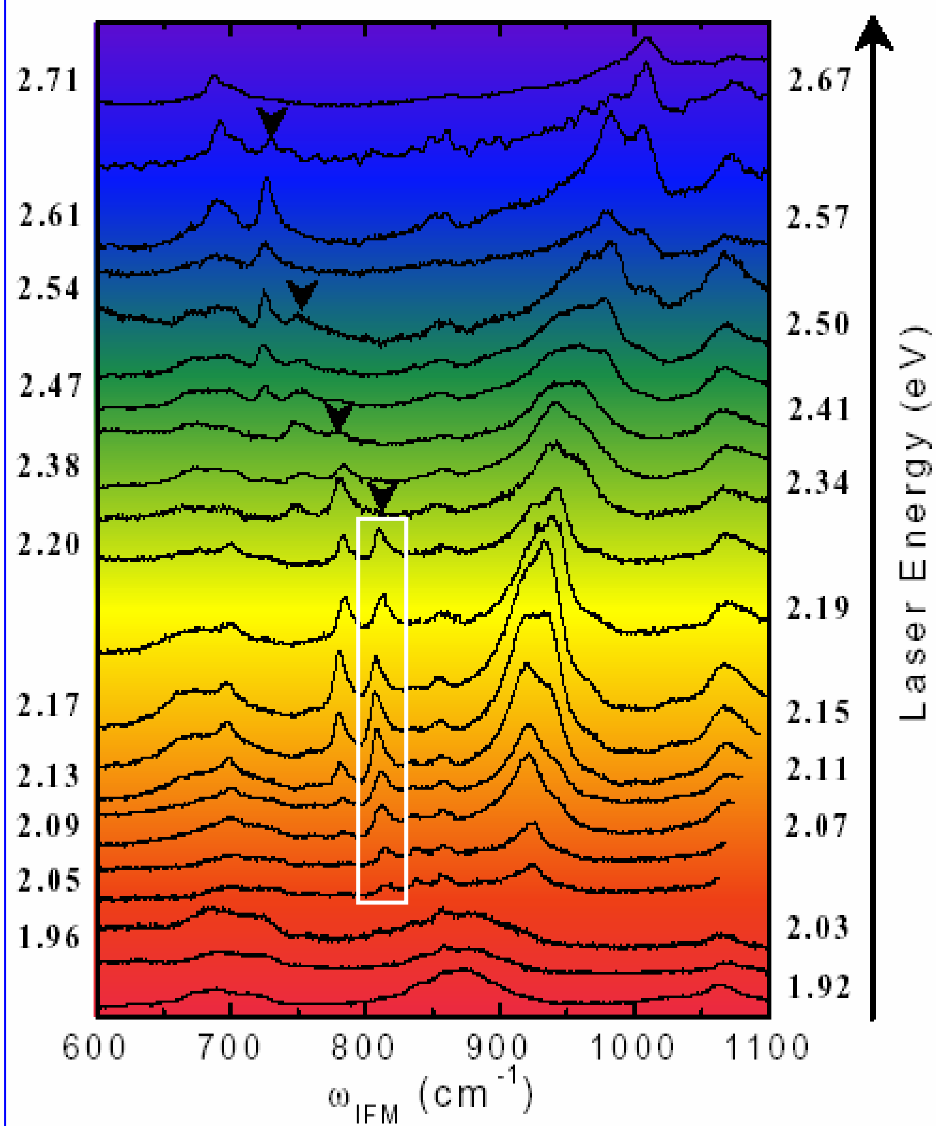

Step-like dispersive behavior of the IFMs

Fantini et al., (unpublished)

- Bright areas indicate strong intensities
- Peak at 780 cm^{-1} is observed for $2.10 \leq E_{laser} \leq 2.40$eV
- Peak at 810 cm^{-1} is observed for $2.05 \leq E_{laser} \leq 2.35$eV

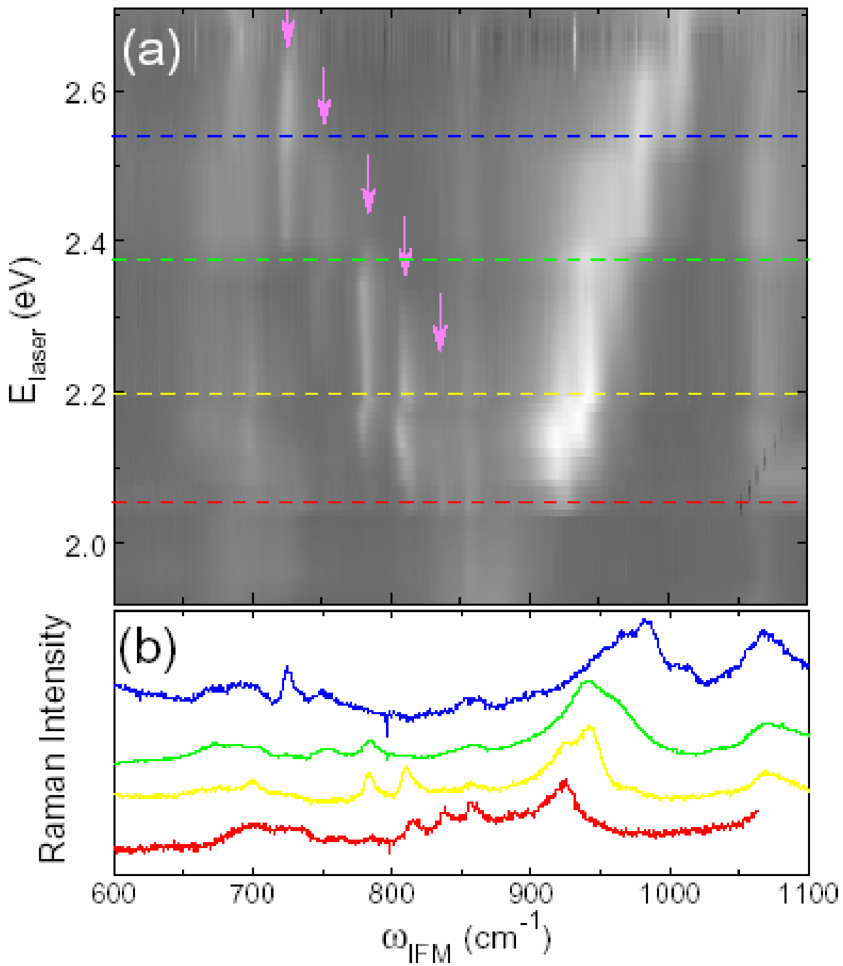

Origin of the IFMs?
Reason for the step-like dispersion?

Fluorescence from SDS-wrapped nanotubes

O'Connel *et al.*, Science 297, 593 (2002)

SDS-wrapping of a single SWNT

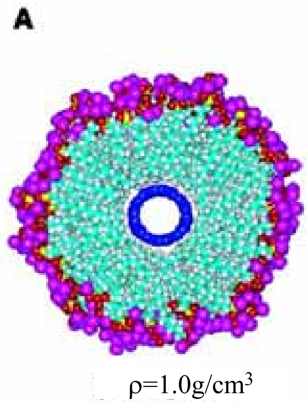

SDS wrapped SWNT in water (simulation)

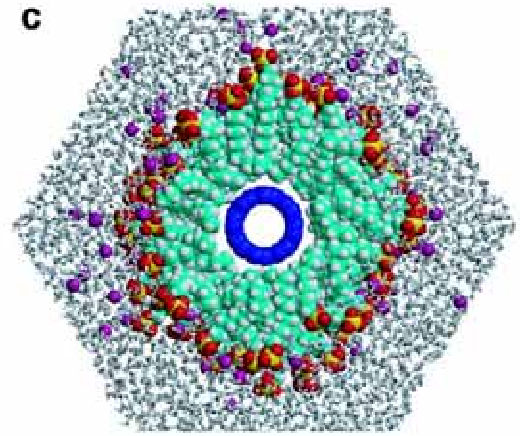

SDS-wrapping of a small SWNT bundle

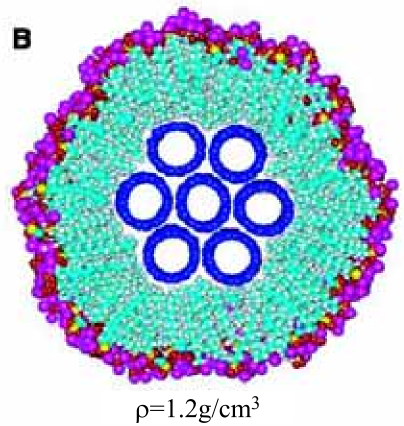

Simulated **element** radial distribution. (0 is the center of the nanotube).

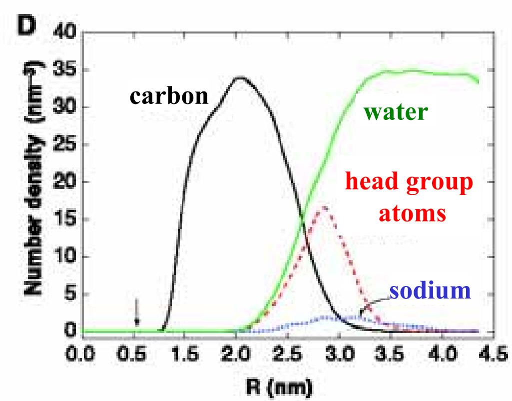

Nanotubes covered by a micelle of Sodium Dodecyl Sulfate (SDS). The wrapping is known to separate the nanotubes in different soluble micelles resulting in a solution of individualized SWNTs.

Fluorescence from SDS-wrapped nanotubes

Structure-Assigned Optical Spectra of Single-Walled Carbon Nanotubes

S. M. Bachilo *et al.*, Science 298, 2361 (2002)

Absorption and Emission

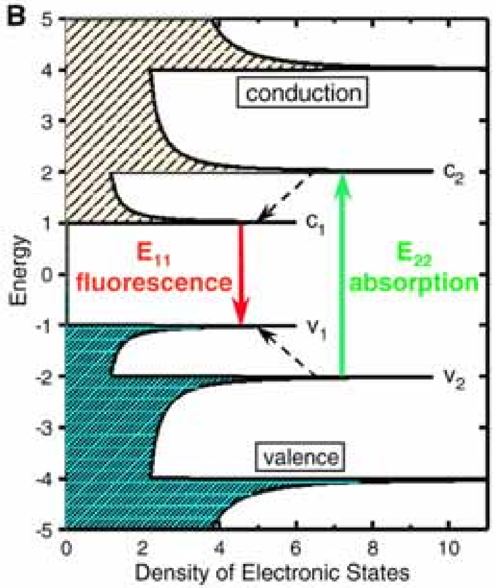

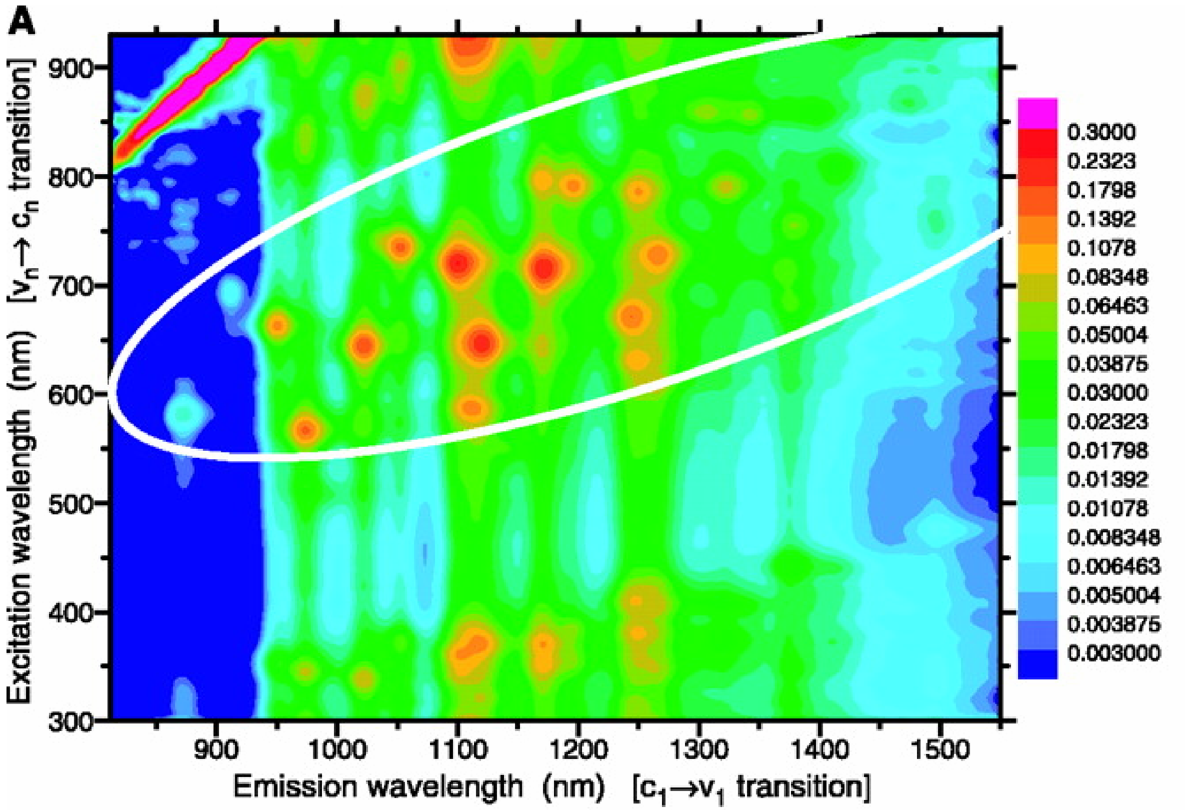

•PL results on SDS-wrapped nanotubes. Each dot on the figure represents the E_{22} & E_{11} transitions observed for one SWNT.

Complemetary spectroscopy technique

Luminescence from semiconducting SWNTs+SDS micelles

M.J.O'Connell et al., Science 297, 593 (2002)

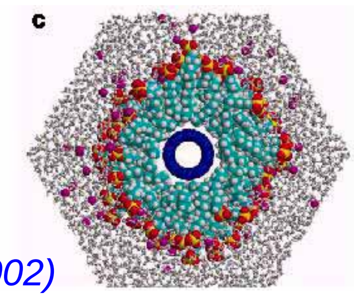

E_{11}/E_{22} + ω_{RBM} (Raman) measurements allow (*n*,*m*) assignment

Experiment

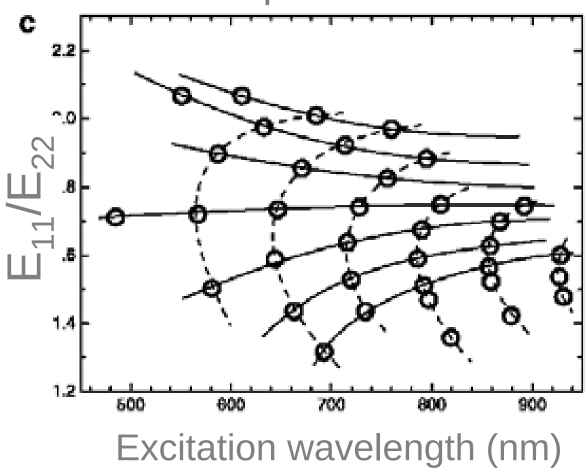

Tight Binding up to 3rd neighbor is used for (*n*,*m*) assignment

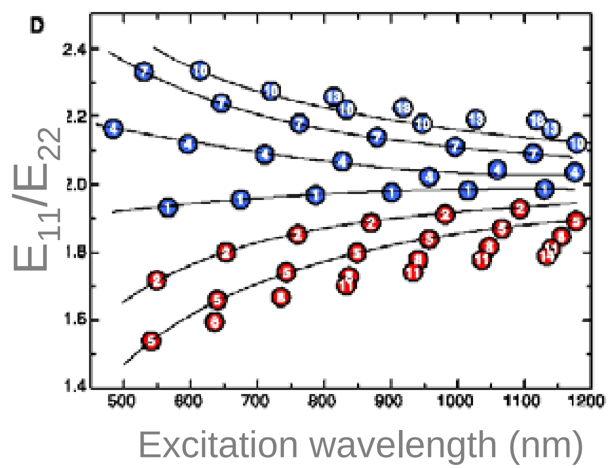

S. M. Bachilo et al., Science 298, 2361 (2002)

Advantages:

- Stronger signal
- Can evaluate many Eii/Ejj

Limitations:

Measurements only for semiconducting SWNTs in aqueous micelles, not isolated SWNTs

Simplest tight binding does not describe E^{S}_{11} very well due to Coulomb effects

(M. Ichida et al., PRB65, 241407(R) 2002)

For small d_t SWNTs σ-π coupling must be considered

Properties of the SDS-wrapped E_{ii} transitions

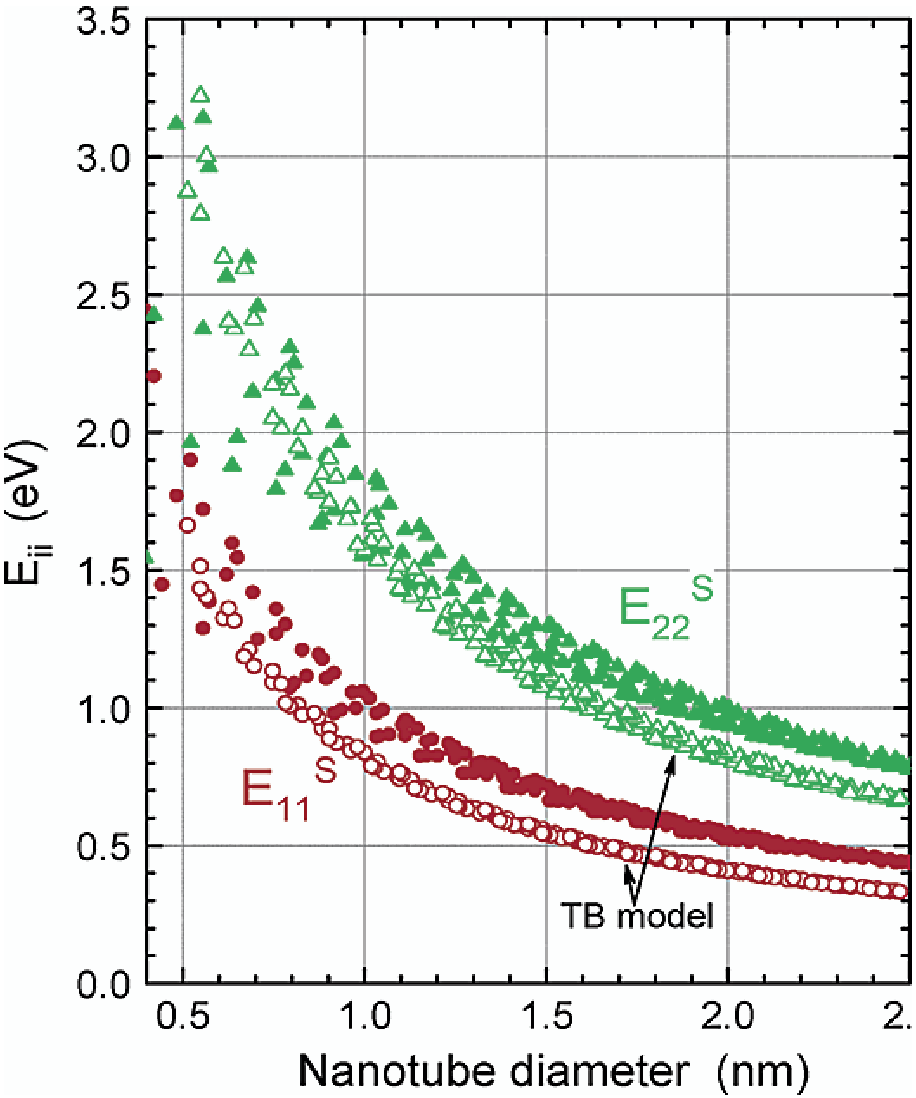

•Large deviation is found between PL results and the Tight Binding (TB) calculations.

•PL data has larger spread of E_{ii} values at constant d_t than TB calculations

•For the PL data the average E_{22}/E_{11} ratio is about 1.7 rather 2.0 as expected by TB. Theorists have proposed many body effects to account for this discrepancies.

•At present there is no good correspondence between E_{ii} found by luminescence on SDS wrapped SWNTs and by Raman spectra from isolated nanotubes on Si/SiO_2 substrates.

Challenges for Carbon Nanotube Research

- Control synthesis process to produce tubes with same diameter and chirality. Progress is being made.
- Until control of synthesis process is achieved, develop effective separation methods:
  - ✓ metallic from semiconducting
  - ✓ by diameter
  - ✓ by chirality
- Develop method for large-scale, cheap synthesis
- Improve nanotube characterization and manipulation
- Develop commercial scale applications

A CHEMICAL SEPARATION PROCESS
For semiconducting and metallic SWNTs

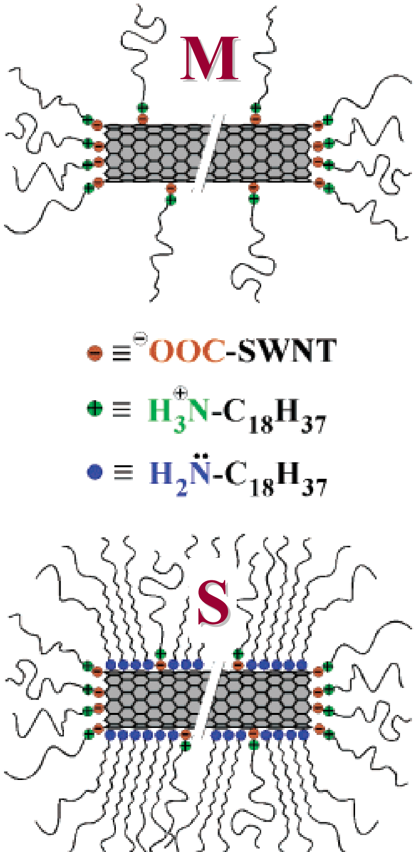

Acid-treated SWNTs were non-covalently functionalized with octadecylamine (ODA) and dispersed in tetrahydrofuran (THF)

Partially evaporate THF $\Rightarrow$ M-SWNTs selectively precipitate & S-SWNT enriched supernatant *
(*currently attributed to an enhanced chemical affinity of ODA for S-SWNTs, rendering M-SWNTs more prone to precipitation*)

Remove ODA by vacuum sublimation

* D. Chattopadhyay, I. Galeska, F. Papadimitrakopoulos, J. Am. Chem. Soc. 125, 3370 (2003)

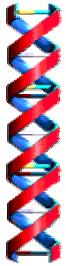

DNA SEPARATION PROCESS

Ming Zheng *et al*.

DuPont Central Research and Development

M. Zheng *et al.*, *Science*, **302**,1546, Nov28th, 2003.

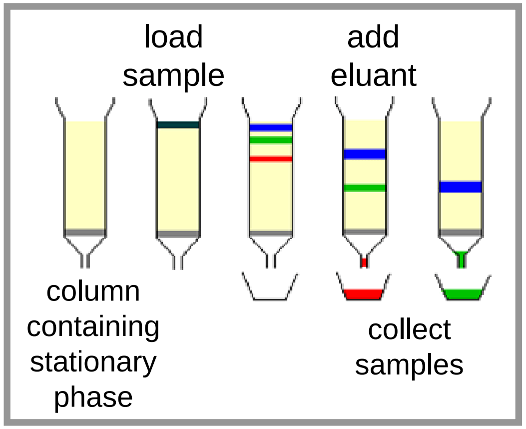

Ion-exchange liquid chromatography

- ✓ Sample – 500 μL of a DNA-SWNT
- ✓ Stationary Phase – strong anion exchange resin positively charged
- ✓ Eluant – aqueous solution with linear salt concentration (0 to 0.9M NaSCN in 20 mM MES buffer at pH7)

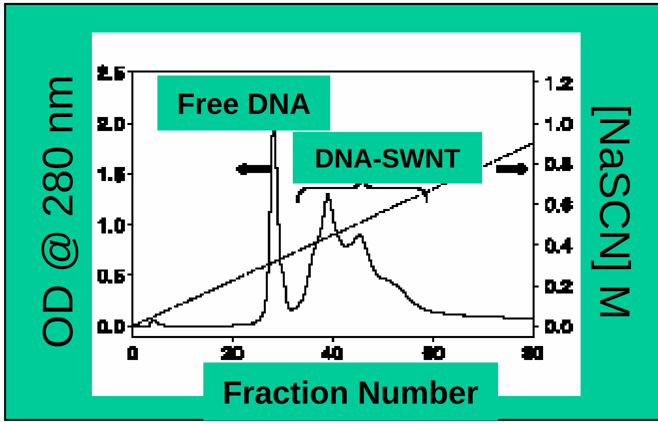

Separation mechanism

- ✓ Hybrid DNA-SWNTspecies: different linear charge densities

- **Met tubes**: lower negative charge density
  higher polarizability ⇒ positive image charge
  elute before **Sem** tubes from the column
- **Small diameter tubes**: elute before **large** diameter SWNTs

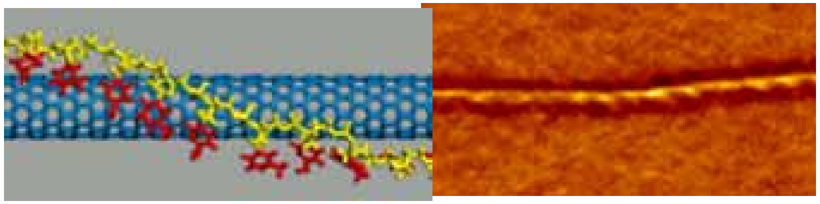

Analyzed samples:

F00 (starting material), F34, F37, F40, F43 (DNA-SWNTs)

Separation Efficiency of DNA-wrapped SWNTs

- ✓ **Resonance Raman Effect at several laser excitation energies are used.**
- ✓ **The DNA-assisted Separation Process:**

  Met *vs*. **Sem** separation and diameter separation

- ✓ **Procedure for evaluating separation efficiency of Sem and Met SWNTs was developed using resonance Raman spectroscopy**

  Enhancement of **Met** in the earlier fraction: **6 times**

  Enhancement of **Sem** in the later fraction: **2 times**

- ✓ **Diameter separation in DNA Process:**

  Small diameter tubes in earlier fractions

  Large diameter tubes in later fractions

Drivers for the Hydrogen Economy:

- ***Reduce Reliance on Fossil Fuels***
- ***Reduce Accumulation of Greenhouse Gases***

Energy Source	% of U.S. Electricity Supply	% of Total U.S. Energy Supply
Oil	3	39
Natural Gas	15	23
Coal	51	22
Nuclear	20	8
Hydroelectric	8	4
Biomass	1	3
Other Renewables	1	1

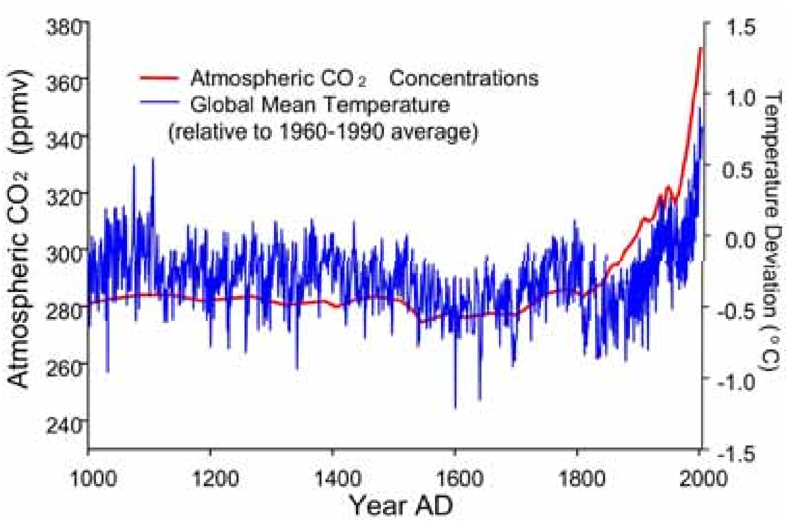

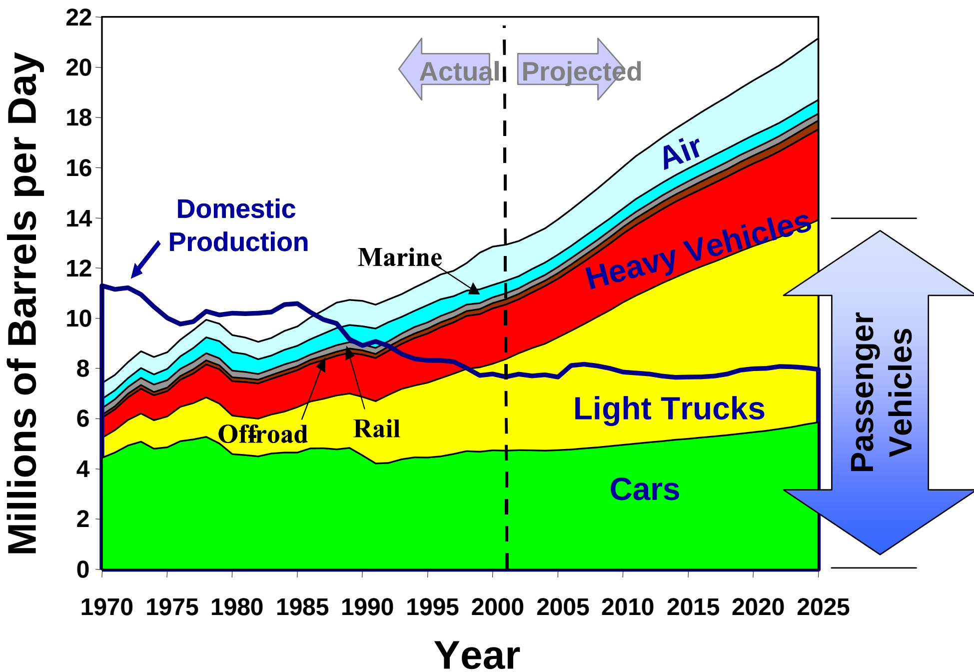

Hydrogen Economy initiative announced by President Bush.

The Hydrogen Economy

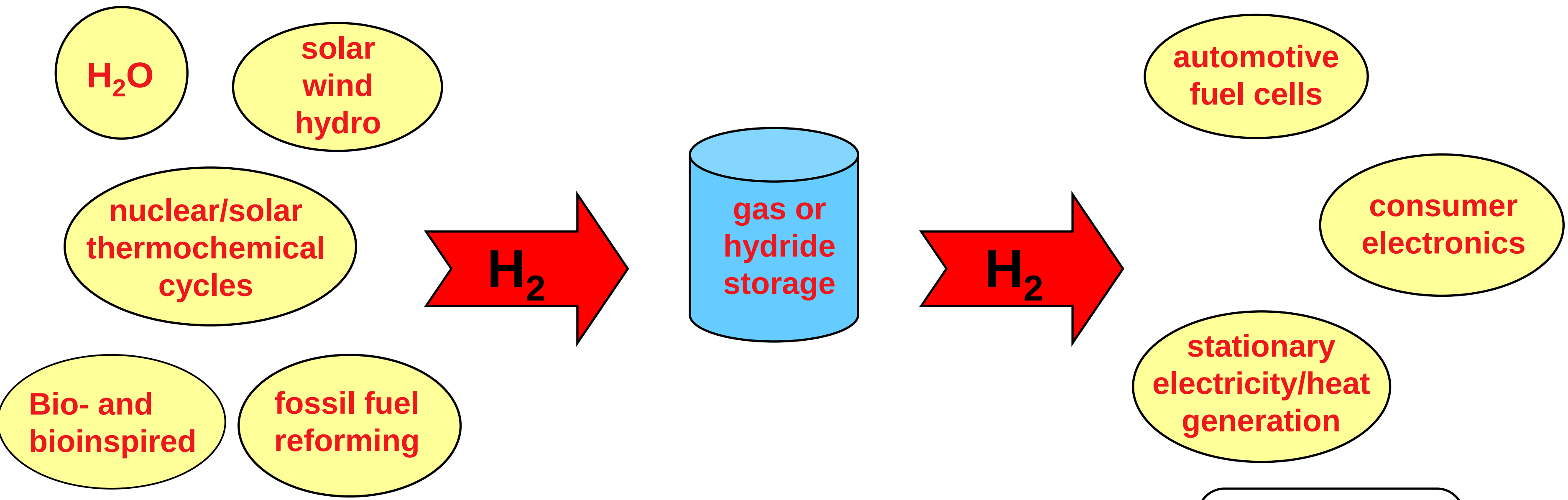

production	***storage***	***use in fuel cells***
9M tons/yr	**4.4 MJ/L (Gas, 10,000 psi)** **8.4 MJ/L (LH2)**	**$3000/kW**
⬇	⬇	⬇
40M tons/yr **(Transportation only)**	**9.72 MJ/L** **(2015 FreedomCARTarget)**	**$35/kW** **(Internal Combustion Engine)**

Fossil Fuel Reforming in Hydrogen Production

- For the next decade or more hydrogen will mainly be produced using fossil fuel feedstocks.
- Development of efficient inexpensive catalysts will be key.
- Modeling and simulation will play a significant role.

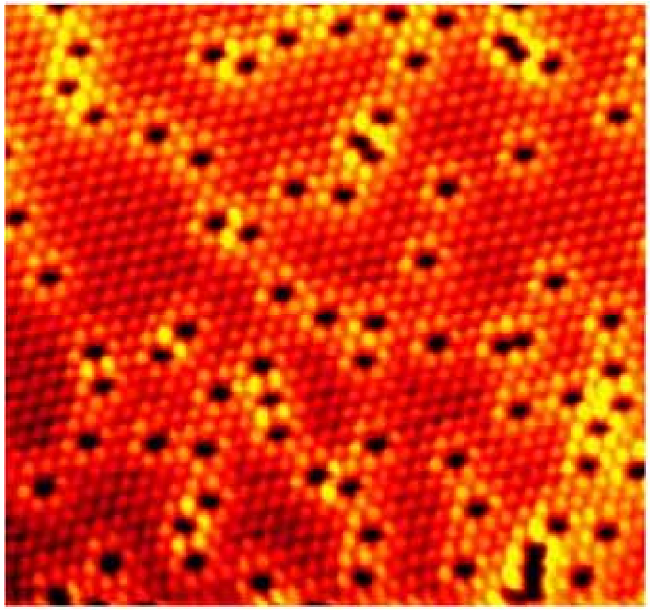

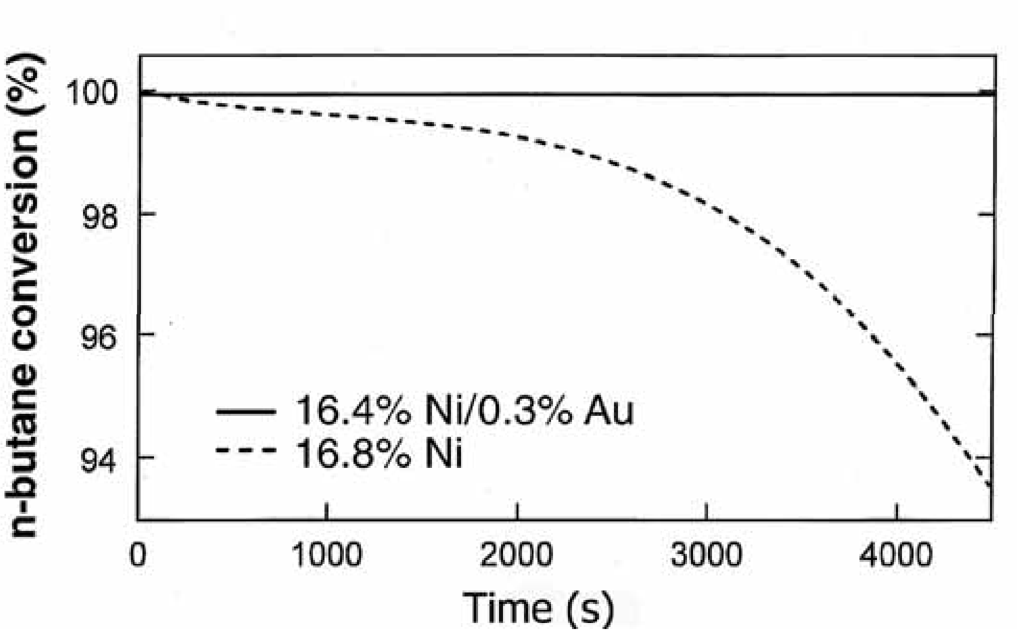

Inspired by quantum chemical calculations, Ni surface-alloyed with Au (black) on the left is used to reduce carbon poisoning of catalyst, as verified experimentally on the right.

Solar Photoelectrochemistry/Photocatalysis for H_2 Production

- Power conversion efficiency (10%) needs to be increased by reducing losses.
- Spectral response needs to be extended into the red
- Costs need to be reduced in the production of the transparent anode.

Low cost TiO_2 porous nanostructures allow deep light penetration into dye-sensitized solar cells to increase their efficiency.

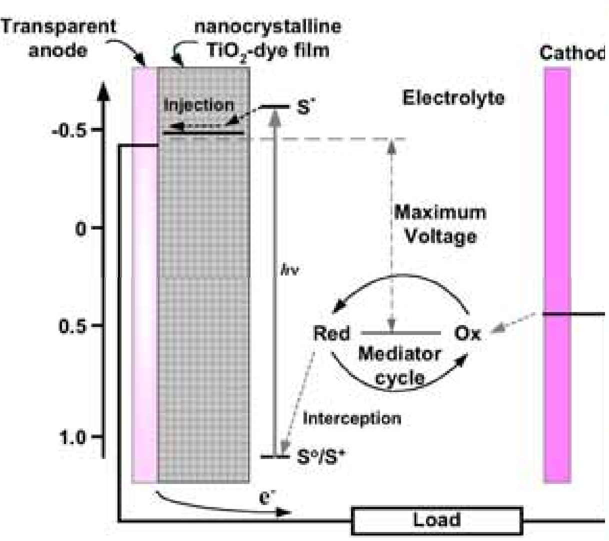

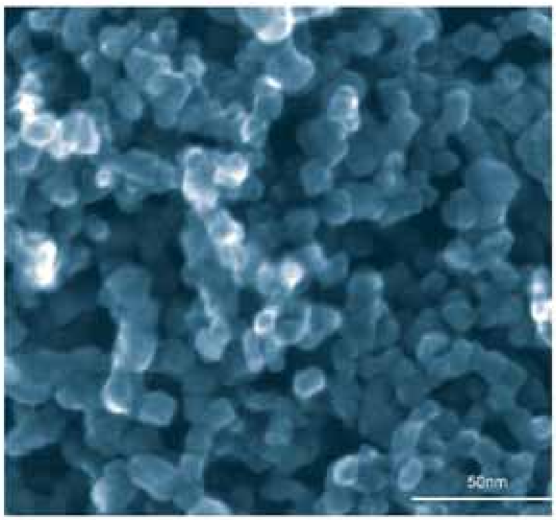

Photochemical solar cells or Grätzel cells use cheap porous TiO_2 with a huge surface area (see right). Dye additives allow absorption of visible light to better match solar spectrum (left).

Hydrogen Storage

Current Technology for automotive applications

- Tanks for gaseous or liquid hydrogen storage.
- Progress demonstrated in solid state storage materials.

System Requirements

- Compact, light-weight, affordable storage.
- System requirements set for FreedomCAR: 4.5 wt% hydrogen for 2005, 9 wt% hydrogen for 2015.
- No current storage system or material meets all targets.

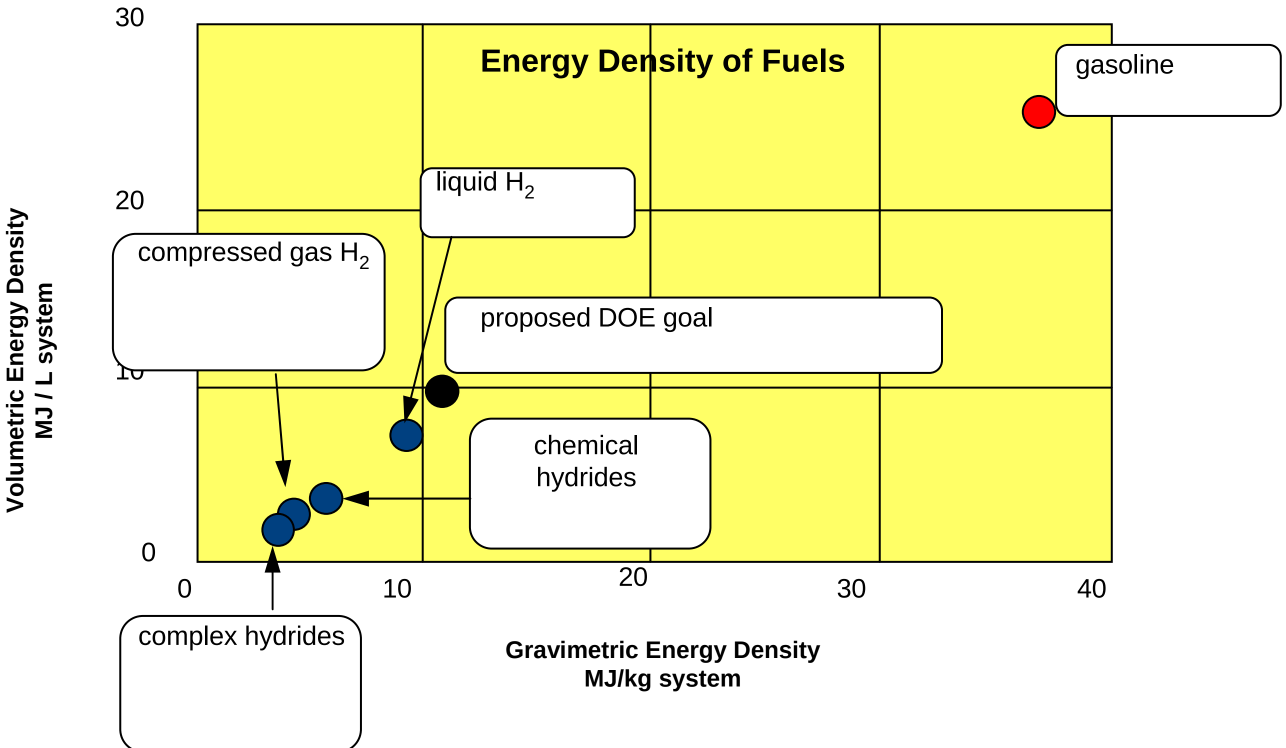

High Gravimetric H Density Candidates

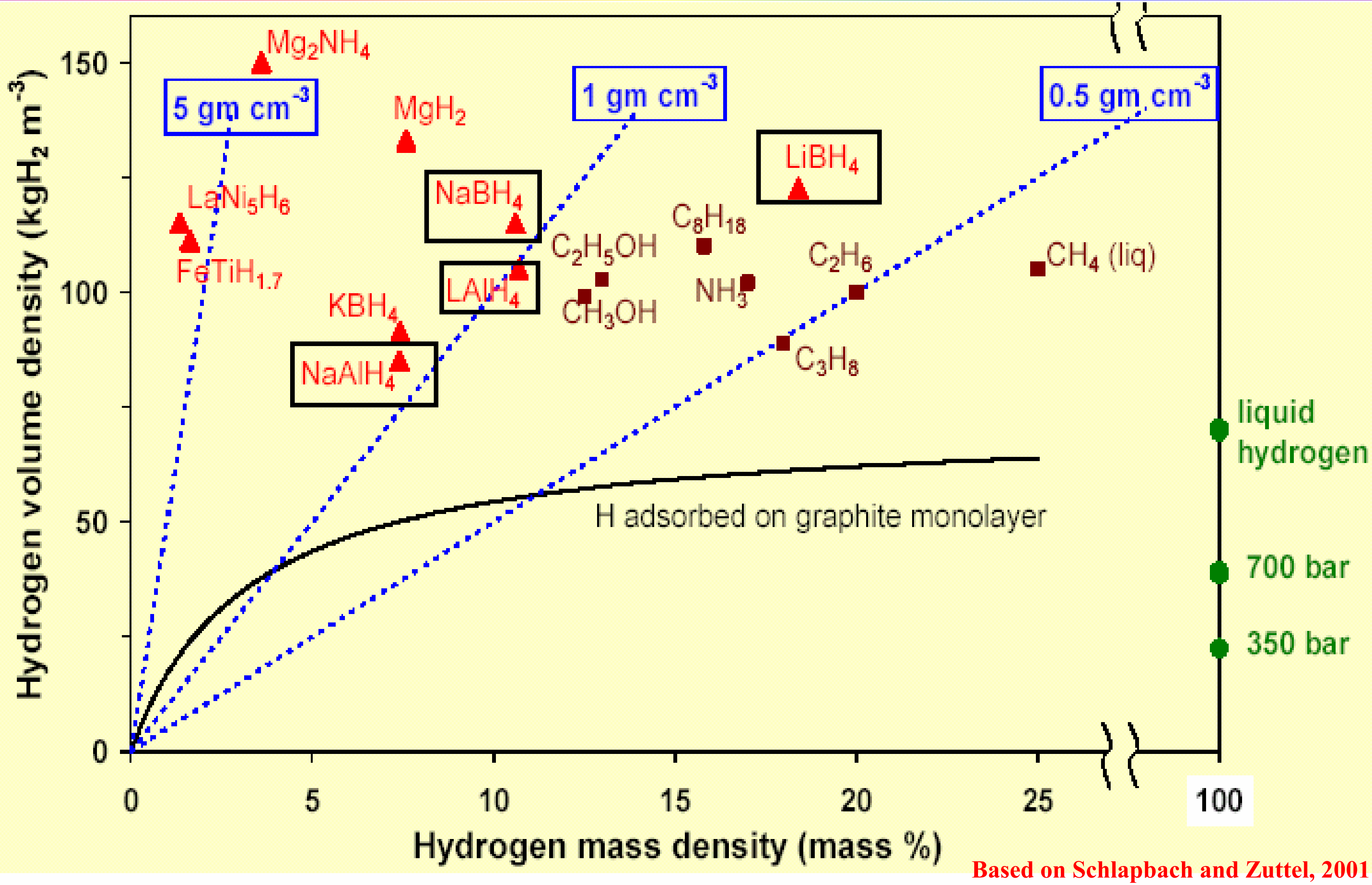

Based on Schlapbach and Zuttel, 2001

Carbon Nanotubes for Hydrogen Storage

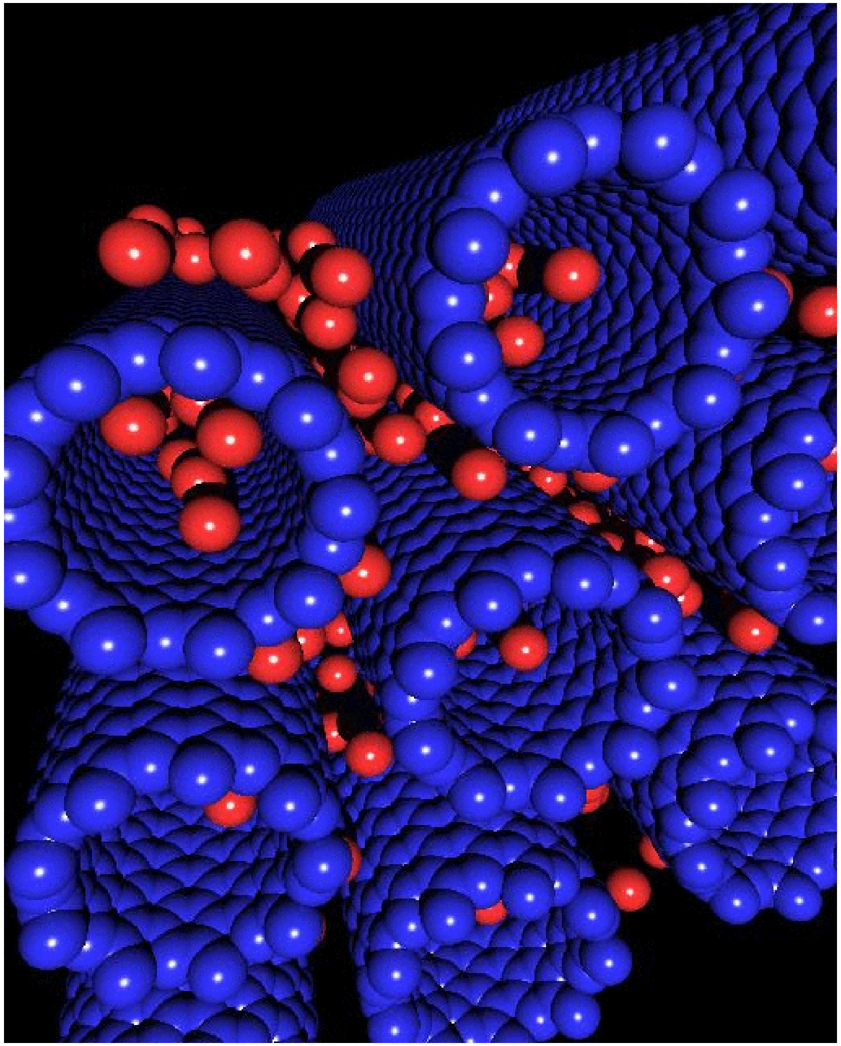

- The very small size and very high surface area of carbon nanotubes make them interesting for hydrogen storage.
- Challenge is to increase the H:C stoichiometry and to strengthen the H—C bonding at 300 K.
- H:C =1 → 8 wt % hydrogen

A computational representation of hydrogen adsorption in an optimized array of (10,10) nanotubes at 298 K and 200 Bar. The red spheres represent hydrogen molecules and the blue spheres represent carbon atoms in the nanotubes, showing 3 kinds of binding sites. (K. Johnson et al)

Nanoscale/Novel Materials

- **Nanoscale materials have high surface areas, novel shapes, with properties much different from their 3D counterparts – especially useful for catalysts and catalyst supports.**

- **Enhanced hydrogen adsorption on high surface area nanostructures may be attained by selective manipulation of surface properties.**

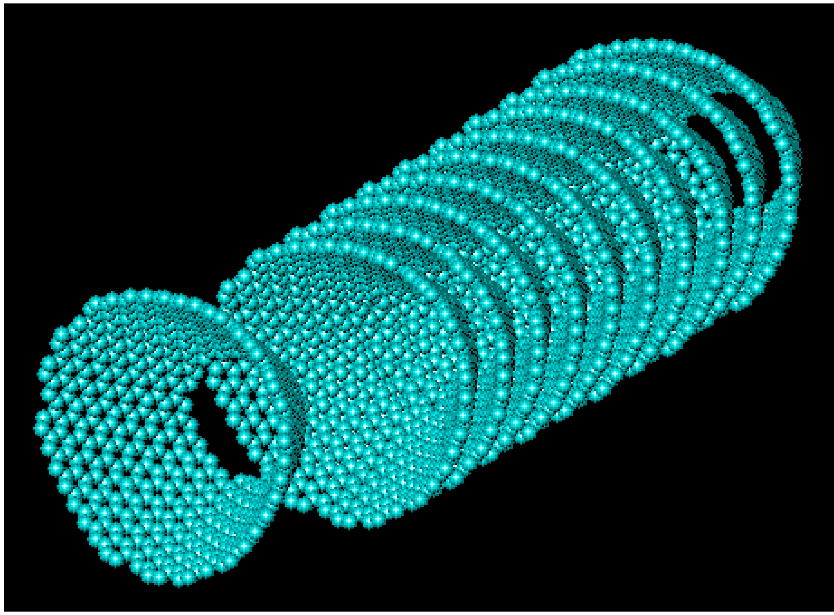

- **Nanostructures also have other opportunities for use for hydrogen storage.**

Nanostructures such as cup-stacked carbon nanofibers (less than 10nm diameter) and other high surface area structures are being developed to support tiny nanocatalyst particles (2nm) in the regions between the cups. Results obtained thus far are encouraging for specific applications.

Theory and Modeling

- AlH_4 is light weight with high potential storage capacity but the kinetics for hydrogen release are too slow.
- Calculations allow exploration of strategies to achieve bonding for H_2 release close to room temperature

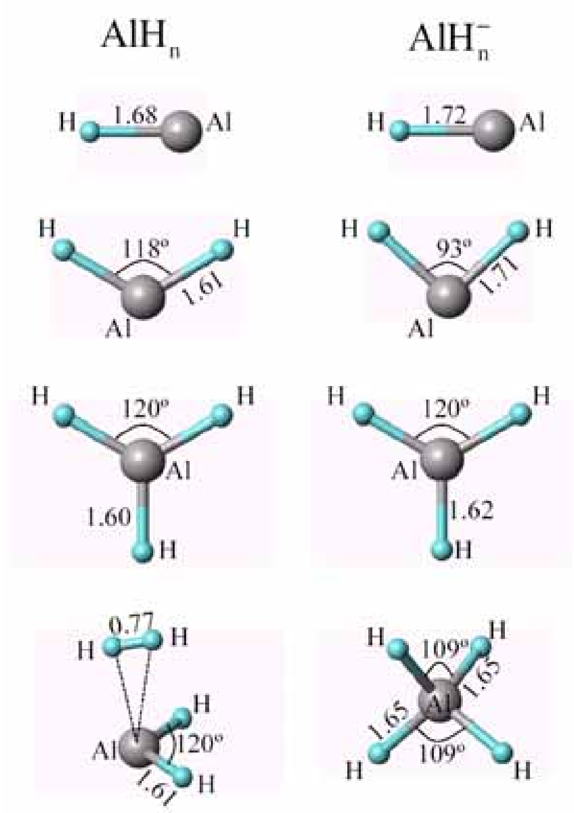

First principles density functional theory shows that neutral AlH_4 dissociates into $AlH_2 + H_2$ but that ionized AlH_4^- tightly binds 4 hydrogens.

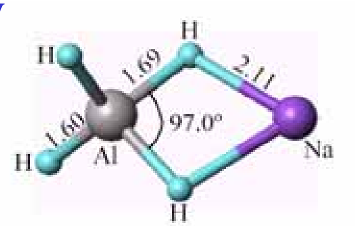

Calculations further show that Ti substitutes for Na in $NaAlH_4$ and weakens the Al-H ionic bond, thus making it possible to lower the temperature of H_2 desorption from 200 ° C to 120 ° C.

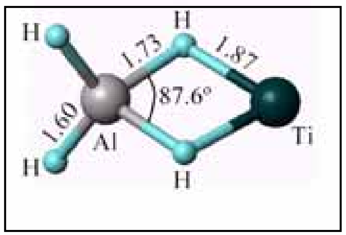

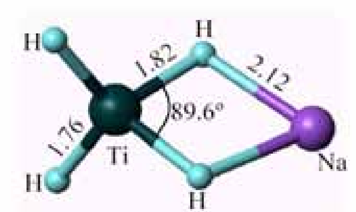

**(unpublished calculations of
P. Jena, co-chair of Hydrogen Storage Panel).**

Messages of DOE Hydrogen Report

- Enormous gap between present state-of-the-art capabilities and requirements that will allow hydrogen to be competitive with today's energy technologies
  - production: 9M tons $\Rightarrow$ 40M tons (vehicles)
  - storage: 4.4 MJ/L (10K psi gas) $\Rightarrow$ 9.72 MJ/L
  - fuel cells: \$3000/kW $\Rightarrow$ \$35/kW (gasoline engine)
- Enormous R&D efforts will be required
  - Simple improvements of today's technologies will not meet requirements
  - Technical barriers can be overcome only with high risk/high payoff basic research
  - Here nanostructures are expected to play an important role
- Research is highly interdisciplinary, requiring chemistry, materials science, physics, biology, engineering, nanoscience, computational science
- Basic and applied research should couple seamlessly

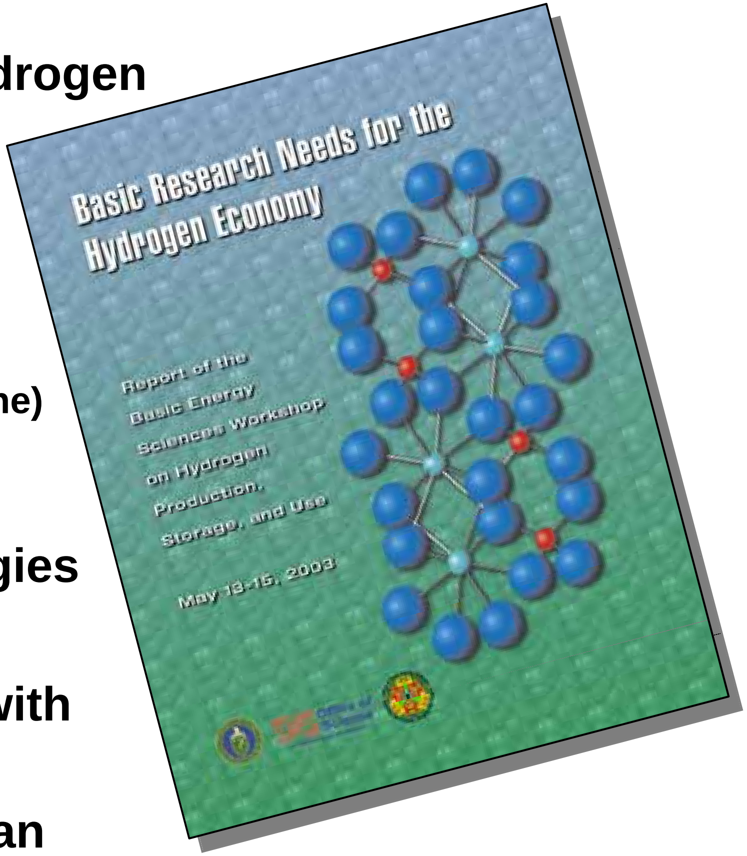

http://www.sc.doe.gov/bes/hydrogen.pdf

Acknowledgements

Collaborators:

Nanotubes

Dr. Gene Dresselhaus (MIT)
Georgii G. Samsonidze (MIT)
S. Grace Chou (MIT)
Dr. Stephen B. Cronin (Harvard)
Dr. Antonio G. Souza Filho (Brazil)
Dr. Ado Jorio (Brazil)
Prof. Riichiro Saito (Japan)
Prof. Morinobu Endo (Japan)

Nanowires

Dr. Yu-Ming Lin (MIT)
Oded Rabin (MIT)
Dr. Marcie Black (MIT)
Prof. Gang Chen (MIT)
Dr. J. Heremans (Delphi Corp.)

Funding:

NSF
DuPont
Intel

NASA

How to do (*n*,*m*) assignment with one E_{laser} ?

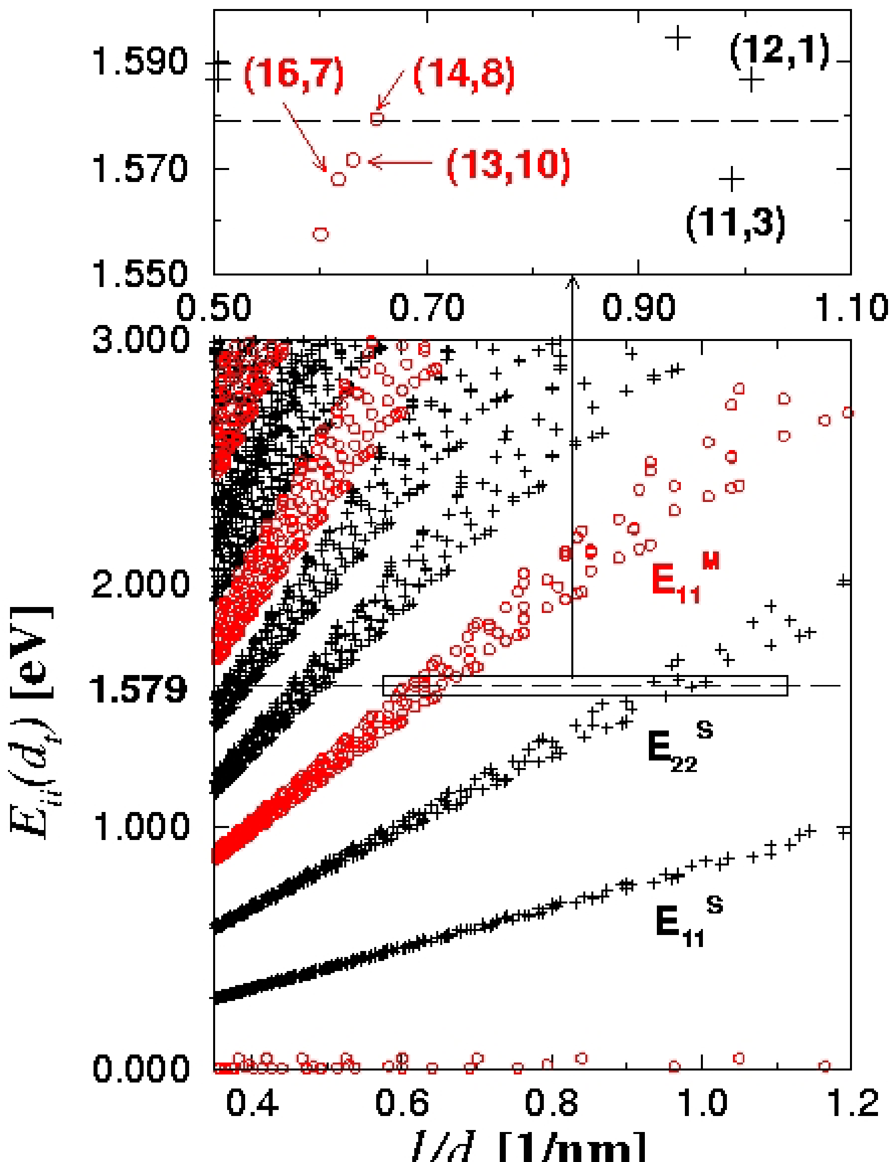

Vertical axis ($1/d_t$)

Radial breathing mode frequency

$\omega_{RBM} = \alpha / d_t$

Horizontal axis (E_{ii})

Laser energy (E_{laser})

+

Stokes/anti-Stokes intensity ratio

Use of a Tunable Laser

A. Jorio *et al.*, *Phys. Rev.* B 63, 245416 (2001)

$$I(E_{laser}) = \int \left| \frac{M}{(E_{laser} - E - i\Gamma_r)(E_{laser} \pm E_{ph} - E - i\Gamma_r)} \right|^2 g(E)\, dE$$

(−) Stokes process
(+) anti−Stokes process

JDOS (Joint Density of States) $g(E) = \mathrm{Re}\left[\sum_i \frac{a_{C-C} E}{d_t \gamma_0 \sqrt{(E - E_{ii} - i\Gamma_J)(E + E_{ii} - i\Gamma_J)}} \right]$

Resonant window ≈ 100 meV

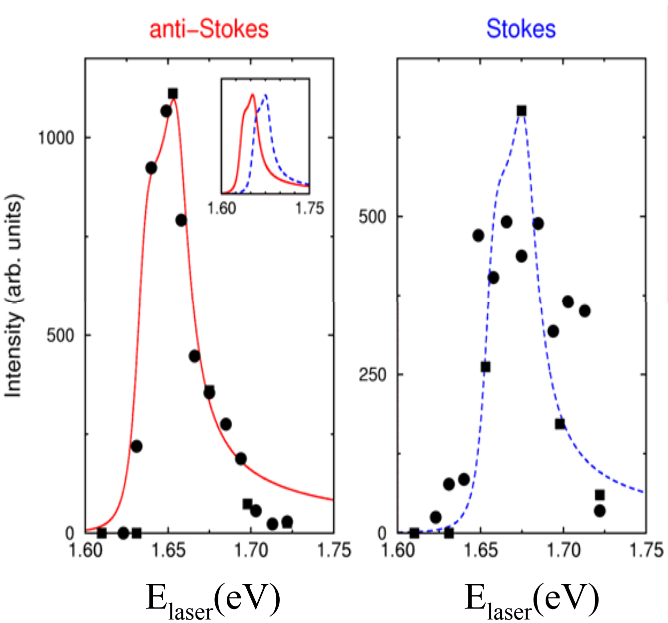

$a_{C-C} = 0.144$ nm
$\gamma_0 = 2.90$ eV

(18,0)

$d_t = 1.43$ nm
$\Gamma_r \sim 8$ meV
$\Gamma_J \sim 0.1–1.0$ meV
$E_{ii} = 1.655 \pm 0.003$ eV

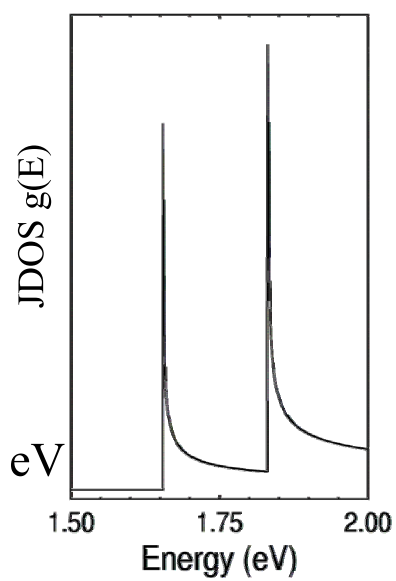

Resonant window reflects the electronic JDOS

$\omega_{RBM} = 248 / d_t$

Nanotube Separation

1. Analytical/Physical Separation

- **Field flow fractionation, size exclusion chromatography, capillary electrophoresis, gel permeation chromatography**

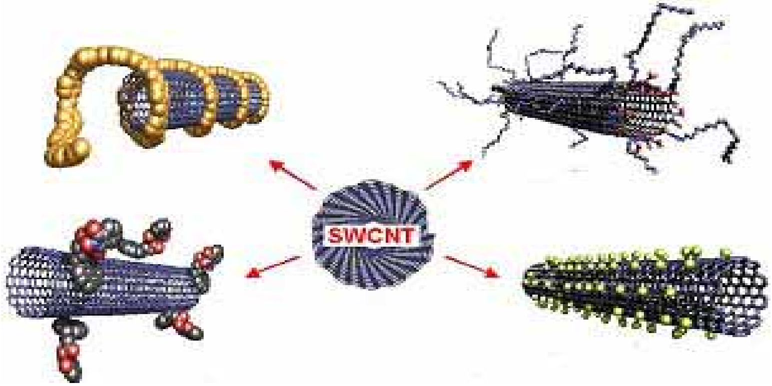

2. Chemical Methods

- **Covalent/non-covalent sidewall functionalization, π-stacking, and dispersion.**

3. Biological Methods

- **Selective binding of bio-molecules**
  Wang *et al. Nature Mat*. **2**, 196 (2002)

Raman Spectroscopy – Provides a Probe to Evaluate Separation Efficiency.

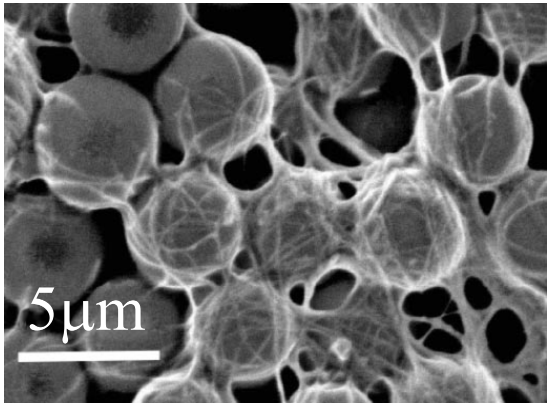

Reciprocal Lattice and k Vectors

R. Saito et al. , Physical Properties of Carbon Nanotubes, Imperial College Press (1998)

- D2 graphite

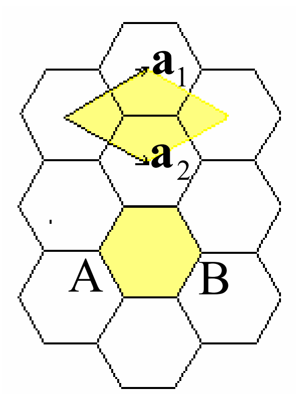

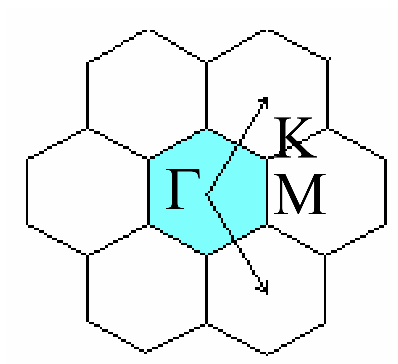

$$\mathbf{a}_1 = (\frac{\sqrt{3}}{2}, \frac{1}{2})a, \qquad \mathbf{a}_2 = (\frac{\sqrt{3}}{2}, -\frac{1}{2})a$$

$$\mathbf{b}_1 = (\frac{1}{2}, \frac{\sqrt{3}}{2})\frac{4\pi}{\sqrt{3}a}, \qquad \mathbf{b}_2 = (\frac{1}{2}, -\frac{\sqrt{3}}{2})\frac{4\pi}{\sqrt{3}a}$$

► 1D Carbon nanotubes

Rolling up 2D graphene sheet

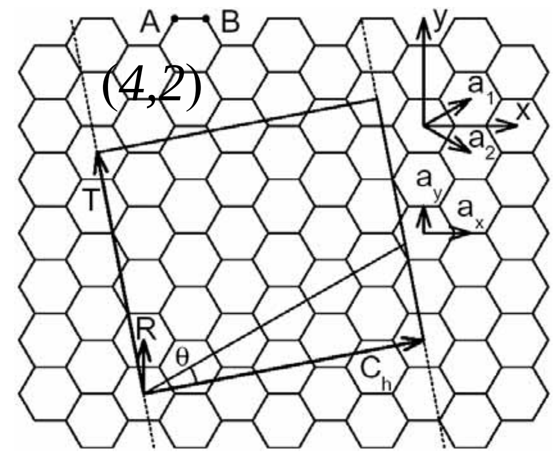

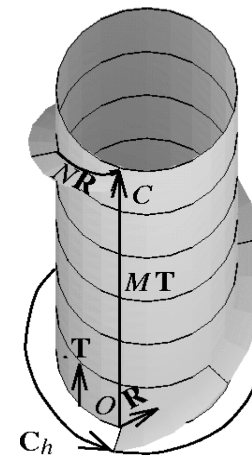

1 Dimensional Wave Vectors ($\mathbf{K_2}$)

Discrete in circumferential direction ($\mathbf{K_1}$)

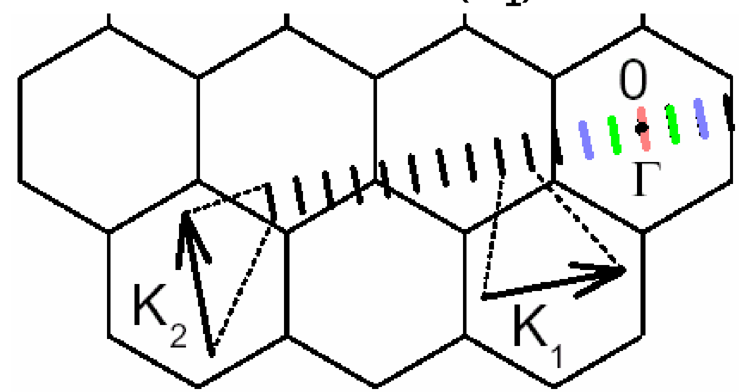

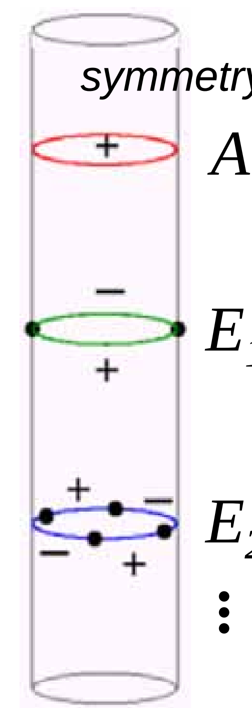

- 1D quantum confinement -

- presence of cutting lines -

Electronic structure – from 2D to 1D

π and π* bands of 2D graphite

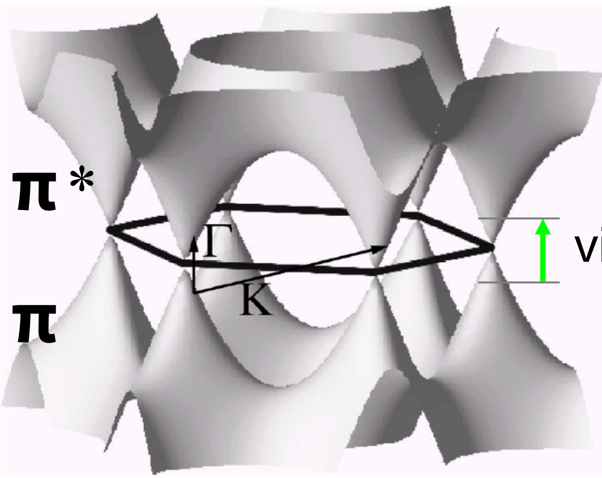

visible range

Dubay and Kresse, Phys. Rev. B ***67****, 035401 (2003)*

E_F

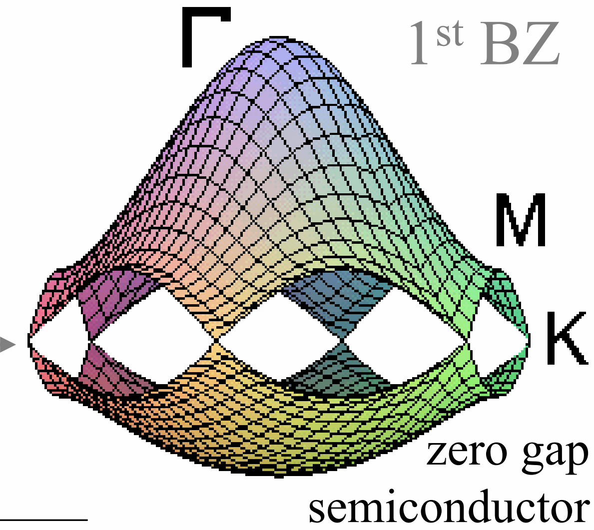

Tight binding energies

$$E_k = \pm t\sqrt{1 \pm 4\cos\frac{k_y a}{2}\cos\frac{\sqrt{3}k_x a}{2} + 4\cos^2\frac{k_y a}{2}}$$

1D electronic dispersion (cutting lines) in carbon nanotubes – *(4,2)*

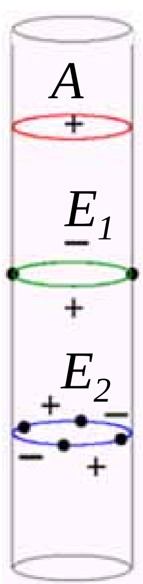

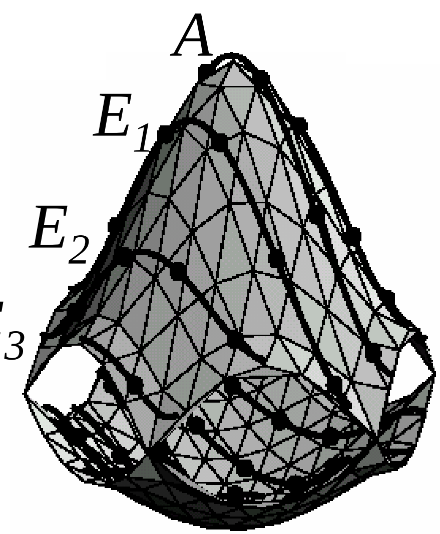

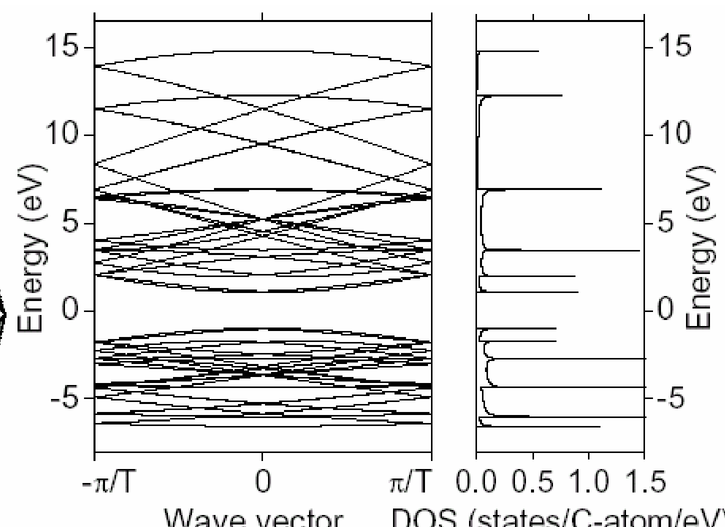

- Presence of van Hove singularities (vHs)
- Molecular-like behaviour with high density of electronic states (DOS)

Electronic Structure

GENERAL MODEL:
From 2D tight binding
+ quantum confinement
↓
Presence of vHS
(van Hove singularities)

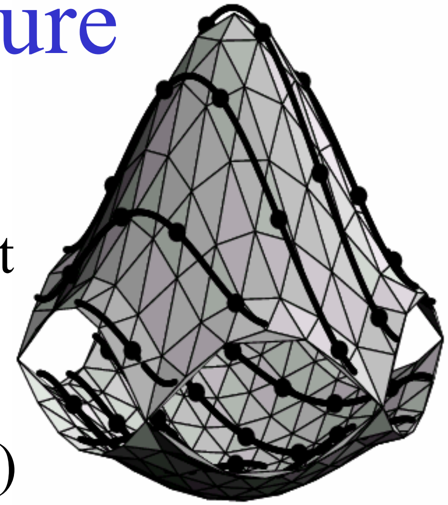

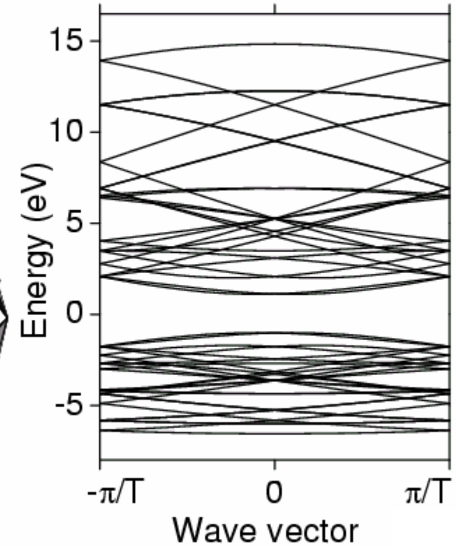

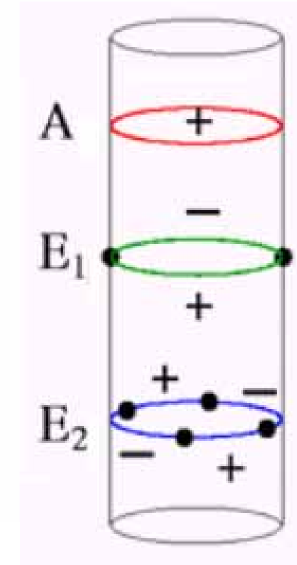

vHS in the density of states (DOS)

Responsible for strong optical effects!

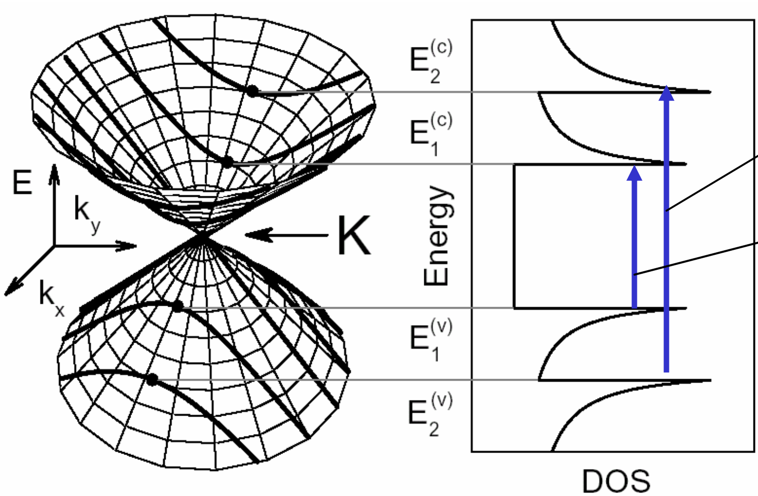

(*4,2*) nanotube (d_t = 0.43nm)

Kataura plot

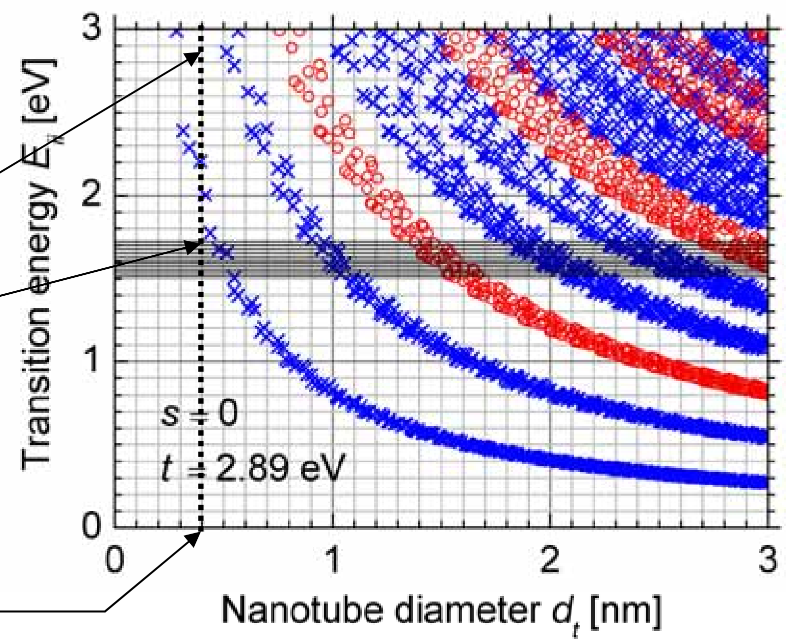

Spectroscopy → determination of E_{ii} experimentally

Kataura's plot

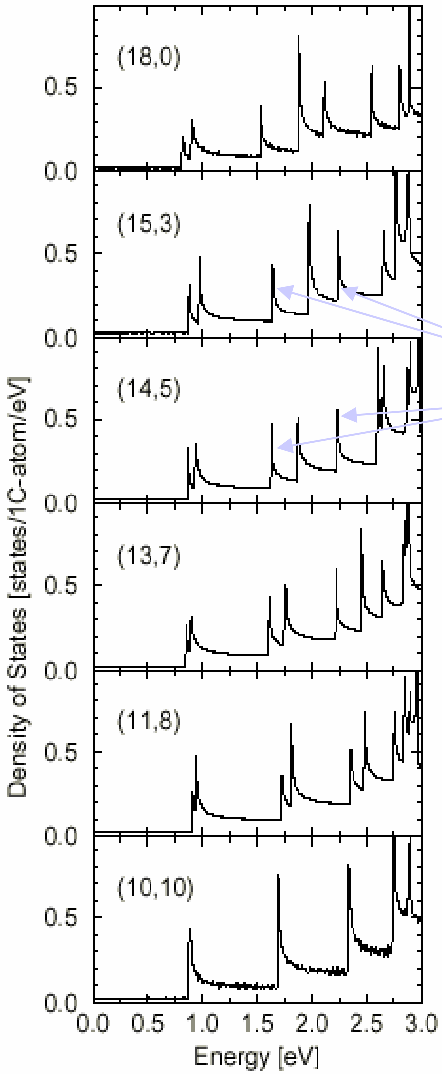

JDOS for different (*n,m*) SWNTs

Each (*n,m*) SWNT has a different set of van Hove singularities (vHSs) in the joint density of electronic states (JDOS)

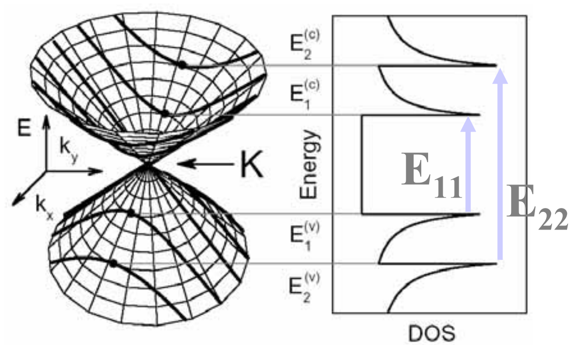

Spectroscopy signal is observed when $E_{photon} = E_{ii}$

vHs position vs 1/diameter

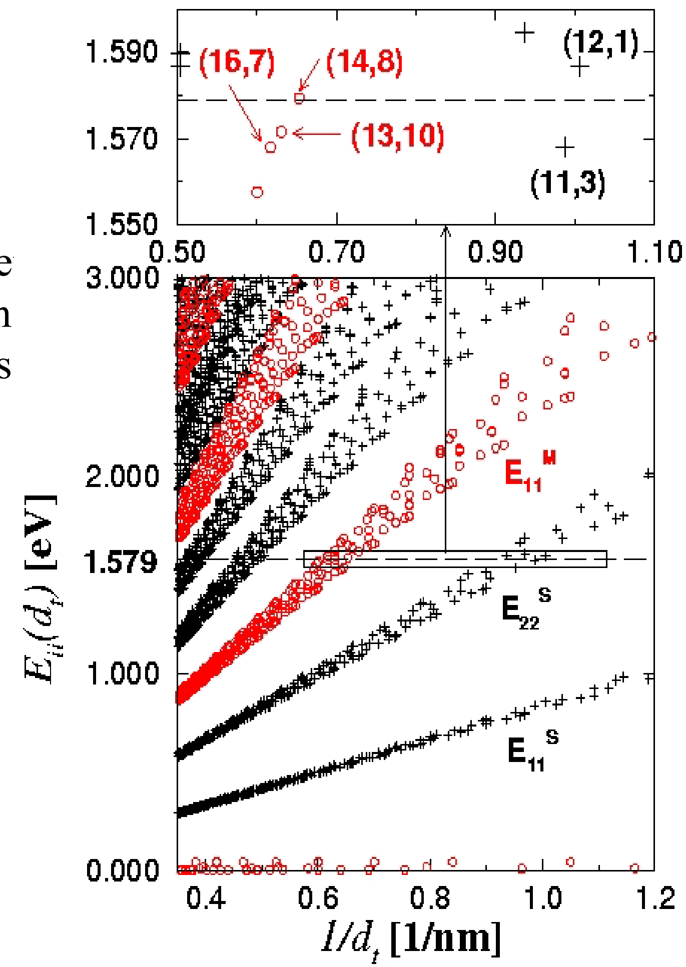

Raman analysis should be based on the Kataura's plot depending on diameter distribution (RBM) and E_{laser}

Resonant Raman Intensity with Tunable Laser

Determination of E_{ii} for a single nanotube

A. Jorio et al.,PRB 63, 245416 (2001)

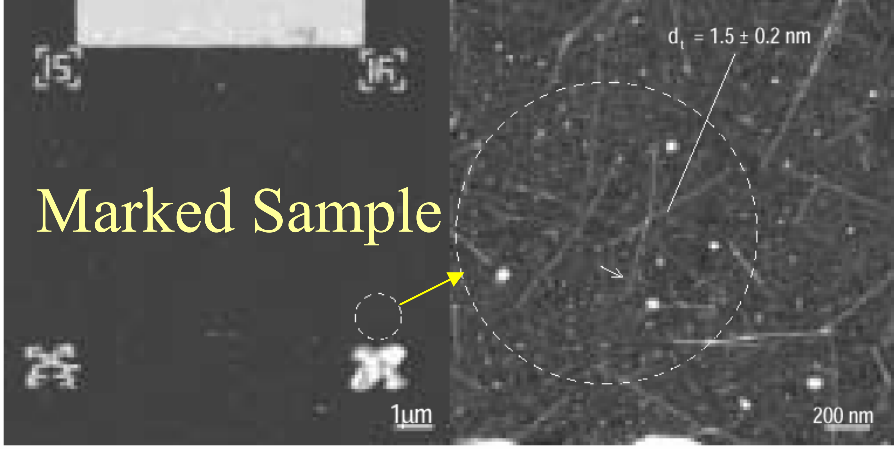

$$
\begin{cases}
I(E_l) = \sum_{\mathbf{k}} |K(\mathbf{k})|^2 , \\
K(\mathbf{k}) = \dfrac{M_{\mathrm{opt}}^{\mathrm{abs}}(\mathbf{k})\, M_{\mathrm{el-ph}}^{\mathrm{S/AS}}(\mathbf{k})\, M_{\mathrm{opt}}^{\mathrm{ems}}(\mathbf{k})}{(E_l - E(\mathbf{k}) - i\Gamma)(E_l \mp \hbar\omega_{\mathrm{ph}} - E(\mathbf{k}) - i\Gamma)}
\end{cases}
$$

$a_{C\text{-}C} = 0.142$ nm

$\gamma_o = 2.90$ eV

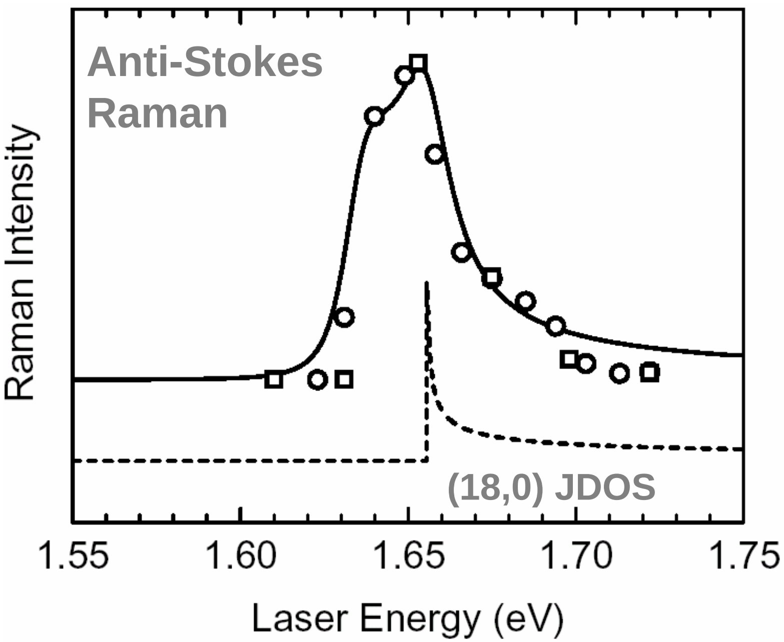

Resonance Raman spectroscopy and a tunable laser gives E_{ii} with high precision (better than 10meV)

Stokes vs. Anti-Stokes resonance Raman

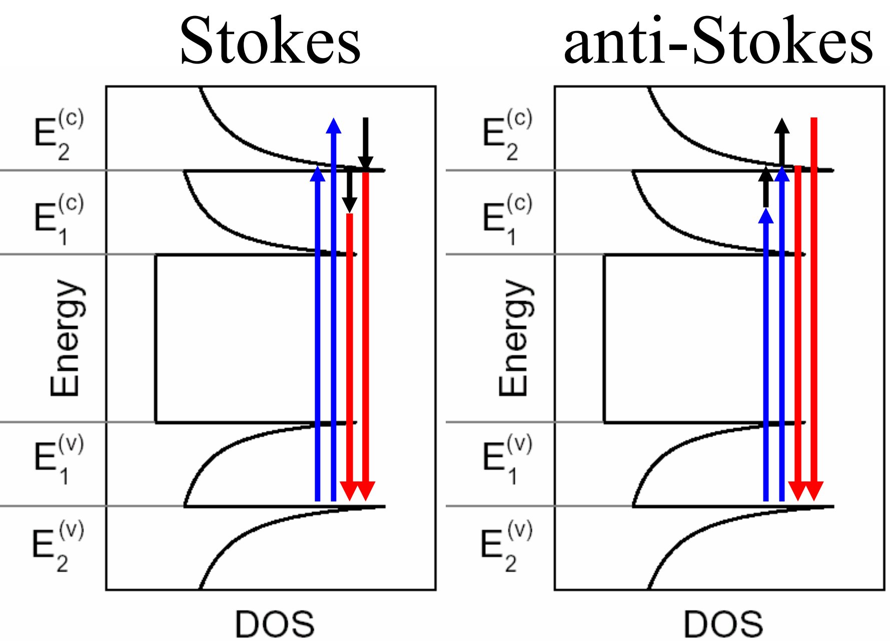

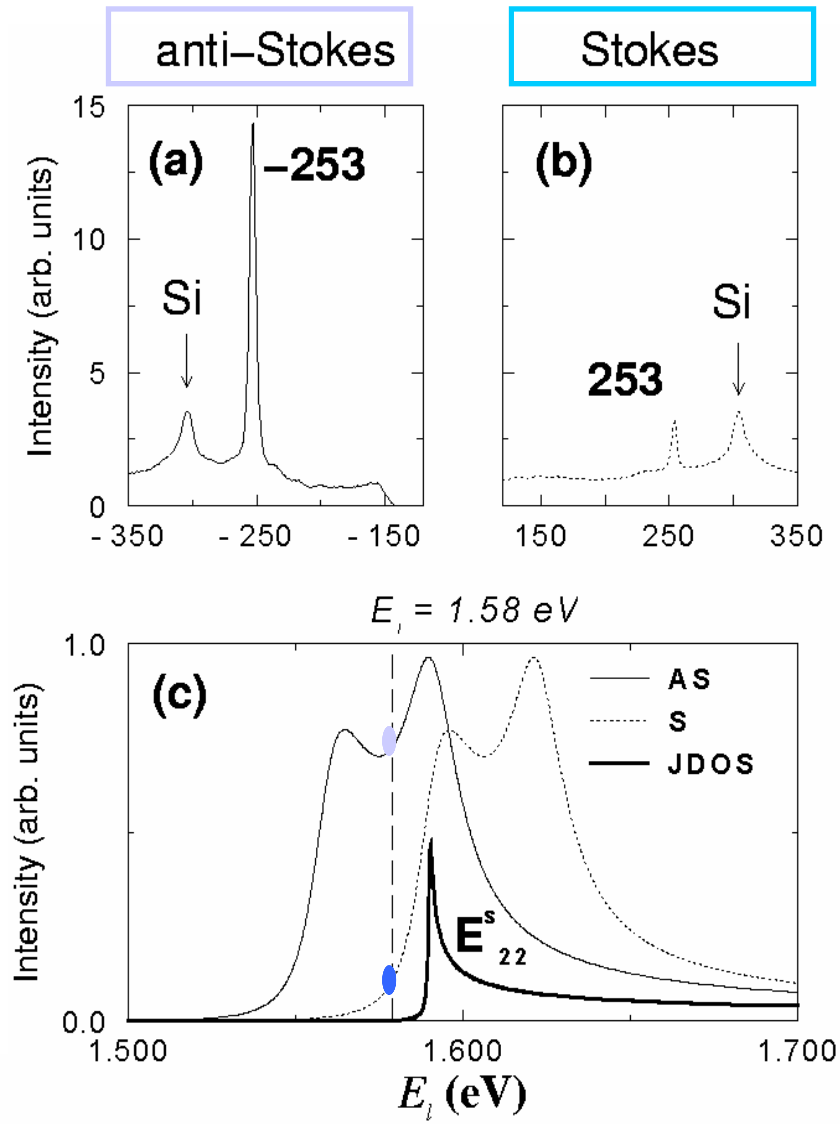

Coherent process with Stokes vs. Anti-Stokes asymmetry – crossing point gives E_{ii} accurately

$$\begin{cases} I\left(E_l\right) = \sum_{\mathbf{k}} \left|K\left(\mathbf{k}\right)\right|^2 , \\ K\left(\mathbf{k}\right) = \dfrac{M_{\mathrm{opt}}^{\mathrm{abs}}\left(\mathbf{k}\right) M_{\mathrm{el-ph}}^{\mathrm{S/AS}}\left(\mathbf{k}\right) M_{\mathrm{opt}}^{\mathrm{ems}}\left(\mathbf{k}\right)}{\left(E_l - E\left(\mathbf{k}\right) - i\Gamma\right)\left(E_l \mp \hbar\omega_{\mathrm{ph}} - E\left(\mathbf{k}\right) - i\Gamma\right)} \end{cases}$$

Single nanotube optical absorption + photoluminescence

Weisman and Bachilo, Nanoletters (2003)

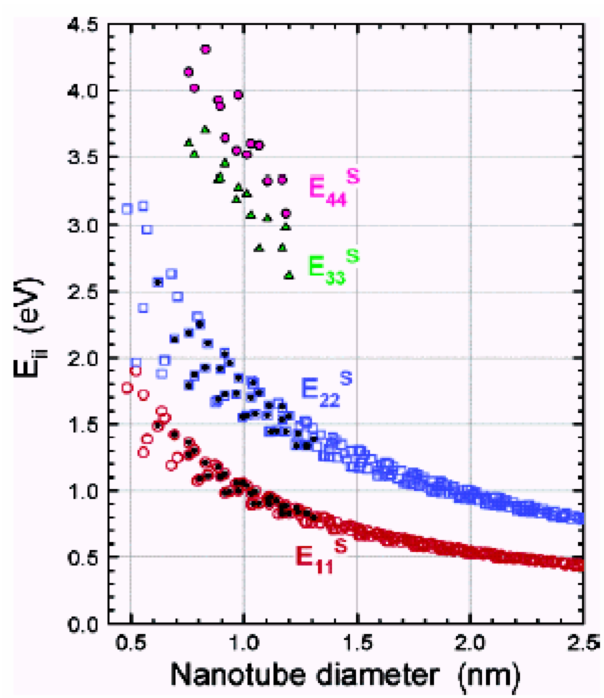

SWNTs isolated in aqueous surfactant suspensions

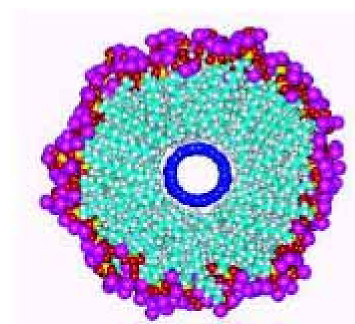

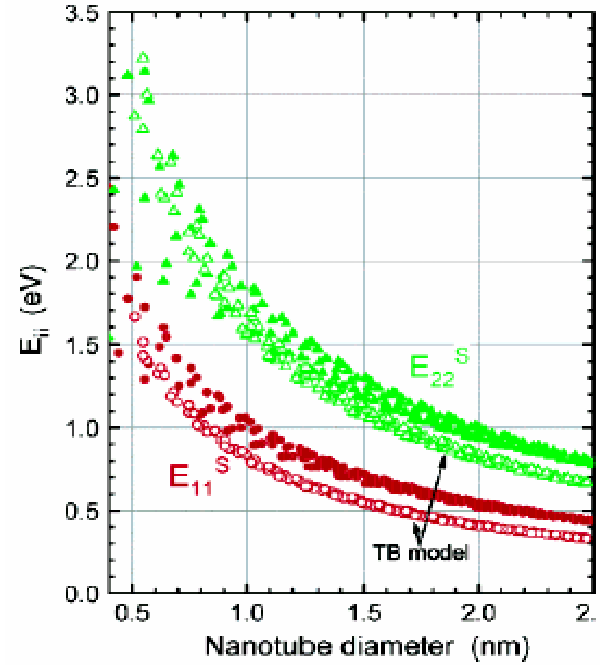

- Experimental results show considerable deviations from usual TB model

- Development of an empirical Kataura plot

$$\bar{\nu}_{11}(\mathrm{mod}\ 1) = \frac{1 \times 10^7\ \mathrm{cm}^{-1}}{157.5 + 1066.9 d_t} - 771\ \mathrm{cm}^{-1}\frac{[\cos(3\alpha)]^{1.374}}{d_t^{2.272}} \quad (1a)$$

$$\bar{\nu}_{11}(\mathrm{mod}\ 2) = \frac{1 \times 10^7\ \mathrm{cm}^{-1}}{157.5 + 1066.9 d_t} + 347\ \mathrm{cm}^{-1}\frac{[\cos(3\alpha)]^{0.886}}{d_t^{2.129}} \quad (1b)$$

$$\bar{\nu}_{22}(\mathrm{mod}\ 1) = \frac{1 \times 10^7\ \mathrm{cm}^{-1}}{145.6 + 575.7 d_t} + 1326\ \mathrm{cm}^{-1}\frac{[\cos(3\alpha)]^{0.828}}{d_t^{1.809}} \quad (2a)$$

$$\bar{\nu}_{22}(\mathrm{mod}\ 2) = \frac{1 \times 10^7\ \mathrm{cm}^{-1}}{145.6 + 575.7 d_t} - 1421\ \mathrm{cm}^{-1}\frac{[\cos(3\alpha)]^{1.110}}{d_t^{2.497}} \quad (2b)$$

Determination of E_{ii} and (*n*,*m*)

1) **Theoretical model (many-body effects...)**
2) **Dependence of E_{ii} on the SWNT environment (SDS, Si/SiO_2, suspended ...)**
3) **Dependence of E_{ii} on experimental technique**

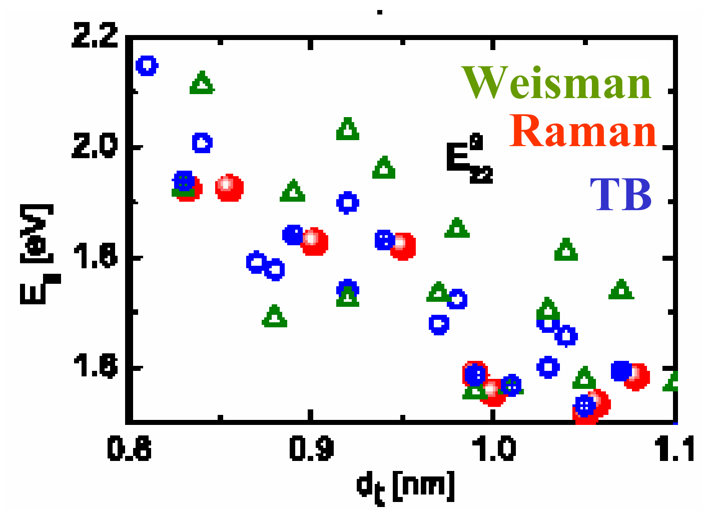

4) **For (*n*,*m*) assignment, Raman is necessary**

$$\boxed{\omega_{RBM} = A/d_t + B}$$

SWNTs isolated on a Si/SiO_2 substrate

A = 248 cm^{-1}nm , B=0

Absorption vs. emission

Bachilo et al., Science 298, 2361 (2002)

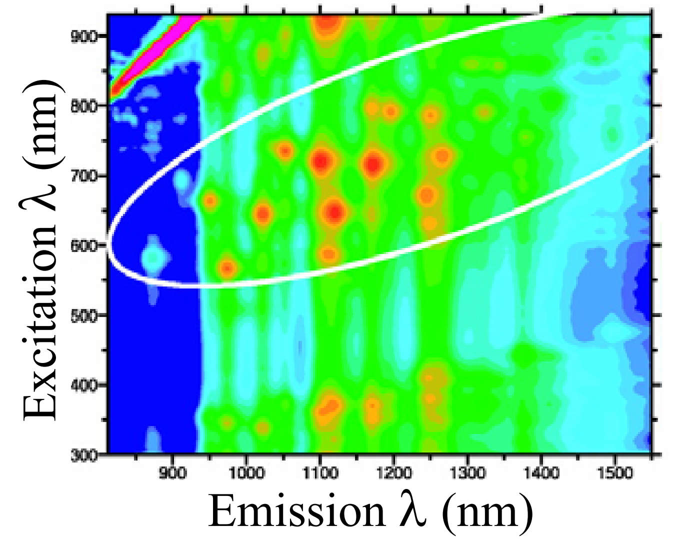

Theoretical Raman plot

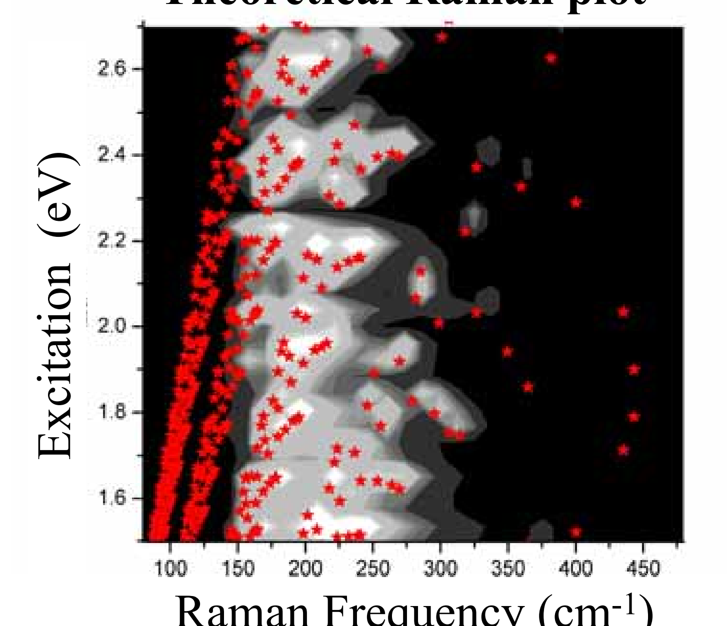

Physics for small d_t SWNTs

New Journal of Physics
An Institute of Physics and Deutsche Physikalische Gesellschaft Journal

The geometry and the radial breathing mode of carbon nanotubes: beyond the ideal behaviour

Jenő Kürti[1,3], Viktor Zólyomi[1], Miklos Kertesz[2] and Guangyu Sun[2,4]
[1] Department of Biological Physics, Eötvös University Budapest, Pázmány Péter sétány 1/A, H-1117 Budapest, Hungary
[2] Department of Chemistry, Georgetown University, Washington, DC 20057, USA
E-mail: kurti@virag.elte.hu

New Journal of Physics **5** (2003) 125.1–125.21 (http://www.njp.org/)
Received 1 July 2003
Published 3 October 2003

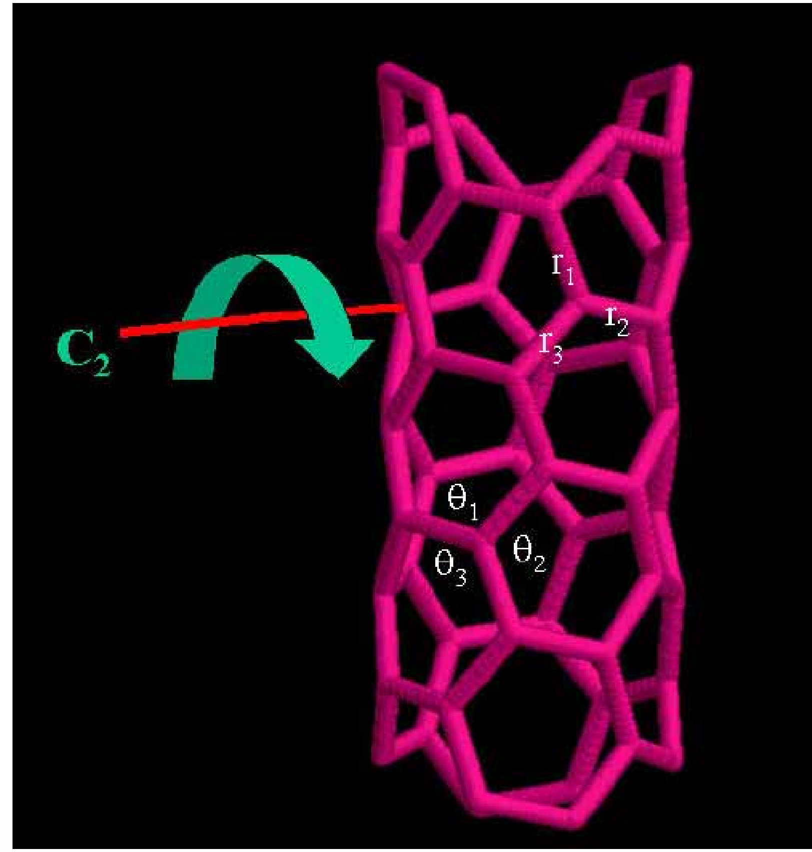

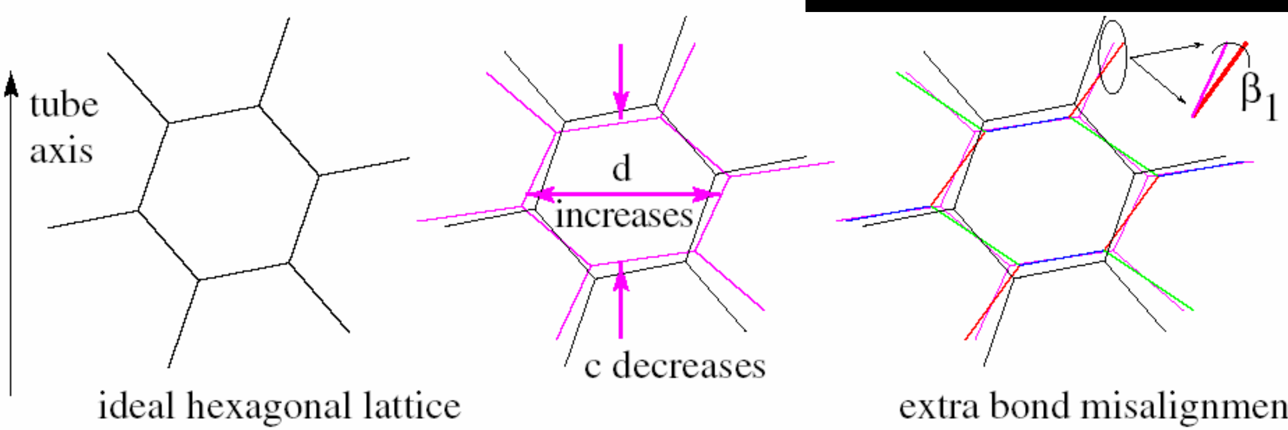

Momentum conservation in the electron scattering by a phonon

$|q| = |k_4 - k_3|$

Phonon confinement

$k_3 \sim k_4$

$k_3 = k_4 \rightarrow \theta = 0 \rightarrow$ zigzag

Phonon van Hove singularities occur at $q \rightarrow 0$

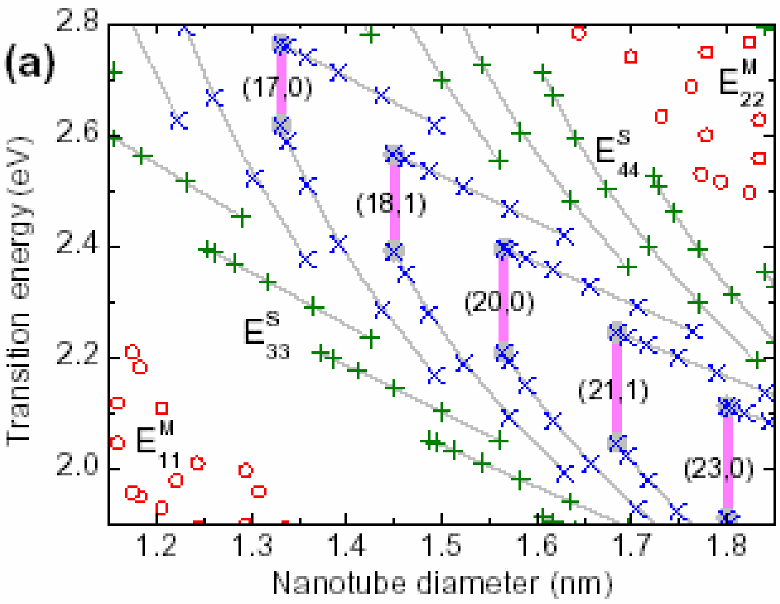

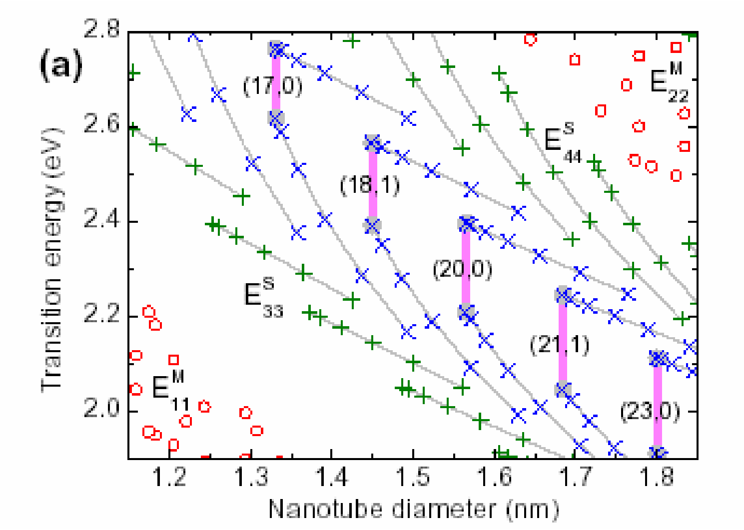

Observation of nanotubes with $\theta \to 0$

$$\omega_{\mathrm{IFM}}^{\pm} = \omega_{\mathcal{O}}^{0} + (v_{\mathcal{O}} \pm v_{\mathcal{A}})6/d_t$$